University of Rhode Island

DigitalCommons@URI

Open Access Dissertations

1996

THE EFFECT OF COMPRESSION FORCE ON THE NEAR-INFRARED SPECTRA OFT ABLET DOSAGE FORMS

Karen Marie Morisseau
University of Rhode Island

Follow this and additional works at: https://digitalcommons.uri.edu/oa_diss

Terms of Use
All rights reserved under copyright.

THE EFFECT OF COMPRESSION FORCE

ON THE NEAR-INFRARED SPECTRA

OF TABLET DOSAGE FORMS

BY

KAREN M. MORISSEAU

A DISSERTATION SUBMITTED IN PARTIAL FULFILLMENT OF THE

REQUIREMENTS FOR DEGREE OF

DOCTOR OF PHILOSOPHY

IN

PHARMACEUTICAL SCIENCES
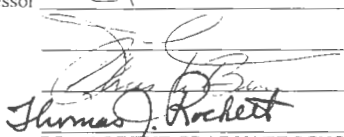
UNIVERSITY OF RHODE ISLAND

1996

DOCTOR OF PHILOSOPHY DISSERTATION

OF

KAREN M. MORISSEAU

APPROVED:

Dissertation Committee

Major Professor

DEAN OF THE GRADUATE SCHOOL

UNIVERSITY OF RHODE ISLAND

1996

ABSTRACT

The United States Pharmacopoeia/National Formulary (USP/NF) sets the standards and maintains monographs for the evaluation of tablets. These include Official Tests for uniformity of dosage units and disintegration testing, and Unofficial Tests for mechanical strength (hardness, crushing strength) and resistance to abrasion (friability). Current methods of analyzing tablet hardness involve the indirect measurement of the mechanical strength of a tablet through destructive and time-consuming procedures. Near-infrared reflectance spectroscopy (NIRS) is gaining acceptance in the pharmaceutical industry as a non-invasive and non-destructive method for the analysis of finished dosage forms and raw materials. This investigation outlines methods used to evaluate various tablet parameters using NIRS and the achievement of successful predictions of those parameters. NIR models for tablet hardness and density were developed for 15% and 20% hydrochlorothiazide and 2% and 6% chlorpheniramine maleate in a 0.5% magnesium stearate and microcrystalline cellulose matrix. NIR calibration models for tablet hardness were developed for flat-faced and convex round tablets containing 6% chlorpheniramine maleate and 0.5% magnesium stearate, with either microcrystalline cellulose or dibasic calcium phosphate dihydrate. Although the NIR response to changing hardness was the same regardless of the drug, separate models were required for tablets of different geometries. Scored tablets also required formulation specific calibrations for NIR hardness determination. Models for upper and lower compression forces were developed for flat-faced round tablets containing 6% chlorpheniramine maleate and 0.5% magnesium stearate, with either microcrystalline cellulose or dibasic calcium phosphate dihydrate. NIRS prediction of these parameters was at least as precise as the reference hardness test. Calibration of compression forces was successful for microcrystalline cellulose-based tablets, but not for the more variable dibasic calcium phosphate dihydrate systems. The methods described in this investigation may serve as a model for the future acceptance of NIRS as an alternative to current compendial methods for tablet hardness.

ACKNOWLEDGMENTS

PREFACE

This document was prepared in the format of the manuscript plan in accordance to section 11-3 of the Graduate Manual at the University of Rhode Island. The dissertation is divided into three sections.

Section I contains a general introduction to the objectives of my research. Section II consists of the main body of this dissertation. This section is composed of four manuscripts, written in the format required for each scientific journal to which they were submitted. An addendum to Manuscript I was inserted between Manuscripts I and II. An addendum to Manuscript IV was included following Manuscript IV. A statement of overall conclusions for the entire dissertation is also included in this section. Section III contains three appendices which include additional information and experimental details useful to the understanding of the work in section II. A bibliography follows Section III, citing all sources used to create this document.

TABLE OF CONTENTS

LIST OF PUBLICATIONS

The following is a list of the journals and meetings the manuscripts were prepared for and their publication status.

Manuscript I

PHARMACEUTICAL USES OF NEAR-INFRARED SPECTROSCOPY

Published in *Drug Development and Industrial Pharmacy* 21(9) 1071-1090 (1995).

Manuscript II

A FEASIBILITY STUDY OF THE EFFECT OF COMPRESSION FORCE ON THE

NEAR-INFRARED SPECTRA OF TABLETS

Presented at 4Pharma Conference, March 1995

Manuscript III

NEAR-INFRARED SPECTROSCOPY AS A NON-DESTRUCTIVE ALTERNATIVE TO
CONVENTIONAL TABLET HARDNESS TESTING

Presented at AAPS Tenth Annual Meeting November 1995 Poster Session
Accepted for publication in *Pharmaceutical Research*

Manuscript IV

EFFECT OF MATRIX AND GEOMETRY ON THE NEAR-INFRARED
DETERMINATION OF TABLET HARDNESS

Submitted to Journal of Pharmaceutical & Biomedical Analysis

LIST OF TABLES

MANUSCRIPT 4

APPENDIX B

APPENDIX C

LIST OF FIGURES

MANUSCRIPT 4

xiv

ADDENDUM TO MANUSCRIPT 4

SECTION I

INTRODUCTION

Near-Infrared Reflectance Spectroscopy (NIRS) is becoming a valuable analytical tool in the pharmaceutical industry. NIRS involves the multidisciplinary approaches of the analytical chemist, statistician and computer programmer. The term "chemometrics" refers to the use of knowledge from other disciplines to derive meaningful chemical information from samples of varying complexity. Chemometrics is defined[1] as the chemical discipline that uses mathematical, statistical and other methods employing formal logic to: a) design or select optimal measurement procedures and experiments, and, b) provide maximum relevant chemical information by analyzing chemical data. Chemometrics has found widespread use in analytical chemistry and is relied upon for the development of NIRS methods. Numerous types of NIRS problems are studied with qualitative and quantitative chemometric methods.

In the NIR region, the radiation can penetrate compacted materials, such as tablets, providing a vast amount of spectral information about the sample. When used in reflectance mode, the NIR light beam is scattered from powder samples after its molecules have absorbed it selectively. The unabsorbed radiation then passes to the several detectors mounted at an angle to the path of the incident rays. The analysis takes approximately 40 seconds per sample. Application of a math treatment, such as second derivative, prepares the raw spectral data for use in a regression and subsequent development of a calibration equation. This type of treatment results in a data file which will yield more information more easily than a raw data file.

Official Standards for the evaluation of tablets are prescribed by the United States Pharmacopoeia[2] (USP) and other compendia and include uniformity of dosage units (weight variation, content uniformity) and disintegration testing. Unofficial tests include those for mechanical strength (hardness, crushing strength) and resistance to abrasion (friability). Tablet hardness or crushing strength is an indication of the mechanical strength

of a tablet. Hardness has also been associated with other tablet properties, such as density and porosity[3].

Tablet hardness depends on the weight of material and the space between the upper and lower punches at the moment of compression. Inconsistent hardness values are likely to result from variation in these parameters. A tablet should be no harder than necessary for adequate handling and shipping. If the tablet is too hard, it may not disintegrate in the required amount of time. If it is too soft, it may not withstand the rigors of shipping, handling and dispensing, and may crumble easily. In production, a hardness of four kilograms (or kilopons) is considered to be minimum for a satisfactory tablet[4].

Variation in tablet hardness may be caused by poor mixing, poor flow, unequal length punches, or a variation in the size and distribution of granules being compressed. Poor mixing of a formulation may lead to poor flow of material, since lubricants and glidants may not have been thoroughly distributed. Poor flow may cause improper filling of the dies, resulting in weight and hardness variation. A slight variation in the lengths of the lower punches can lead to variation in the fill volume and affect tablet hardness. Finally, if there are too many large granules present, the proportion of large and small particles may change the fill weight in each die[5].

Results of mechanical tests give an indication of how the tablet will behave during handling. The crushing strength of a tablet (axial or radial) has been described as a function of the compressional pressure employed during its compaction[6]. The mechanical strength of a tablet plays an important role in the development and control procedures. Crushing strength is the most widely used test of mechanical strength. It is defined as the compression force which, when applied diametrically to a tablet, just fractures it[7].

The Erweka Hardness Tester, which is commonly used in the pharmaceutical industry, measures horizontal crushing strength by applying a load at 90° to the longest axis. This type of hardness tester is subject to two sources of inherent error: (1) the possibility of an incorrect zero and (2) a scale that does not accurately indicate the true load

applied. Other commercially used instruments include the Strong-Cobb, Monsanto and Pfizer hardness testers. Variations in crushing strength values obtained from different types of hardness testers are due to inaccuracies in instrument scale values, incorrect zero adjustment, and varying methods of applying the load. This necessitates calibration when comparing results from different types of testers. The physical dimensions and shape of the tablet may also contribute to the property of crushing strength.

The conventional methods of hardness testing for tablets also involve a subjective, operator error. The scale on the Erweka Hardness Tester is divided into segments of 0.25 kg units. Very often, the sample under evaluation may produce a reading that falls in between two divisions and it is up to the operator to decide upon the result. Consistency in reading the scale is very important. It is imperative that an accurate and reliable method of testing be used to evaluate tablet hardness.

There is reason to believe that the NIR signal would vary if the compression force used to manufacture tablets was changed. Many drug attributes, such as particle size, density, moisture content and surface area can have a direct effect on the compaction process. Current "wet" methods of analyzing tablets involve the indirect measurement of the mechanical strength of a tablet through destructive and time-consuming procedures. Many of these tests do not give an entirely accurate indication of how the tablet will behave during handling.

Intuitively, a harder tablet would have a smoother surface, thus changes in hardness (compression force) would be expected to alter the NIR spectra. Presumably, increased compression force causes a harder tablet to be smoother, thus causing less light scattering, leading to greater absorbance and a higher baseline[8]. However, not all of the tablets within a batch or between batches would have the same hardness properties. It is not known to what extent it would be feasible to develop standard procedures to quantify compaction force. The use of NIRS could provide an alternative method of quantifying the compaction properties of a tablet.

4

HYPOTHESIS TESTED IN THIS Ph.D. PROJECT

There is considerable interest in the area of quantification and prediction of tablet parameters using near-infrared spectroscopy (NIRS)[9,10]. If certain process parameters were altered, a change in the NIR spectra of the sample would be expected. It has been shown that the NIR signal is modified by changes in particle size, morphology and crystallinity.[11] For instance, a very rough surface of many small particles would enhance scattering and absorption of infrared radiation. Thus we can conclude that changes in compression force may have a substantial effect on the intensity of the NIR signal of a drug in a tablet.

The current literature contains no data that indicates to what extent the NIR signal is modified by the compression force used to manufacture the tablet. Questions remain as to what extent NIRS can be used for finished dosage forms. If a relationship between the compression force and the NIR spectra cannot be established, then NIRS would be of limited value.

The hypothesis to be tested in this research is that NIRS can be utilized for the nondestructive determination of tablet hardness in a manufacturing environment, and offers potential as an alternative to traditional methods of hardness testing. Although this project is limited to a small number of drugs and matrices, it is hoped that the general principles will be applicable to many or all drugs. Thus, it is hoped that the project will be of material value in advancing the possible use of NIRS for compendial standards.

REFERENCES

1) Massart, D. L., et al, <u>Data Handling in Science & Technology</u>, (New York: Elsevier Publishing, 1988), vol. 2, <u>Chemometrics: a textbook</u> , pp. 5.

2) United States Pharmacopoeia XXIII/National Formulary XVIII, USP Convention, Inc., Rockville, MD, Rand McNally, Taunton, Massachusetts, pp. 1838-1982 (1995).

3) Marshall, K. and Rudnic, E. M., "Tablet Dosage Forms", in <u>Modern Pharmaceutics</u>, second edition, G. S. Banker and C. T. Rhodes, editors, Marcel Dekker, Inc., New York, NY, pp. 355-425 (1990).

4) King, R. E., "Tablets, Capsules and Pills", in <u>Remington's Pharmaceutical Sciences</u>, Osol, A., et al, editors, Mack Publishing Co., Easton, Pennsylvania, pp. 1553-1584 (1980).

5) Gunsel, W. C., et al, "Tablets", in <u>The Theory and Practice of Industrial Pharmacy</u>, L. Lachman, Lieberman, H. A. and Kanig, J. L., editors, Lea & Febiger, Philadelphia, pp. 305-345 (1970).

6) Higuchi, T., et al, *J. Amer. Pharm. Assoc.*. Sci. Ed. 42, p. 194 (1953).

7) Brook, D. B. and Marshall, K., *J. Pharm. Sci.* 57, p. 481 (1968).

8) Kirsch, J. D. and Drennen, J. K., *J. Pharm. Biomed. Anal.*, 13, 1273-1281 (1995).

9) Duff, G. A. and Ciurczak, E. W., presented at PittCon, March (1993).

10) Ciurczak, E. W. and Pope, J. M. presented at PittCon, March (1993).

11) Olinger, J. M. and Griffiths, P. R. *Appl. Spectr.*, 47(6):687-694 (1993).

OBJECTIVES

The objectives of this research project were:

1) To evaluate the utility of Near-Infrared Reflectance Spectroscopy (NIRS) for the measurement of tablet hardness.

2) To describe the relationship between NIR signal and tablet compaction force or hardness.

3) To compare traditional "wet" methods of tablet analysis to NIRS methods and calibrate a NIRS instrument to tablet hardness.

4) To develop a NIRS method of quantifying the compaction properties of a tablet, which might replace or augment existing compendial tests and demonstrate the potential utility of the technique as an alternative to current methods of tablet hardness testing.

5) To examine the effect of tablet geometry and excipient matrix on the NIR/compression force relationship.

6) To evaluate any differences in NIR response due to scoring of a tablet.

7) To examine the utility of NIRS as a quality control mechanism in determining adherence to batch requirements for hardness.

SECTION II

Pharmaceutical Uses Of Near-Infrared Spectroscopy

Abstract

Near-infrared spectroscopy (NIRS) has been used extensively in the food and agricultural industries for the past twenty years. Recent technological advances have made NIRS an attractive analytical method for use in the pharmaceutical industry. NIRS has been shown to be useful as a qualitative and a quantitative method. A review of pharmaceutical applications of NIRS as well as quality control and regulatory issues is presented.

Introduction

In recent years, near-infrared spectroscopy (NIRS) has become an important analytical technique in industry. It has been used extensively in the food and agricultural industries for the determination of moisture, protein and starch content in grains[1]. The use of NIRS to solve pharmaceutical problems is increasing because of technological advances in NIR analytical instrumentation and computer software. Though the spectroscopy itself is not new, its applications and its use of chemometrics are new and innovative.

It is now recognized that NIRS offers significant advantages for a broad range of quantitative applications. NIRS is a rapid analytical technique that uses the diffuse reflectance of a sample at several wavelengths to determine the sample's quantitative composition. Sophisticated software stores calibration equations which correspond to the spectral features of a sample. In the pharmaceutical industry, NIRS has been shown to be useful in determining the percentage of active ingredient as well as in identifying specific tablet formulations. NIRS has potential as both a qualitative and quantitative method in the

pharmaceutical industry[2]. Other pharmaceutical uses include raw material identification[3] as well as monitoring content uniformity in powder mixing operations[4].

The NIR region of the infrared spectra was discovered by William Herschel in the early 1800's. It deals with the absorption of electromagnetic radiation in the range of 800 to 2500 nm[5]. The segment from 1100 to 2500 nm is known as the Herschel region, and is the range most often used in the analysis of pharmaceutical products.

NIR is more often used as a secondary analytical technique than a primary technique. When used as a primary technique, standards are prepared from reference materials, just as they are for other primary analytical techniques. A library of known spectra is created, then the instrument response is plotted for each sample, yielding a calibration curve. Sophisticated mathematical techniques are applied to the data via computer software, and the results may be calculated within a few minutes.

Historical Background

Near Infrared Spectroscopy (NIRS) has been used in the food industry for over twenty years to determine the components of feeds and grains. A major stimulus to interest in analytical applications of NIRS has been the success achieved in the analysis of agricultural products. Pioneering work by Karl Norris and coworkers at the United States Department of Agriculture (USDA) resulted in the development of methods for determination of components of forage crops. Norris is credited as with being the first to use NIRS to analyze chemically complex solid samples. He was also the first to utilize multivariate methods of analysis for quantifying the complex NIR spectra[6]. NIR reflectance spectra are widely accepted in the food and grain industry for the determination of protein, fat, moisture, and other factors. It is also used for compositional analysis of dairy products and meats.

Before 1990, most publications on NIRS concerned applications in the agriculture and food industries. NIRS research is ongoing in nearly all analytical disciplines. Since 1990,

more NIRS papers were published in the field of general chemistry than in the field of agriculture[7].

Many of the well known analytical meetings, such as PittCon, Federation of Analytical Chemistry and Spectroscopy Societies (FACSS), American Association of Pharmaceutical Sciences (AAPS) and Eastern Analytical Society (EAS) have recently included technical sessions and posters involving NIRS. In October, 1993, the Association of Analytical Chemists (AOAC) held a special symposium on Pharmaceutical Process Control and Quality Assessment by Non-Traditional Means. The conference, the first of its kind, consisted solely of topics relating to applications of NIRS in pharmaceutical manufacturing and the use of neural networks in drug fingerprinting.

It is anticipated that adoption of NIRS methods and related technologies will be explosive because they offer the potential for major improvements in quality control, record keeping, and control of product uniformity. However, the requirements for pharmaceutical quality control are more severe than in other fields. Analytical methods are required to be extremely accurate, specific and precise. In addition, since active components are often present in small quantities, the methods must be very sensitive. Absorption in the near infrared region is generally weak, which is an advantage for major components since no sample dilution is needed. However concentrations of minor components are often at or near the detection limit of the instrument[8].

Fundamentals And Instrumentation

Theory

NIRS deals with the absorption of electromagnetic radiation in the range of 700 to 2500 nm[9]. It is a rapid analytical technique, using the diffuse reflectance of a sample at several wavelengths to determine the sample's composition.

The absorption of infrared radiation is the result of transitions between molecular vibrational and rotational states (twisting, bending). Upon interaction with infrared radiation, portions of the incident radiation are absorbed at specific wavelengths. One of

the features of an infrared spectrum is that absorption in a specific region can be correlated to functional groups in the molecule (e.g., fingerprint region 7690-15,380 nm). Multiple vibrations occur simultaneously and produce a complex absorption spectrum that is uniquely characteristic of the functional groups that make up the molecule and of the overall configuration of the molecule.

The NIR region of the spectrum contains overtones and combination bands which are mainly due to hydrogen vibrations (OH, CH, NH). These overtones and combination bands are much weaker than the fundamental vibrations, so the molar absorptivities are between 10 and 1000 times smaller than those of the corresponding infrared bands. Due to the smaller molar absorptivities, it is possible to use undiluted samples and obtain remarkable depth of penetration into solid samples. The NIR range is adequate for studying most organic compounds.

There are some important differences between the near infrared region and other infrared (IR) spectrophotometry. Conventional laboratory IR instruments can operate in either the near, mid, and far IR regions, depending on the energy source and the detectors used. The wavelength range used for NIR is just beyond the visible end of the electromagnetic spectrum, from about 700 nm to 2500 nm. Other regions of the IR spectrum are referred to in terms of wavenumbers. Thus the near infrared region is from 14,300 to 4000 cm^{-1}, the mid infrared range is 4000 to 200 cm^{-1}, and the far infrared range is from 200 to 10 cm^{-1}.

Instrumentation

NIR instrumentation comprises four categories: monochromator, filter, selective diode, and Fourier-transform near-infrared (FT-NIR). Most laboratory NIR instruments depend on the dispersion-type monochromator for generating the monochromatic beam. Holographic gratings, which are produced by a photo etching process, have replaced the old mechanically grooved and replicated gratings. The newer gratings are easier to manufacture and cost less than their predecessors.

12

The energy sources used in most NIR instruments are long-lasting, tungsten-halogen lamps with quartz envelopes. A lamp which is used for 40 hours per week may be expected to last approximately 100 weeks. Detectors may be silicon photo voltaic sensors (360 to 1000 nm range) or lead sulfide (900 to 2600 nm range). Both types integrate diffusely reflected light.

NIR radiation is readily scattered by particles, making reflectance analysis an ideal technique for the analysis of solids. When the light from a NIR source is directed on a sample, both specular and diffuse reflected light are generated by the sample. However, only the diffuse reflected light contains the desired chemical information. An integrating sphere is used to segregate the diffuse and specular reflectance and to focus the diffuse reflected radiation onto the detector. A scanning grating monochromator between the source and the sample is used to obtain the desired spectrum.

Instrumentation developed for NIRS can be implemented either *at-line*, where a technician routinely extracts a sample from the process stream and transfers it to the instrument; *on-line,* where the sample is moved automatically to the instrument mechanical device; or *in-line*, where a fiber optic probe is place directly in the process stream.

Since ordinary glass is transparent in the NIR wavelength range, the optical components of NIR instrumentation don't have to be made of fragile materials. This lack of response by glass as well as quartz enables these materials to be used as transparent containers and also permits the use of optical fibers to transmit the spectra.[10] Glass cannot be used in instruments designed for the mid and far IR regions.

Marketed Equipment And Suppliers

Pharmaceutical Applications

NIRSystems of Silver Spring, Maryland (formerly Pacific-Scientific) supplies most of the NIR laboratory instrumentation used by the pharmaceutical industry. These instruments are scanning monochromators with interchangeable ("modular") sampling systems that include transmission, reflectance, and fiber optic models. NIRSystems manufactures a Rapid Content Analyzer™, which can be fitted with specially designed sample holders to analyze the contents of transdermal patches, tablets, capsules, and various pharmaceutical packaging. The company, a division of the Swedish company Perstorp Analytical, specializes in process and laboratory instrumentation primarily for food and agricultural, pharmaceutical, chemical, and polymer applications.

Process and Laboratory Applications

NIR instruments are manufactured for use in process, at-line, on-line and laboratory applications. Bran & Luebbe Analyzing Technologies, of Buffalo Grove, IL is a German-based company that supplies NIR instruments for use in raw materials release and identification. Buehler also supplies instruments for raw materials release and identification. Other manufacturers of NIR instrumentation include the following:

ABB Process Analytics, Lewisburg, WV

Axiom Analytical, Irvine, CA

Dickey-John, Auburn, IL

Guided Wave, Inc., El Dorado Hills, CA

Infrared Engineering, Inc., Waltham, MA

Katrina, Inc., Hagerstown, MD

LT Industries, Inc., Rockville, MD

Ocean Optics, Dunedin, FL

Perkin-Elmer, Pomona, CA

Trebor Industries, Inc., Gaithersburg, MD

Calibration

NIR instruments collect full spectra of a sample and use the statistical technique of chemometrics to infer physical and chemical parameters from a spectral scan. Chemometrics is a technique which links analytical information to properties other than concentration of chemical species. Chemometric methods are applied to the design and implementation of analyses so that the most efficient and informative experiments are carried out. They are also applied to the experimental results to enhance accuracy in interpretation. Calibration techniques, such as multiple linear regression (MLR), principal components regression (PCR) and partial least squares (PLS) may be utilized via the instrument software, and are linear functions of the reflectance of absorbance.

A calibrated mathematical model is created to calculate the parameters. Calibration involves taking spectra from a great many samples varying over the measurement range and also measuring the desired parameters. A rugged chemometric model for a complex sample may require thousands of samples taken from all possible situations, in and out of specification, that it may encounter. Samples selected for calibration must contain all the variables affecting the chemical and physical properties of the samples to be analyzed. In order to characterize each source of variation, it is recommended that 15 to 20 samples be run for each variable.

Because NIR bands are mixtures of overtones and combinations, the intensity of the absorbance at any particular wavelength does not necessarily respond linearly to a change in concentration. In the case of a mixture, band mixing may further disrupt any linear relationship between the intensity and the concentration. For these reasons, the simple application of Beer's Law ($A = ebc$, where A = absorbance, e = absorptivity, b = path length, and c = concentration) to NIR bands may not generate equations suitable for quantitation.

To avoid this problem, calibration equations are generated using multiple regression techniques. A series of samples representing the concentration range of interest are selected

and their spectra obtained. This group of spectra is divided into two groups: a calibration, or training set and a test, or prediction set. The spectra of the calibration set are used to correlate the constituent of known concentration with those of the prediction set.

The quality of the calibration equation is determined by a number of factors, including the multiple correlation coefficient (MCC), the F-value, and the standard error of estimation (SEE). These parameters are measures of the fit between the actual training set concentrations and the values predicted by the calibration equation. Ideally, it desirable to obtain a MCC value as close to 1.0 as possible, indicating 100 % correlation. The value of the SEE should be as minimal as possible, since it indicates the standard deviation of the differences between the actual and predicted values for the calibration set.

One of the major drawbacks of NIRS is the degree of difficulty in calibration of the instruments. A calibration is required for each constituent in the sample. The mathematical models used can depend critically on the character of the sample, its preparation, and operator technique. Laboratories that analyze many samples will be the most satisfied users of this technique; labs that analyze only a few samples a week may have trouble justifying the setup time.

Another issue is that of "transferability" of the calibration model, including transferable correlation coefficients, that would be usable on all instruments. A model built on extensive samples and spectra is much more readily transferable than one developed with only a few samples. Although some progress has been made in making calibration transfers between instruments, the situation is far from ideal, and careful monitoring is needed to obtain satisfactory results.

QC and Regulatory

The pharmaceutical industry's interest in NIR technology is in the production of better products at a lower cost, while the regulatory interest is in product control and uniformity and the detection of deviations from the approved formulations.

Validation of a NIRS method is necessary for acceptance by regulatory bodies. The error of the primary method must be well known. Accuracy, linearity, reproducibility, specificity, sensitivity, and robustness of the method must be demonstrated. The accuracy of the NIR results is obtained by comparison with the reference analytical method. Specificity of the method can be determined through the use of instrument software which qualifies the sample. Since sample placement is an important source of error, the same sample should be measured, removed and remeasured several times to determine reproduciblity. Robustness of the assay may be tested by varying the operating conditions.

The major pharmacopoeias allow manufacturers to use alternative analytical methods for compliance testing. However, these alternatives must be validated in order to demonstrate that they arrive at the same conclusions as the conventional methods. Official approval of a NIR method requires acceptable performance using different instruments with the same samples. This may be difficult because there is no agreed upon model for instrument calibration; each company uses its own model and each type of sample requires a different model. It is usually necessary to customize a model to a particular sample and instrument. It may be possible to satisfy in-house quality control specifications for product consistency within one facility. However, these results must be reproducible at other manufacturing sites.

The United States Food and Drug Administration (U.S.F.D.A.) recently approved (May 1992) the use of a NIRS method in place of compendial methods for moisture content, identification and assay for ampicillin trihydrate[11]. This was the first time the U.S.F.D.A. approved the use of a NIRS method for release testing of a bulk pharmaceutical product for human consumption. The method was developed at Gist-brocades bv, a Netherlands-based pharmaceutical company. Validation studies using the NIR method showed that it offered faster and more accurate results, eliminated the use of solvents, and produced no waste products. This approval is likely to be followed by other computer-based technologies which will rapidly come into use in the pharmaceutical

industry. It is anticipated that "adoption of these technologies will be explosive because they offer the potential for major improvements in the control of product uniformity and quality and better record-keeping..." at a significantly lower cost[12].

Canada's pharmaceutical regulatory agency, the Health Protection Branch (HPB), recently (December, 1993) approved the use of a NIR method for identification of raw materials and packaging components developed at Merck Frosst Canada, Inc. to replace compendial methods of identification[13]. The submitted method utilized a database of reference spectra of 185 different raw materials and packaging components. It contained examples of successful identification and differentiation between HDPE (high-density polyethylene) and LDPE (low-density polyethylene) using NIRS.

Pharmaceutical Applications

Moisture Determination

The classical methods for water determination are based on weight loss by drying or on Karl-Fischer Titration. The presence of water is indicated by a NIR absorption band in the 1900 to 2000 nm region due to the combination of fundamental bending and stretching vibrations of the OH bond. Moisture levels in grains[14] have been measured using the OH absorption at 1950 nm. The absorption maximum and peak shape depend on the degree of hydrogen bonding occurring within the environment where the water is located. The stronger the hydrogen bond, the longer the wavelength of the NIR absorption maximum.

The physical and chemical properties of water and their functions of temperature were determined by NIRS by Lin and Brown[15]. Properties determined included density, refractive index, dielectric constant, surface tension, ionization constant, as well as various thermal and thermodynamic properties. It was concluded that NIRS, when used with multivariate regression, can be used as a simple, fast and universal approach for the simultaneous determination of the physical and chemical properties of water.

NIR methods for the determination of water in freeze-dried products were developed by Jones, et al[16]. The authors were able to analyze 40 samples per hour using this method, and found good agreement (correlation coefficients up to 0.95) between NIR predicted values and the Karl Fischer reference values. It was concluded that the NIR method provided more accurate and precise data than Karl Fischer titration since it avoided the need to open the vials and risk contamination from atmospheric moisture.

Kamat, et al[17] reported a method of determining residual moisture in lyophilized sucrose through the intact glass vials. The peaks attributable to water appeared at 1450 and 1940 nm. Results indicated a water concentration in the range of 0.72 to 4.74 % with an RSD of 6.7 %. A prediction error of 0.27% was reported with a single scan.

Sinsheimer and Poswalk[18] measured the 1900 nm moisture band in solids, solvent systems, and a micellar system of dioctyl sodium sulfosuccinate (DSS). For solvent systems, they concluded that the range of conformity to Beer's Law is limited to the lower concentrations in weakly basic solvents.

Boehm and Liekmeier[19] studied the moisture content of solid dyes and organic solvents. They identified three working ranges for quantitative water determination (Table 1). Nonpolar, organic solvents, such as carbon tetrachloride, were analyzed at 2400 nm, the most sensitive band. An indigo dye was analyzed at the 1900 nm wavelength.

Table 1. Working ranges for quantitative water determination with NIRS [19]

Absorption bands (nm)	Working range for quantitative analysis
1400	0.1 to 5 %
1900	0.02 to 0.5 %
2700	10 to 200 ppm

NIRS was applied by Corti, et al[20] to the analytical control of the active ingredient and water content of tablets of ranitidine chlorhydrate. The maximum acceptable water content for ranitidine tablets was 2 %. The reference value using the Karl Fischer (reference) method was 1 %. Comparison of NIRS values to Karl Fischer values indicated higher errors occurring with samples having a water content of less than 1 % (by reference method). None of the NIRS values exceeded 2 %.

Solid dosage forms

Current methods of tablet analysis are destructive in nature, and do not allow for 100% quality control testing. NIRS is a non-invasive and non-destructive method which, in theory, would allow 100% inspection of every tablet. It is theoretically possible to determine the amount of drug in every tablet in every batch, and check to ensure that a tablet is placed in its correct container. In this respect, NIRS is attractive from both a quality control and a regulatory perspective. In addition to being a non-destructive method, other advantages of NIRS over other quantitative methods include relative ease of sample preparation and fast analysis.

Several authors have reported methods for the identification of active components in tablet[21,22] and liquid[23] dosage forms, as well as for raw material identification[24].

A general method for the rapid verification of identity and content of solid dosage forms was devised by Ryan, et al[25]. The authors evaluated the use of mid (MIRS) and near infrared spectrometers to analyze tablet and capsule dosage forms containing either lovastatin, simvastatin, enalapril, finastride, or placebo in the range of 0.2 to 40 mg of drug. The minimum amount of active drug (in the presence of excipients) detected by both methods was 1% (w/w). It was reported that NIRS could not allow for differentiation between an α-hydrogen atom on the lovastatin ester group and an additional α-methyl group in simvastatin. However, the MIRS method was able to distinguish between the two structures, since it is well suited for structural elucidation and identification of compounds.

21

Lodder and Hieftje[26] described a NIRS method of analysis of intact aspirin tablets. The method involved the use of a double-reflecting aluminum sample holder which preserved the integrity of the tablet during the analysis.

Lodder, et al[27] reported a NIRS method for the detection of adulterated nonprescription drugs. This work was triggered by the 1982 incidents[28]. of potassium cyanide-laced Extra Strength Tylenol® capsules in the Chicago area that resulted in seven deaths The adulterants tested included potassium cyanide, sodium cyanide, ferric oxide, aluminum metal shavings, arsenic trioxide, and sodium fluoride . The detection limit for potassium cyanide was 2.6 mg, or two orders of magnitude less than the lowest reported lethal dose in humans (2.941 mg/kg, or 306 mg for a 70 kg person). One shortcoming of a NIRS method in this situation is that it is not possible to predict what contaminant might be placed in a particular product. The authors' results indicated that a variety of contaminants could be detected in intact capsules by using four wavelengths.

Drennen and Lodder[29] developed a non-destructive NIRS assay for determination of the degradation products for intact aspirin tablets. The authors concluded that the salicylic acid formed by hydrolysis of aspirin significantly changed the spectrum of aspirin tablets after exposure to moisture and that this correlation to salicylic acid resulted from salicylic acid formation rather than a correlated process. The mass of salicylic acid formed by hydrolysis in intact aspirin tablets was measured by NIRS with a reported error of 0.04% of the total tablet mass (400 ppm).

Ciurczak[30] reported a powder mixing study which utilized NIRS to check for homogeneity. For this study, aspirin and vitamin B12 were the active ingredients. Aliquots were taken at various times and analyzed via NIRS. A comparison was made between visual matching, spectral matching and principal component analysis. Visual matching provided an approximation, while spectral matching (using computer software) gave somewhat better results. Principal component analysis was the more rigorous method, in that it was able to distinguish between the penultimate and the true final mix.

The author suggested that the use of NIRS could save many hours of analysis time in a routine mixing study.

Ciurzcak, et al[31] described a method of determination of the mean particle size of pure, granular substances. The method is based on the theories of reflected light, namely the Kubelka-Munk equation,

$$\frac{(1 - R)^2}{2R} = \frac{K}{S}$$

where K is the absorption coefficient and S is the scattering coefficient. Reflectance, R , increases as the mean particle size decreases, while R decreases as the absorptivity increases. Graphs were constructed from $\log \frac{1}{R}$ values and used to assess the particle size of pure samples of ascorbic acid, aspirin, and aluminum oxide. The absorbance values for each spectrum at 1658 nm (the major peak) were plotted against the absorbance values at 1784 nm (the baseline), resulting in a linear plot with a correlation coefficient of 0.99999. The authors concluded that this method could be used as a quality control tool when new materials are received.

The suitability of NIRS as an alternative to several compendial methods has been demonstrated by Plugge and Van Der Vlies [32,33] with ampicillin trihydrate. Their work led to the U.S.F.D.A.'s acceptance of NIRS as an official method of testing for the identification, water content and assay of ampicillin trihydrate. The NIR method was compared to a hydroxylamine colorimetric method as described in the Code of Federal Regulations (CFR). Other workers[34,35] have reported the development of NIR methods for quality control in pharmaceutical analysis, but this was the first time that a regulatory agency approved the use of a NIR method for release testing of a bulk pharmaceutical product for human consumption. The U.S.F.D.A. has accepted NIRS as the official method for determination of the lincomycin content in an agricultural mixture containing soybean meal [36], but until 1992 there had not been any approved pharmaceutical uses.

Liquid Dosage Forms

Dubois, et al[37] reported a method of determination of five components in a liquid formulation of otic drops. The product contained two active components (phenazone and lidocaine), two solvents (ethanol and glycerol) and one antioxidant (sodium thiosulfate). Results indicated that the NIRS method was well suited to the quantitation of both of the solvents and one of the active compounds (phenazone). The concentration of lidocaine in the formulation (1 %) was at the detection limit of the instrument, thus the accuracy of the method was insufficient.

Kumar and Raghunathan[38] used NIRS to examine the nature of the water pool formed in the reverse micellar system, lecithin/nonpolar solvent/water. The three nonpolar solvents used in the study were benzene, carbon tetrachloride and cyclohexane. The NIR spectra indicated the presence of two types of water in the lecithin reverse micellar solutions. One was water-dispersed in the organic phase and the other was water-solubilized in the reverse micellar interior. Results revealed that the amount of water present in the organic phase was negligible at all water concentrations in all three solvents.

Grant, et al [39] investigated the quantitative analysis of solutions containing various concentrations of sodium hydroxide, sodium chloride and sodium carbonate using NIRS. It was observed that the addition of these salts caused changes in the absorption spectrum of water, even though sodium carbonate and sodium chloride do not themselves absorb in the NIR region.

Other Possible Uses

The hydroxyl value is an indicator for the stages of an esterification reaction. Hansen reported a NIRS method by which the shifting of the hydroxyl value of a reaction could be monitored [40]. This work suggests that it may be possible to monitor the degradation of a reaction, and possibly be useful in stability testing of raw materials.

Tudor, et al [41] investigated the use of near-infrared Fourier-transform (FT) Raman spectroscopy in the molecular structural analysis of drugs and biomedical polymers. The

authors developed a technique by which the concentration of a drug within a polymer vehicle could be determined over a wide drug concentration range. The FT-Raman spectrum of diclofenac dispersed in a sodium alginate matrix was monitored, as well as the spectrum of the alginate alone. It was concluded that this method illustrated the potential for quantification of degradation kinetics in certain polymers using FT Raman infrared spectroscopy.

Conclusion

Recently, there has been a large increase in the amount of research in the near infrared region. NIRS has been shown to be a valuable tool for a number of important applications. It has gained official acceptance in the food and agricultural industries, and is now becoming more recognized in the pharmaceutical industry. Specially designed instrumentation for use in the pharmaceutical industry has become more widely available, and is made more powerful by software improvements.

References

1) Osborne, B. G. et al, in "Near Infrared Spectroscopy in Food Analysis", Longman Scientific & Technical, UK, pp. 2 (1986).

2) Lafford, T. A., et al, *Analyst* 117(10) p.1543 (1992).

3) Gemperline, P. J. and Webber, L. D., *Anal. Chem.* 61, 138 (1989).

4) Ciurzcak, E. W., *Pharm. Tech.* 9, 140 (1991).

5) Willard , H. H. et al, "Infrared Spectroscopy", Chapter 11, in, Instrumental Methods of Analysis, 7th edition, Wadsworth Publishing Company, Belmont, California, p. 287 (1988).

6) McClure, W. F., *Anal. Chem.* 66(1), 43A (1994).

7) ibid.

8) Dubois, P., et al, *Analyst* 12(112), 1675 (1987).

9) Willard, H. H., et al, "Infrared Spectroscopy", Chapter 11, in, Instrumental Methods of Analysis, 7th edition, Wadsworth Publishing Company, Belmont, California, p. 287 (1988).

10) Corti, P., et al, *Farmaco* 48(1), 3 (1993).

11) Plugge, W. and Van der Vlies, C., *J. Pharm. Biomed. Anal.* 11(6), 435 (1993).

12) Association of Analytical Chemists, Conference Publication, November (1993).

13) Carroll, J. E., *DatelinePerPharma* 1(1), 1 (February 1994).

14) Norris, K. H. and Hart, J. R., Proceedings of the 1963 International Symposium on Humidity and Moisture: Principles and Methods of Measuring Moisture in Liquids and Solids, Vol. 4., Reinhold, New York, p. 19 (1965).

15) Lin, J. and Brown, C. W., *Appl. Spectr.* 47(10), p. 1720 (1993).

16) Jones, J. A., et al, "Development and transferability of near infrared methods for determination of moisture in a freeze-dried injection product", presented at the "Fourth International Symposium on Pharmaceutical and Biomedical Analysis", Baltimore, MD, (April 1993).

17) Kamat, M. S., et al, *Pharm. Res.* 6(11), 961 (1989).

18) Sinsheimer, J. E. and Poswalk, N. M., *J. Pharm. Sci.* 57(11), p. 2007 (1968).

19) Bohme, W. and Liekmeier, W., *Int. Labmate* 14(1) (1986).

20) Corti,P., et al, *Pharm. Acta Helv.* 65, p. 28 (1990).

21) Ciurczak, E. W. and Maldacker, T. A., *Spectroscopy* 1(1), p. 36 (1986).

22) Corti, P., et al, *Pharm. Acta Helv.* 65, p. 28 (1990).

23) Ciurczak, E. W and Torlini, R. P., *Spectroscopy* 2(3), p. 41 (1987)

24) Ciurczak, E. W, et al, *Spectroscopy*, 1(7), p. 36 (1986).

25) Ryan, J. A., et al, *J. Pharm. Biomed. Anal.* 9(4), p. 303 (1991).

26) Lodder, R. A., and Hieftje, G. M., *Appl. Spectr.* 42(4), p. 556 (1988).

27) Lodder, R. A., Selby, M. and Hieftje, G. M., *Anal. Chem..* 59(15), p. 1921 (1987).

28) Church, G. J., *Time* 120, p. 16 (October 18, 1982).

29) Drennen, J. K. and Lodder, R. A., *J. Pharm. Sci.* 79(7), p. 622 (1990).

30) Ciurczak, E. W., *Pharm. Tech.*, 15(9), p. 140 (1991).

31) Ciurczak, E. W., *Spectroscopy*, 1(7), p. 36 (1986).

32) Plugge, W. and Van Der Vlies, C., *J. Pharm. Biomed. Anal.* 10(10-12), p. 797 (1992).

33) Plugge, W. and Van Der Vlies, C., *J. Pharm. Biomed. Anal.* 11(6), p. 435 (1993).

34) Lonardi, S., et al, *J. Pharm. Biomed. Anal.* 7:, p. 303 (1989).

35) Kamat, M. S., et al, *Pharm. Res.* 6, p. 961 (1989).

36) Whitfield, R. G., *Pharm. Manuf.* 4, p. 31 (1986).

37) Dubois, P., et al, *Analyst* 12(112), p. 1675 (1987).

38) Kumar, V. V. and Raghunathan, P., *Lipids* 21(12), p. 764 (1986).

39) Grant, A., et al, *Analyst* 114(7), p. 819 (1989).

40) Hansen, W. G., *Appl. Spectr.* 47(10), p. 1623 (1993).

41) Tudor, A. M., et al, *J. Pharm. Biomed. Anal.* 8(8-12), p. 717 (1990).

Addendum to Manuscript I

The importance of NIRS may be affirmed by its increasing appearance in the literature. NIRS has been used to measure such properties as sample composition and identification[1], moisture content[2,3], content uniformity[4], homogeneity of mixing[5], and degradation products[6]. Other reports[7] of pharmaceutical uses of NIRS describe a method to screen tablets in the development of a new coating process. Since reflective techniques are sensitive to surface texture[8,9], NIRS is also suitable for particle size measurements. A comprehensive review was written by Weyer[10], citing 164 NIRS references in agriculture and chemical processing. Workman[11] outlined 156 references to the use of NIR for process applications, including pharmaceutical uses. McClure[12] described NIRS instrumentation in great detail and discussed several engineering and agricultural applications.

Since 1990, NIRS has received more attention from the pharmaceutical industry, as noted by several reviews describing useful applications. Mac Donald and Prebble[13] presented an overview of NIRS in the pharmaceutical industry, and included results of their own experiments with identification, blending, and water determination. Aldridge, et al[14] described a NIRS method for nondestructive identity testing of blister packed tablets. The NIR method required only seven minutes to analyze ten tablets, compared to only 40 tablets per day using conventional TLC.

In the food industry, NIRS has been used for the qualitative determination of hardness[15,16] of wheat kernels. Wheats are classified as hard or soft according to their milling performance. Hard wheats produce larger, more angular particles during the grinding process than soft ones. This angling occurs because hard wheats have cleavage planes associated with the cell walls in the endosperm; the cells come away more cleanly and remain more intact[17]. Soft wheats fracture at random, frequently across cell walls, resulting in fragments containing mainly starch. NIRS can be used to discriminate hard

and soft wheat kernels through differences in particle size of ground meal. The ground meal from the hard varieties reflects less energy than soft ones ground in the same fashion[18].

Calibration Transfer Between Instruments

In a recent commentary stemming from the 1995 American Chemical Society Meeting at the short course on practical NIR (the first NIR short course offered by the A.C.S.), consultant Emil Ciurczak stated that " it is more important for instruments to perform in a reproducible manner than for them to represent absolute values of some mythical standard."[19]   In other words, Ciurczak stressed that it is doesn't matter that a single wavelength of one instrument may be 2 nm off from an absolute standard, as long as it always identifies that point the same way every time. The National Institute of Standards and Technology (NIST) in Gaithersburg, MD has no single standard available for wavelength accuracy in transmission NIRS. A reflectance standard exists but has not yet been widely accepted. The reflectance standard is based on polystyrene, however, and consistency in batches of such polymers has not yet been achieved. At this time, the responsibility of establishing proper calibration is on the manufacturer of the instrument.

Bouveresse and Massart[20] described a modified algorithm for standardizing NIR spectrophotometric instruments. The authors used locally weighted regression, which gives more weight to the standardization samples which are in the same spectral intensity range as the samples to be predicted and less weight to the samples farthest from this range. This approach enabled standardization of samples of a different nature.

Standards for Quantitative NIR Analysis

The American Society for Testing and Materials (ASTM) recently published an official document[21] providing a guide to spectroscopists for the multivariate calibration of infrared spectrometers. The scope of the publication, entitled "Standard Practices for Infrared, Multivariate, Quantitative Analysis", includes the use of multivariate

calibrations for the determination of physical or chemical characteristics of materials. The practice applies to the near-infrared (780 to 2500 nm) through the mid-infrared (4000 to 400 cm-1) spectral regions. This document is the first official standard for the application of chemometric multivariate analysis to near-IR and IR instruments[22].

Validation of NIRS Methods

Validation aspects of a NIRS method are similar to those of other analytical methods. The principal elements of ensuring linearity, accuracy, selectivity and reproducibility of a quantitative method are required. The validation process determines the amount of error due to variation between the values in the population. It is used to check for the existence of a relationship between the calibration set and the validation set.

Calibration models are developed by regression analysis to determine the relationship between calibration set spectra and the constituent value of interest for those samples. Partial Least Squares (PLS) is a useful type of regression for small populations and involves application of a series of simple linear regressions. Using cross validation in a PLS regression, the sample population is separated into several segments, usually four, then one segment is validated as an unknown against the remaining segments. The segment that is validated is sequentially moved through the entire population until all the samples in the population are fully validated. The procedure results in the calculation of the mean square error of cross validation (MSECV) for the population. In other words, the program will determine the number of factors (a factor is equivalent to a sample in the file) required to characterize a sample set without overfitting it. Overfitting the population would render the calibration incapable of predicting analytical results on samples outside the population.

When cross validation is performed on a sample set that required (e.g.) six factors, four lines result on the plot of MSECV versus factors. The number of factors that will overfit the spectra is indicated at the point on the plot where the line points upward. The ideal number of factors will be displayed to the left of that point, at the

factor where the plot is closest to the x-axis. Of the values reported in the regression results, a critical value to examine is the ratio of the current MSECV to the minimum MSECV. It is recommended that this ratio be as close to 1.25 (not 1.00 or equal to the lowest value) as possible to determine the correct number of factors. This is in contrast to other regression procedures where the point of highest correlation is the value of interest[2,3].

Manufacturers of NIRS instrumentation include software packages which allow the operator to predict analytical results on data files that have been stored, thus allowing for validation of the calibration equation, and testing for errors in the developed calibration. This enables calibration equation performance testing in terms of precision. If the laboratory values relevant to the sample spectra were entered into the computer file, performing the prediction function on the data results in the calculation of predicted results and residual values. This may be followed by a statistical summary (see Appendix 1 for definition of terms used in statistical summary report) which includes bias, standard deviation of differences, root mean square, and standard error of bias, as well as slope and intercept information. Using this information, the operator can determine if there is a bias or slope difference between a calibration set of samples, or a slope difference between a calibration set of samples and a validation set. Slope variations indicate that the calibration samples and the prediction samples are quite different, more than just a bias offset, and that this calibration is not applicable to this type of sample. It is not acceptable practice to make a slope adjustment to a calibration.

A bias may be observed when the NIR instrument values are consistently higher or consistently lower than the laboratory values. This translates to a shift in the Y-intercept of a plot of NIR versus lab values (the slope may not be affected). The ideal situation is when this plot shows points scattered evenly along a line that is 45° to the x-axis, thus zero bias. A bias adjustment is required when the value for the bias is more than double the standard error of the bias in the positive or negative direction.

The main problem associated with using empirical models is that they are based on correlation rather than causation[24]. Construction of these models involves finding measurements that simply correlate well with an analyte. The validity of these models depends the ability of the calibration set to accurately represent the samples in the prediction set. A good rule of thumb is to make sure that any type of variation observed in the prediction set also varies in the calibration set over the same range as the variation occurring in the prediction set[25]. Usually, the complete prediction set is not available at the same time as the creation of the calibration set, and unusual phenomena may be associated with some of the prediction samples.

One source of prediction error is the inherent accuracy and precision of the reference method used. If the reference method produces erroneous analyte values that are consistently high or low, this bias will be reflected in the prediction results. Imprecise (but accurate) reference values may also increase prediction error, in a nonsystematic way. Thus it is very important to minimize the errors in the reference values that are to be used to create an empirical model.

Other sources of prediction error relate to the reproducibility, stability and repeatability of the NIR instrument. Reproducibility (precision) is validated by making repeated measurements of the same sample, removing it between runs. Small changes in conditions may occur due to multiple insertions of a sample onto the instrument. Stability refers to similar changes that may occur over a longer period of time (hours or days). Repeatability refers to the instrument's ability to generate consistent measurements under the same conditions (without removing the sample from the instrument), over a relatively short period of time (seconds or minutes). All of these factors must be addressed to assure the validity of the NIR calibration model.

Current NIR News

In 1995, the European Patent Office[26] granted a patent to Dr. Paul Aldridge of Pfizer Central Research in Groton, Connecticut for an Apparatus for mixing and detecting

32

on-line homogeneity. This patent involves the use of a NIR fiber-optic probe interfaced on-line with a blender. Sekulic, et al[27] recently described the use of this Apparatus for on-line monitoring of powder blend homogeneity. An 8-quart twin-shell V-blender was interfaced with a fiber optic probe at the axis of rotation. Spectra were collected at prescribed intervals, and data analysis was performed by a series of software packages. Variability in the NIR spectra as a function of time was measured, and it was shown that this variability reached a minimum sooner than traditional blending times suggest.

Official approval of a NIR method as an alternate method for identification and assay of tablets was granted in June 1995 to Glaxo Wellcome in the United Kingdom[28]. The company received official approval from the Medicines Control Agency (MCA) for the use of NIR as an alternate method for identification and assay of Zovirax® 200 mg tablets. The MCA is the agency within the U. K. Department of Health which is responsible for licensing of medicinal products, inspection and enforcement. The quantitative calibration was developed in the Analytical Development Laboratories and is a four-factor PLS equation.

Update on manufacturers of NIRS instrument hardware and software

An extensive product review of recent NIR technology was published by Noble[29]. Enormous progress has been achieved in chemometrics and computing power, making many new applications possible. There are over twenty manufacturers of NIR spectrophotometers in the United States. There are many more vendors of sampling components and software packages for data analysis. Multivariate calibration methods are essential for quantitative NIR analysis. Most instrument vendors offer software that is capable of using multivariate algorithms, such as partial least-squares (PLS), multilinear regression (MLR) and principal component analysis (PCA). Some of the vendors also license software from third-party vendors of statistical analysis software. The best known third-party packages include *Pirouette* (Infometrix, Seattle, WA),

MATLAB (The Mathworks, Inc., South Natick, MA), *LabCalc* and *Grams 386* (Galactic Industries, Salem, NH).

Conclusions

Although the use of NIRS methods in the pharmaceutical industry is increasing, many scientists are reluctant to accept it as a viable alternative to current testing methods. The process of developing a calibration and selecting a model is challenging project, as is the validation of the method. Traditionally, pharmaceutical scientists are not trained in chemometric methods, and this remains a stumbling block to the understanding and implementation of NIR technology. Instrument manufacturers and software vendors are aware of this, and now design their products in more user-friendly ways than before. It will be several more years before sufficient data is published to convince the skeptical that NIRS is a usable and extremely useful technology.

References

1) Corti, P., et al, *Pharm. Acta Helv.*65, 28 (1990).

2) Kamat, M. S., et al, *Pharm. Res.* 6(11), 961 (1989).

3) Jones, J. A., et al, "Development and transferability of near infrared methods for determination of moisture in a freeze-dried injection product", presented at the "Fourth International Symposium on Pharmaceutical and Biomedical Analysis", Baltimore, MD (April 1993).

4) Ryan, J. A., et al, *J. Pharm. Biomed. Anal.* 9(4), 303 (1991).

5) Ciurczak, E. W., *Pharm. Tech.* 15(9), 140 (1991).

6) Drennen, J. K. and Lodder, R. A., *J. Pharm. Sci.* 79(7), 622 (1990).

7) Buchanan, B. R., et al, *Pharm. Res.* 13(4), 616-621 (1996).

8) Kubelka, P., *J. Opt. Soc. Am.* 38, 448 (1948).

9) Kortum, G., in Reflectance Spectroscopy: Principles, Methods & Applications, Springer-Verlag, New York (1969).

10) Weyer, L. G., *Appl. Spectr. Reviews* 21(1&2), 1-43 (1985).

11) Workman, J., *J. Near Infrared Spectrosc.* 1, 221-245 (1993).

12) McClure, W. F., *Anal. Chem.* 66(1), 42A-53A (1994).

13) MacDonald, B. F. and Prebble, K. A., *J. Pharm. Biomed. Anal.* 11(11), 1077-1085 (1993).

14) Aldridge, P. K., et al, *Appl. Spectr.* 48(10) 1272-1276 (1994).

15) Osborne, B. G. and Fearn, T., *J. Sci. Food Agric.* 34, 1011-1017 (1983).

16) Windham, W., et al. *Cereal Chemistry* 70, 662-666 (1993).

17) Osborne, B. G. and Fearn, T., Near Infrared Spectroscopy in Food Analysis, Wiley & Sons, Inc., New York, pp. 117-161 (1986).

18) ibid, pp. 104-116.

19) Ciurczak, E. W., *Spectroscopy* 10(9), 19-20, 1995.

20) Bouveresse, E. and Massart, D. L., *Anal. Chem.*, 67(8), 1381-1389, 1995.

21) American Society for Testing and Materials, "Standard Practices for Infrared, Multivariate, Quantitatibe Analysis", (E 1655), pp. 1-25, 1995.

22) Workman, J. and Brown, J., *Spectroscopy*, 11(2), 48-51, 1996.

23) Reference Manual for Near Infrared Spectral Analysis Software (NSAS) Version 3.30 a, NIRSystems, Inc./Perstorp Analytical Co., Silver Spring, MD, pp.3-1 to 3-62, 1995.

24) Thomas, .E. V., *Anal. Chem.*, 66(15), 795A-804A, 1994.

25) ibid.

26) Aldridge, P. K., Pfizer, Inc. Apparatus for mixing and detecting on-line homogeneity. European patent Publication 0 631 810 A1, 1993.

27) Sekulic, S. S., et al, *Anal. Chem.*, 68(3), 509-513, 1996.

28) Entrop, P., *Dateline:Pharma*, a Perstorp Analytical publication, October 1995.

29) Noble, D., *Anal. Chem.*, 67(23), 735A-740A, Dec. 1, 1995.

<center>**Manuscript II**</center>

A Feasibility Study of the Effect of Compression Force on the Near-Infrared Spectra of Tablets

1.1   Abstract

The primary objective of this research was to evaluate the utility of near-infrared reflectance spectroscopy (NIRS) for measuring tablet hardness. Flat, white tablets with no orientation (scoring, etc.) were manufactured on a Stokes Rotary Tablet Press. The formulations evaluated were: 1) placebo matrix (microcrystalline cellulose and magnesium stearate), 2) hydrochlorothiazide (HCTZ) 15 % with placebo matrix, and (3) chlorpheniramine maleate (CTM) 2 % with placebo matrix. Five or six levels of tablet hardness (2 to 12 kg) were used for each formulation. Tablets were evaluated by conventional USP testing methods for weight, hardness, thickness and friability. NIR reflectance analysis was performed on 20 tablets from each batch using a NIRSystems Rapid Content™ Analyzer. Tablet evaluations showed hardness variation of 5-10% and weight variation of < 1 %. NIR analysis of these tablets showed an upward shift in the raw spectra with increasing hardness. Softer tablets had more variable spectra. Principal component analysis correctly (by distance) identified tablets that were two hardness units apart. Results confirmed that there is a difference in raw NIR spectra due to changes in tablet compression force.

1.2 Introduction

Near-infrared reflectance spectroscopy (NIRS) has received widespread attention as a nondestructive method for the rapid measurement of the composition of many products[1,2,3]. NIRS determines these parameters through the measurement of diffuse reflectance. Diffuse reflectance is light that has been transmitted through a portion of the sample and emerges from the illuminated surface due to internal light scattering[1]. This type of reflectance is affected by the absorbance and light-scattering properties of the product.

Current methods of tablet hardness testing, drug identity and content are destructive in nature and may not always give an accurate representation of the batch being evaluated. NIRS is a noninvasive and nondestructive method that, in theory, would allow for 100% testing. In this respect, NIRS is attractive from both a quality control and a regulatory perspective.

The purpose of this study was to investigate the feasibility of NIRS for the measurement of tablet hardness.

1.3 Experimental

1.3.1 Tablet Manufacture

Half-inch round, flat-faced tablets were manufactured using one of the sixteen stations of a Stokes B-2 Rotary Tablet Press. Hydrochlorothiazide and chlorpheniramine maleate were the active components chosen for the formulations, in addition to microcrystalline cellulose (Avicel® PH102, FMC Corporation) and magnesium stearate. Both are relatively low-dosage drugs and would thus not be expected to interfere with the process of direct compression. The components of each formulation (Table 1) were accurately weighed on a Mettler balance for a batch size of one kilogram. Each blend was mixed for ten minutes in a Turbula mixer, then transferred to a labeled plastic bag to await compressing.

Table 1. Formulations used in feasibility study.

Formulation	Components	Percent
placebo blend	Avicel® PH102	99.5 %
	magnesium stearate	0.5 %
HCTZ 15%	hydrochlorothiazide	15.0 %
	Avicel® PH102	84.5 %
	magnesium stearate	0.5 %
CTM 2%	chlorpheniramine maleate	2.0 %
	Avicel® PH102	97.5 %
	magnesium stearate	0.5 %

Tablet hardness was varied to achieve a range of 2 to 12 kilograms (kg) as measured by the Erweka Hardness Tester. (Note: 1 kg is equivalent to 1 kilopon, a commonly used hardness unit). Approximate batch size was 300 tablets for each of five to six levels of hardness.

Tablets were evaluated for weight, hardness, friability and thickness. Twenty tablets from each batch were weighed using a Mettler balance. The thickness of five tablets from each batch was measured using an Ames Dial Comparator (B. C. Ames Co., Waltham, MA, Model No. 3). Thickness data was converted from inches to millimeters using Microsoft® Excel. The conversion equation was: (25.4 mm/in) x (# Ames lines x 100) x (0.001 inch/line).

Hardness testing was performed on twenty tablets from each batch using an Erweka Hardness Tester. Hardness data were subject to a two-sided T-test using Minitab® (Version 8, Addison-Wesley Publishing Co.) to rule out equal means between hardness levels. Randomness of the sample selection process was tested by applying a nonparametric runs test. Hardness values were expressed in kilograms.

Friability testing was performed using a Roche Friabilator. Twenty tablets from each batch were weighed on a Mettler balance before and after undergoing four minutes (100 revolutions) in the friabilator. The weight difference was calculated and expressed in terms of percent loss due to abrasion or fracture.

1.3.2   Near-Infrared Analysis

A NIRSystems Rapid Content Analyzer® Model 5000 was used for the analysis of tablet samples. This instrument consists of a reflectance detector module and a monochromator module (Figure 1) The reflectance module consists of detectors sited at a 45° angle to the light incident on the sample (Figure 2), which reduces the effect of specular, or stray, energy reaching the detectors. The reflectance detector module is equipped with a sample holder specifically designed to hold tablets. Figure 3 is a schematic drawing of the sample holder, which includes the iris. The lever shown at the bottom,

right corner in the diagram is used to control the width of the iris, thus centering a tablet of practically any diameter on the detector surface.

The instrument was interfaced with a Compaq Presario personal computer installed with NSAS™ (Near-Infrared Spectral Analysis Software) version 3.13 and IQ^2™ (Identify, Qualify and Quantify) Chemometric Software version 1.13 (NIRSystems, Silver Spring, MD). A color monitor and dot matrix printer were also part of the system. PrintAPlot® software version 3.0 (Insight Development Corporation, San Ramos, CA) was used to create color output files for spectral plots. Plots were downloaded to a laser printer in a remote location.

NIR reflectance parameters were set at 32 scans per sample in the range of 1100 to 2500 nm. A ceramic (Coor's Standard) reference scan was taken before each set of samples. Single tablet NIR scans were run on 20 samples from each batch of tablets. The sample to be measured was placed directly above the detector surface and centered with the iris. Before positioning each sample, the detector surface was gently cleaned of debris. Each sample scan took approximately 42 seconds to complete.

Reflectance spectra were collected for the active components (in powder form), the individual excipients used in the blends, and the powdered blends before compaction. The sample to be measured was loosely packed into a 50 ml glass beaker, up to a volume of 20 ml. The beaker was tapped lightly three times to level the powder surface. The spout of the beaker was aligned the same way for each sample. The sample was scanned once, then tapped three times on the counter, and rescanned, with the spout shifted 45° from the original alignment. A third scan was taken after the beaker was tapped and rotated another 45° . The same beaker was used for all components. The three scans were averaged and overlayed on a plot.

A spectral library of each "product" (batch) was created through the use of IQ^2™ . Spectral data from each hardness level of HCTZ tablets were entered into the HCTZ product library. Likewise, CTM spectral data were entered into the CTM product library.

41

Through the software's internal validation program, principal components were calculated. Identification by correlation and by distance was evaluated. "Correlation" is one of the modes of spectral matching used by the NSAS software. In correlation mode, the products in the spectral library are compared by correlation to see if they match a potential sample for analysis. In the "distance" mode, the program uses the distance between the library records and potential samples. A minimum of three spectra in the library is required for the distance mode to work.

1.4   Results

1.4.1   Results of Tablet Evaluation

Tablet weights were very consistent, with a relative standard deviation of less than 1% (most batches had a relative standard deviation of 0.5% or less). Specifications for tablet hardness were set at 10%. Table 2 summarizes the average hardness, weight, thickness and friability for the placebo blend. Relative standard deviations (RSD) for the mean hardness values for the placebo tablets ranged from 4.50% to 11.2%.

Table 3 summarizes the average hardness, weight, thickness and friability for HCTZ 15% tablets. The RSD's for hardness ranged from 3.3% to 14.6%, following a trend of increasing variation with a decrease in hardness. The standard error of the Erweka Hardness Tester was calculated to be 0.34 kg.

A summary of average hardness, weight, thickness and friability for CTM 2 % tablets appears in Table 4. The RSD's for hardness ranged from 3.18% to 8.49%. This formulation produced tablets with the least amount of deviation from the target hardness.

Overall, the variation (RSD) in tablet hardness (Figure 4) was observed to be inversely proportional to the hardness value, a trend which was generally reflected in the friability data (decrease in hardness results in an increase in friability). It is logical to expect that a softer tablet may have more variability with respect to values for hardness.

42

The raw and second derivative spectra of CTM, Avicel® PH102 and magnesium stearate are shown in Figures 5 and 6. Avicel® and Avicel®-containing blends were of a free-flowing and uniform nature. CTM powder contained clumps and was not free-flowing. Figures 7 and 8 display the raw and second derivative spectra of HCTZ along with Avicel® PH102 and magnesium stearate. HCTZ powder was crystalline, uniform and free-flowing. Observation of these spectra show distinctly different patterns or fingerprints for each component of the formulations. The second derivative treatment of the spectra reduces the contribution of physical characteristics of the components, resulting in a smoothing of the data and a reduction of baseline shift and noise.

The NIR absorbance (log 1/R) versus wavelength (nm) was plotted for each batch of tablets. When the raw spectra from all batches of a blend were overlayed on the same plot, a general upward shift in absorbance was observed in response to an increase in hardness. Plotting the second derivative spectra at several hardness levels also demonstrated an increase in absorbance at the peak maxima, although less obvious. The raw and second derivative spectra of the placebo blend tablets at five hardness levels are shown in Figures 9 and 10, respectively. Figures 11 and 12 are the raw and second derivative spectra of HCTZ 15% tablets at five levels of hardness. The raw and second derivative spectra of CTM 2% tablets at six hardness levels are shown in Figures 13 and 14.

Observation of the spectra in Figures 12 and 14 demonstrate the smoothing effect of the second derivative math treatment. The spectra appear to be nearly superimposed upon each other, except for small changes at absorbance maxima. Linear regression was performed on the spectral data at absorbance maxima. Numerous single wavelengths were chosen based on the appearance of an effect from increased tablet hardness. The results of these analyses are summarized in Tables 5 and 6. CTM 2% absorbance at eight single wavelengths was found to be significantly increased with an increase in tablet hardness.

HCTZ 15% absorbance at eight (out of ten wavelengths chosen) was also significantly increased in response to an increase in tablet hardness.

A spectral library was created for each of the two blends containing active components, using the second derivative spectra. Each level of hardness represented a separate product, from which the calculation of principal components was generated. The principal component analysis (PCA) for HCTZ 15% resulted in the successful identification of each product by distance. Seven HCTZ 15% samples (47 correct/ 7 incorrect) were incorrectly identified when the library was validated by correlation. The correlation method also identified four out of ten conflicting pairs of products in this library. This information is useful for future updating of the library, since there may be a better set of samples for use in this spectral library.

1.5   Conclusions

The results of this feasibility study indicate that there is a change in the NIR signal as a function of tablet hardness. Three tablet formulations were manufactured of varying compression forces and analyzed by NIRS. An increase in tablet hardness resulted in a consistent upward shift in NIR absorbance. Tablet samples of different hardness levels were successfully differentiated by principal component analysis. NIRS has the potential as an alternative method of tablet hardness testing.

Table 2. Summary of Placebo Matrix Tablet Evaluation

Lot Number	Mean Hardness (kg) n=20	Mean Weight (g) n=20	Mean Thickness (mm) n=5	Friability % loss
KM17 (h=12kg)	9.625 ± 0.43 (rsd=4.50%)	0.3233 ± 0.0008 (rsd=0.24 %)	3.81	0.61
KM19 (h=8kg)	8.14 ± 0.38 (rsd=4.73 %)	0.3246 ± 0.0009 (rsd=0.29 %)	3.99	0.31
KM21 (h=6kg)	6.11 ± 0.34 (rsd=5.56%)	0.331 ± 0.003 (rsd=0.84 %)	4.14	0.30
KM23 (h=4kg)	4.66 ± 0.33 (rsd=7.02 %)	0.333 ± 0.002 (rsd=0.52 %	4.29	0.45
KM25 (h=2kg)	2.09 ± 0.23 (rsd=11.2 %)	0.321 ± 0.001 (rsd=0.34 %)	4.78	2.65

Table 3. Summary of Hydrochlorothiazide 15% Tablet Evaluation

Lot Number	Mean Hardness (kg) n=20	Mean Weight (g) n=20	Mean Thickness (mm) n=5	Friability % loss
KM47 (h=12kg)	10.09 ± 0.52 (rsd=5.2 %)	0.3272 ± 0.0015 (rsd=0.45%)	3.40	0.15
KM45 (h=9kg)	8.96 ± 0.31 (rsd=3.3 %)	0.3254 ± 0.0013 (rsd=0.41%)	3.58	0.15
KM43 (h=6kg)	4.85 ± 0.30 (rsd=6.1%)	0.326 ± 0.0018 (rsd=0.56%)	3.94	0.46
KM41 (h=4kg)	3.46 ± 0.30 (rsd=8.5%)	0.3264 ± 0.0017 (rsd=0.53%)	4.19	0.76
KM39 (h=2kg)	1.61 ± 0.24 (rsd=14.6%)	0.325 ± 0.0015 (rsd=0.46%)	4.79	2.30

Table 4. Summary of Chlorpheniramine Maleate 2% Tablet Evaluation

Lot Number	Mean Hardness (kg) n=20	Mean Weight (g) n=20	Mean Thickness (mm) n=5	Friability % loss
KM51 (h=12kg)	11.2 ± 0.36 (rsd=3.18 %)	0.3239 ± 0.0016 (rsd=0.49%)	3.91	0.08
KM53 (h=9.5kg)	9.49 ± 0.44 (rsd=4.6 %)	0.326 g ± 0.002 (rsd=0.49 %)	4.06	0.15
KM61 (h=8kg)	7.58 ± 0.49 (rsd=6.53 %)	0.326 ± 0.001 (rsd=0.44 %)	4.27	0.15
KM55 (h=6kg)	6.31 ± 0.47 (rsd=7.5 %)	0.325 ± 0.002 (rsd=0.68 %)	4.47	0.31
KM57 (h=4kg)	4.10 ± 0.30 (rsd=7.32 %)	0.322 ± 0.001 (rsd=0.32 %)	4.80	0.78
KM59 (h=2kg)	2.38 ± 0.20 (rsd=8.49 %)	0.325 ± 0.003 (rsd=0.81 %)	5.33	1.54

Table 5. HCTZ 15%: Linear regression of second derivative absorbance data at single wavelengths

Equation: Hardness = y-intercept + slope (Abs at x nm)

	Linear Regression			ANOVA	
nm	y-intercept	slope	r^2	F	p
1334	-11	1221	0.524	3.31	0.167
1364	-0.75	-758	0.239	0.94	0.404
1396	-28.1	976	0.958	91.56	0.002
1432	-26.1	-1331	0.975	118.34	0.002
1800	6.86	-613	0.072	0.23	0.664
1882	-27.3	614	0.933	56.57	0.005
2000	-28.9	653	0.933	42.06	0.007
2218	-27.6	1048	0.933	41.45	0.008
2270	-19.2	-1143	0.968	90.56	0.002
2344	-56.6	-1914	0.985	202.98	0.001

Table 6. CTM 2% linear regression of second derivative absorbance data at single
wavelengths

Equation: Hardness = y-intercept + slope (Abs at x nm)

Linear Regression				ANOVA	
nm	y-intercept	slope	r^2	F	p
1330	-32.2	2991	0.883	30.18	0.005
1366	-14.7	-2163	0.631	6.83	0.059
1396	-51.5	1728	0.957	89.89	0.001
1434	-40.8	-2034	0.963	104.44	0.001
1458	-27.9	-5510	0.987	296.32	0.000
1926	-59.9	-995	0.918	44.91	0.003
2018	-64.9	1794	0.973	142.61	0.000
2102	-78.9	-2478	0.923	47.63	0.002

Figure 1. Rapid Content Analyzer™ monochromator and detector units.

Figure 2. Photograph of Rapid Content Analyzer™ detectors.

Figure 3. Diagram of sample holder for Rapid Content Sampler. Lever at bottom right is used to control the iris opening for centering tablets.
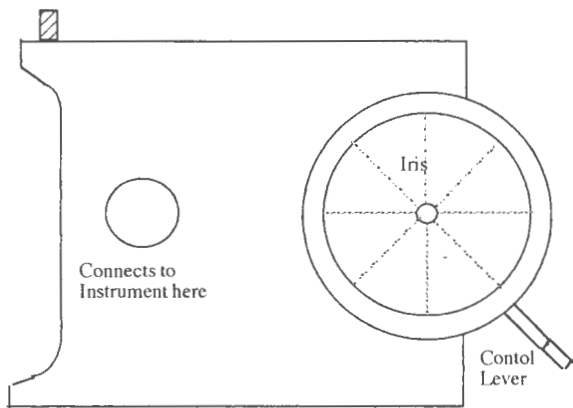
Figure 4. Percent variation in hardness versus tablet hardness.
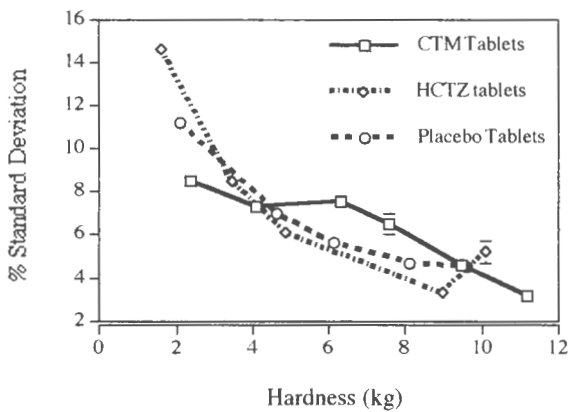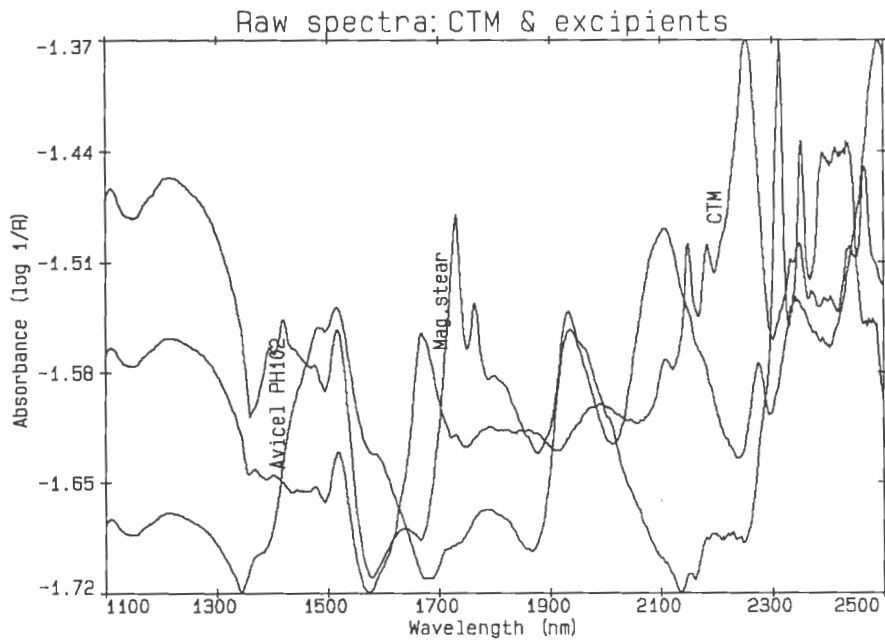
Figure 5. NIR reflectance spectra of CTM and excipients used in blend.
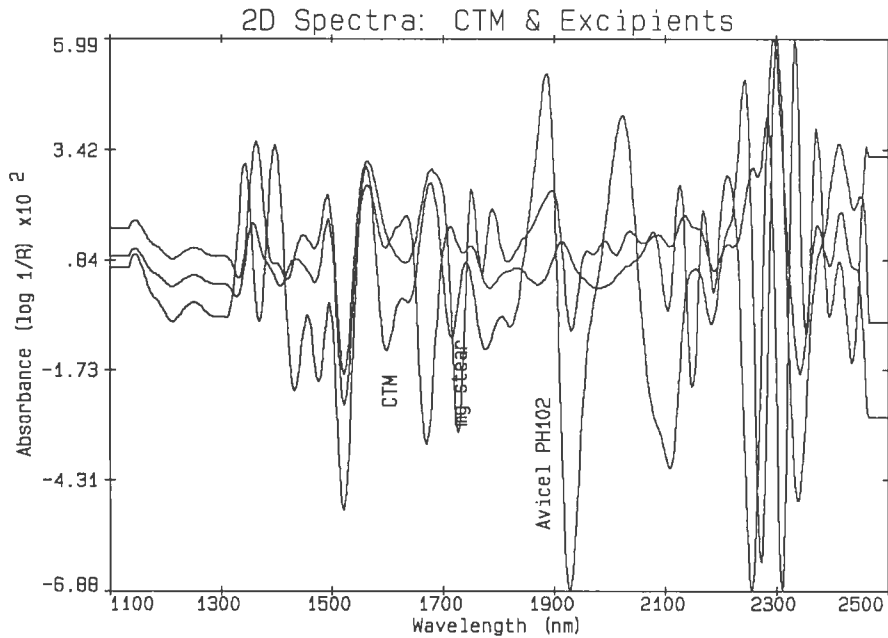
Figure 6. NIR second derivative spectra of CTM and excipients in blend.
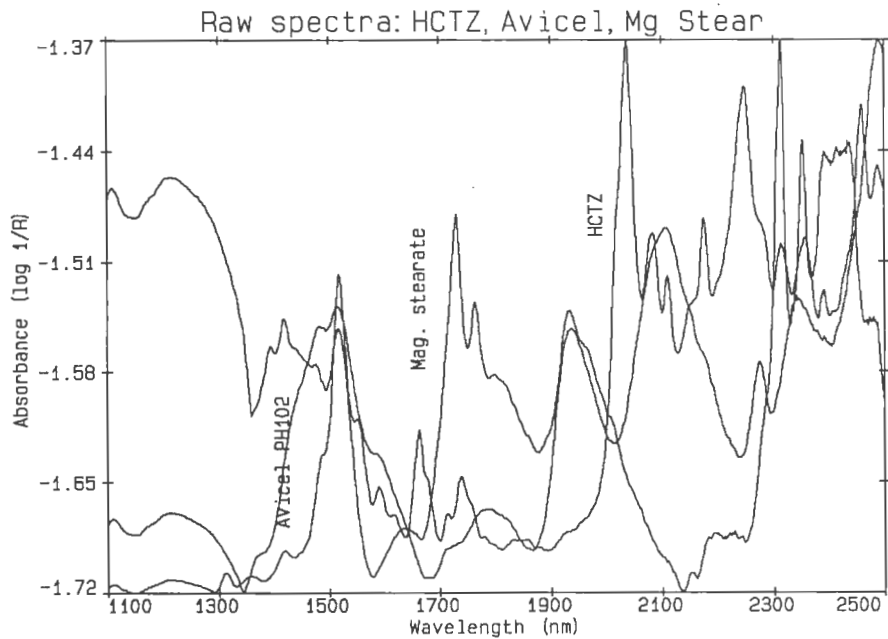
Figure 7. NIR reflectance spectra of HCTZ and excipients used in blend.
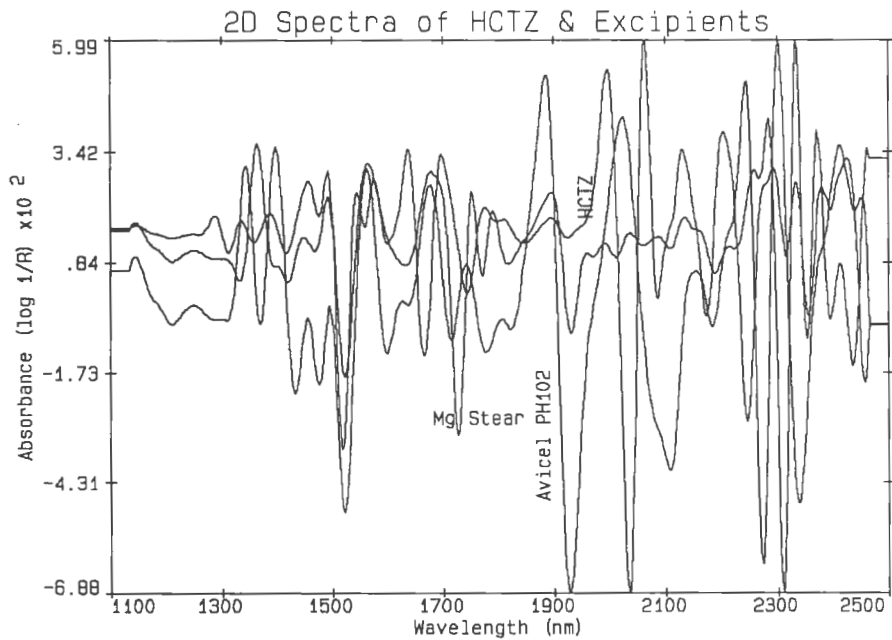
Figure 8. NIR second derivative spectra of HCTZ and excipients in blend.
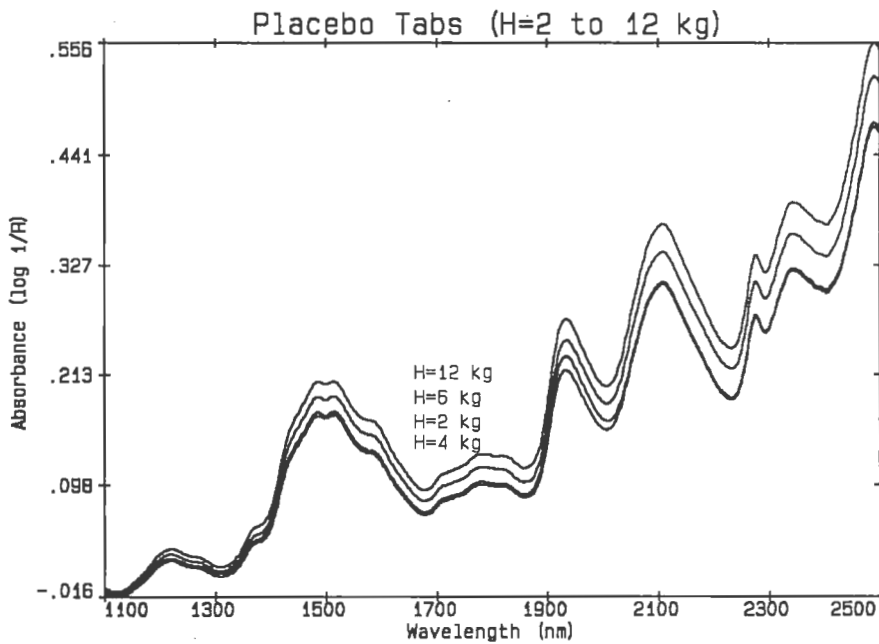
Figure 9. NIR reflectance spectra of placebo blend.
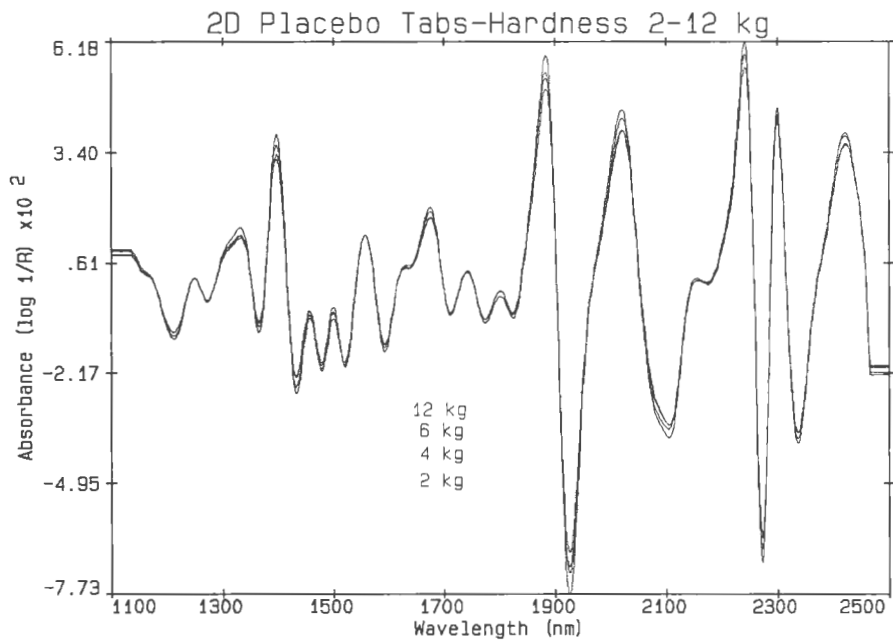
Figure 10. NIR second derivative spectra of placebo blend.
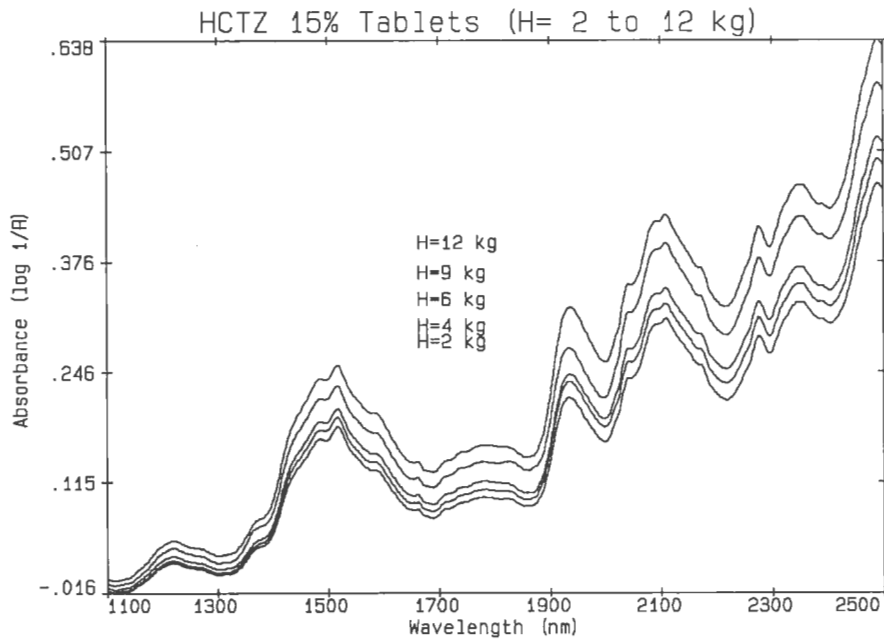
Figure 11. NIR reflectance spectra of HCTZ 15% (hardness 2 to 12 kg).
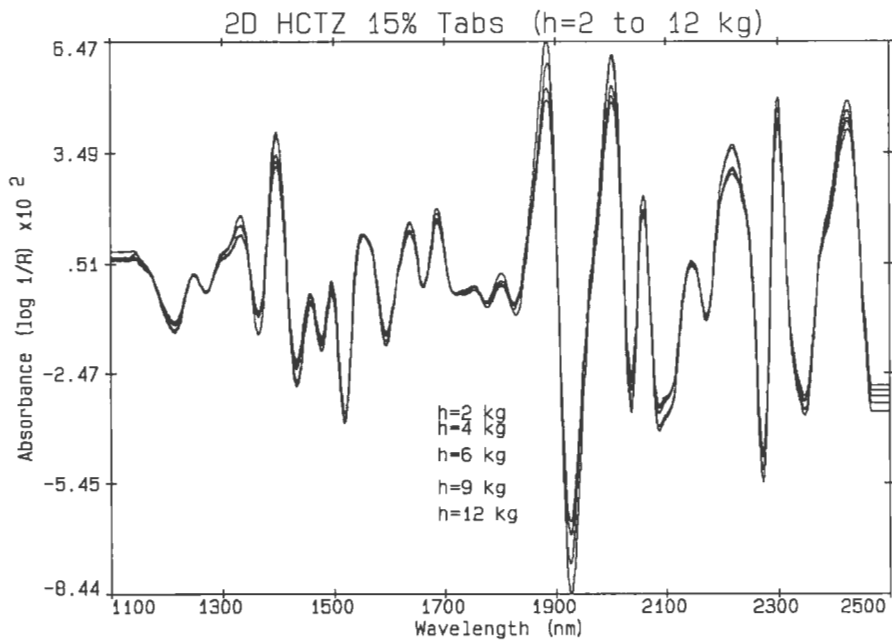
Figure 12. NIR second derivative spectra of HCTZ 15% (2 to 12 kg).
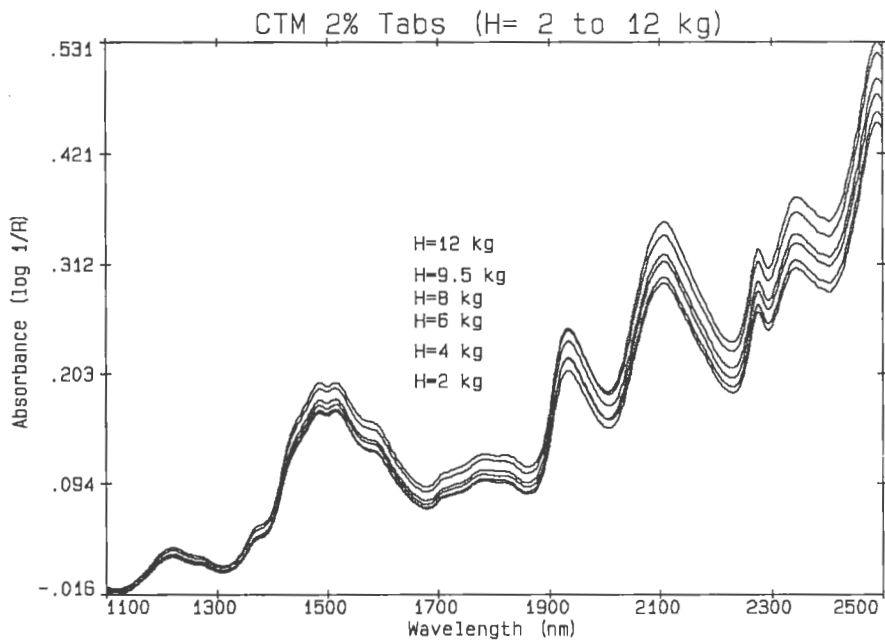
Figure 13. NIR reflectance spectra of CTM 2% (hardness 2 to 12 kg).
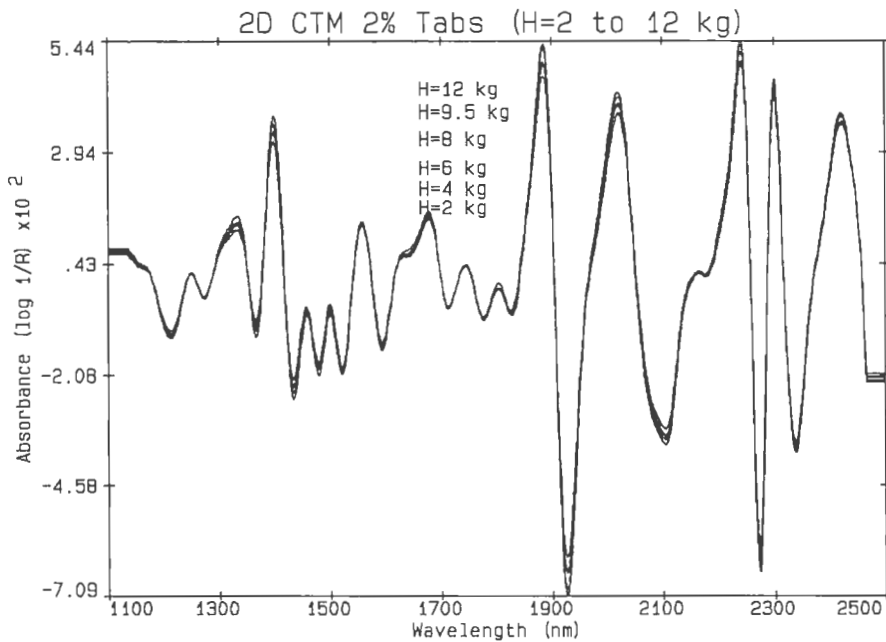
Figure 14. NIR second derivative spectra of CTM 2% (2 to 12 kg).

References

1) Corti, P., et al,, *Pharm. Acta Helv.* 65(1), 28 (1990).

2) Ciurczak, E. W. and Maldacker, T. A., *Spectroscopy* 1(1), 36-39 (1986).

3) Dempster, M. A., et al, *J. Pharm. Biomed. Anal.* 11(11/12), 1087-1092 (1993).

4) Baer, R. J., et al, *J. Assoc. Off. Anal. Chem.*, 66(4), 858-863 (1983).

Manuscript III

Near-Infrared Spectroscopy as a Non-Destructive Alternative to Conventional Tablet Hardness Testing

*presented at AAPS Tenth Annual Meeting November 1995 poster session

1.1   Abstract

In the present study, near-infrared reflectance spectroscopy (NIRS) was used to evaluate and quantify the effect of compression force on the NIR spectra of tablets. Flat, white tablets with no orientation (scoring, etc.) were manufactured on a Stokes Rotary Tablet Press. NIRS was used to predict tablet hardness on the following four formulations: hydrochlorothiazide (HCTZ) 15 % and 20% in a placebo matrix (microcrystalline cellulose and magnesium stearate), and chlorpheniramine maleate (CTM) 2 % and 6% in a placebo matrix. Five or six levels of tablet hardness from 2 to 12 kg were used for each formulation. Twenty tablets from each batch were evaluated by conventional USP methods for weight, hardness, thickness and friability. This laboratory tablet data was compared to NIR reflectance data using an NIRSystems Rapid Content Sampler. Multiple linear regression and partial least squares regression techniques were used to determine the relationship between tablet hardness and NIRS spectra. An increase in tablet hardness produced an upward shift (increase in absorbance) in the NIRS spectra. A series of equations was developed by calibrating tablet hardness data against NIR reflectance response for each formulation. The results of NIRS hardness prediction were at least as precise as the laboratory hardness test ($SE = 0.32$). A method is presented which has the potential as an alternative to conventional hardness testing of tablets.

1.2   Introduction

A variety of chemometric and statistical techniques are used in modern spectroscopic methods to extract useful information from raw spectroscopic data. Linear calibration methods such as multiple linear regression (MLR), principal component analysis (PCA) and partial least squares regression (PLS) are commonplace in near-infrared spectroscopy, as well in NMR and UV/VIS methods. A discussion of these mathematical techniques may be found in various other references[1, 2]. Multivariate calibration is a process for creating a model that correlates component concentrations or properties to the absorbance of a set of known reference samples. The reference method is the analytical method that is used to determine the reference component concentration or property values that are used in the calibration. The mathematical expression relating component properties to absorbance is known as a calibration model. The calibration process is one of the most important steps in NIR analysis. Errors in NIR prediction most often arise from errors in the reference method, instability of the NIR instrument, and inappropriate choice of the calibration model.

With sophisticated computer software, the general analyst may use these calibration algorithms with relative ease. Using the NIR spectral software, the analyst can acquire spectra, correlate them to laboratory data, develop a calibration equation and apply that equation to similar, new samples to predict constituent concentrations or properties.

A feasibility study was previously performed (Manuscript II) in order to investigate the effect of tablet hardness on the NIR spectra. Results of the initial work indicated that there is a detectable shift in the NIR spectra in response to a change in tablet hardness for a given formulation. These results were promising enough to warrant further investigation of the NIR method. The purpose of this study was to calibrate a NIR instrument to tablet hardness and demonstrate the potential utility of the technique as an alternative to current methods of tablet hardness testing.

66

1.3 Experimental

1.3.1 Tablet Manufacture

Table 1 lists the formulations used for this study. The components of each formulation were accurately weighed on a Mettler balance for a total weight of one kilogram. Each formulation was blended for ten minutes in a Turbula T2C shaker/mixer, then transferred to a labeled plastic bag to await compressing.

Tablets were manufactured by direct compression using one of the sixteen available stations of a Stokes B2 Rotary Tablet Press. One-centimeter tooling was used to make flat, white tablets having no orientation or scoring. The target tablet weight was 324 mg and the batch size was approximately 300 tablets. The tablet press was monitored until the desired level of hardness was achieved. Five to six hardness levels, with target hardness levels of 2, 4, 6, 8, 10, and 12 kilograms on the Erweka Hardness Tester (which measures crushing strength), were used for each of the four formulations, for a total of 27 batches of 300 tablets each.

1.3.2 Evaluation of Tablets

Twenty tablets from each batch were evaluated for weight, hardness, thickness and friability. The USP tolerances for weight variation[3] allow a percentage difference of 7.5 for an average tablet weight of 130 to 324 mg. Tablets weighing more than 324 mg may differ by no more than 5%. The USP requires that twenty tablets be individually weighed and their average weights calculated. The weights of no more than two of the tablets may differ from the average weight by more than the prescribed percentage. No single tablet weight may differ by more than double that percentage. In this study, the target weight was 324 mg +/- 5.0%. Tablet thickness and friability were measured according to the protocol described in Manuscript II.

Tablet hardness was measured using the Erweka Hardness Tester. Hardness testing was performed on twenty tablets from each batch after all non-destructive physical tests were completed. This order of testing allowed direct correlation of data to a specific

67

Table 1. Composition of tablet formulations manufactured for NIR analyses.

Formulation	Components	Percent
Placebo Blend	Avicel® PH102	99.5 %
	magnesium stearate	0.5 %
HCTZ 15%	hydrochlorothiazide	15.0 %
	Avicel® PH102	84.5 %
	magnesium stearate	0.5 %
HCTZ 20%	hydrochlorothiazide	20.0 %
	Avicel® PH102	79.5 %
	magnesium stearate	0.5 %
CTM 2%	chlorpheniramine maleate	2.0 %
	Avicel® PH102	97.5 %
	magnesium stearate	0.5 %
CTM 6%	chlorpheniramine maleate	6.0 %
	Avicel® PH102	93.5 %
	magnesium stearate	0.5 %

tablet sample. Hardness specifications are generally chosen by the manufacturer, based on the desired performance of the tablet. For this study, the desired tolerances for hardness were set at +/- 10.0%.

The mean, standard deviation and relative standard deviation (RSD) were calculated for weight, hardness and thickness for each batch using Microsoft® Excel. The laboratory values for tablet hardness were entered into the NSAS™ computer files for the corresponding NIR spectra.

Tablet density (weight per volume) values were calculated with Microsoft® Excel (Version 5.0, Microsoft Corporation, USA) using equation (1):

$$density \frac{g}{cm^3} = \frac{weight(g)}{thickness(cm)} \times \pi r^2 \qquad \text{equation (1),}$$

where r = radius of 0.5 cm.

The RSD of the density values were tabulated and compared with the RSD of the laboratory hardness values. The calculated density values were entered into the NSAS™ computer files for the corresponding NIR spectra. For practical purposes, surface porosity was disregarded, i.e., it was assumed that the tablets were flat.

The standard error (standard deviation) was calculated for each laboratory (reference) method. The overall and single product values for the reference standard errors were used for comparison to the NIR standard errors.

1.3.3   Near-Infrared Spectroscopic Analysis

A NIRSystems Rapid Content Analyzer® Model 5000 was used for the analyses of tablet samples. This instrument and corresponding setup were described in Manuscript II. NIR reflectance parameters were set at 32 scans per sample in the range of 1100 to 2500 nm. A ceramic (Coor's Standard) reference scan was taken before each set of samples. Single tablet NIR scans were run on 20 samples from each batch of tablets. The sample to be measured was placed directly above the detector surface and centered with the iris.

Before positioning each sample, the detector surface was gently cleaned of debris. Each sample scan took approximately 42 seconds to complete. For each sample tablet, the lab hardness value for the corresponding NIR spectra was entered into the computer as the constituent value for hardness. The NIR spectral data were mathematically transformed to their second derivative spectra using a segment of 20 and a gap of 0. The segment size refers to the number of wavelengths the computer averages into one data point to improve the signal to noise ratio. Gap size is the distance in nanometers between wavelength segments. These two parameters will vary according to the math treatment in use.

Of the twenty spectra collected per batch, thirteen spectra per batch were selected for inclusion in the calibration set. To test for bias in the data, several calibration sets were created for each formulation, either by random computer selection or simply using the first thirteen spectra. The remaining seven spectra were used to create a validation sample set. Each of the HCTZ calibration sets contained a total of 65 samples (13 x 5 hardness levels), while the CTM calibration sets contained 78 samples (13 x 6 hardness levels). The placebo calibration sets contained 72 samples (13 x 4 hardness levels).

Multilinear regression (MLR) and partial least squares (PLS) regression were performed on the second derivative of the calibration spectra using NSAS™ . MLR utilizes one or more wavelengths in the development of a calibration model, whereas PLS involves the use of the full spectrum. Tablet hardness data was calibrated with NIR data and equations were developed for the various formulations. Numerous calibration equations were generated with each regression type. PLS was used with cross validation (segment size of four) and a maximum number of eight factors. The equations were deemed to be initially acceptable if they had a correlation coefficient of 0.95 or better and a standard error of estimation (SEE) of 0.32 to 0.5 kg. Further statistical analysis (root mean square error, bias, multiple correlation coefficient) was performed using NSAS™ when each calibration equation was applied to a validation set of tablet spectra. These statistics describe the

ability of the equation to predict the hardness of the samples. The definitions of these statistical terms are listed in Appendix 1.

Validation of each model was performed by applying it to a set of validation (or prediction) samples to test the model's predictive ability. These predicted values were then statistically compared to laboratory hardness values measured for these samples and checked for agreement of the model with the reference method. The standard error of prediction (SEP), also known as the RMS error[1], was also calculated.

1.3.4 Effect of Sample Position on NIR Spectra

A validation study was undertaken to evaluate the effect of sample position on the resulting NIR spectra. A comparison was made between spectra taken from (A) one tablet in ten positions without the use of the iris, which is normally used to center the tablet before analysis, (B) ten tablets in one position, both sides, using iris, and (C) one tablet scanned 20 times using iris.

In Part A, one tablet was scanned in ten positions on the instrument's detector surface without the use of the iris. Samples 2 through 10 were scanned with an edge of the tablet touching the approximate center area of the detector surface. Figure 1 illustrates the approximate placement of each tablet sample on the detector surface. All positions were in reference to the center position, which was located by the iris. The positions were identified as follows: 1) approximate center of detector surface, 2) above center at 12 o'clock or $0°$, 3) $45°$, 4) $90°$, 5) $135°$, 6) $180°$, 7) $225°$, 8) $270°$, 9) $315°$ and 10) 12 o'clock again ($360°$).

In Part B, one tablet was scanned twenty times in the center position. The tablet was scanned, removed, then repositioned between scans using the iris to center the tablet on the detector surface.

In Part C, twenty tablets were scanned once using the iris to position the sample in the center of the detector surface.

71

Figure 1. Diagram of tablet position in reference to center position on NIR detector surface. Center position was determined using the iris.

0,360°

315°   45°

270°   90°

225°   135°

180°
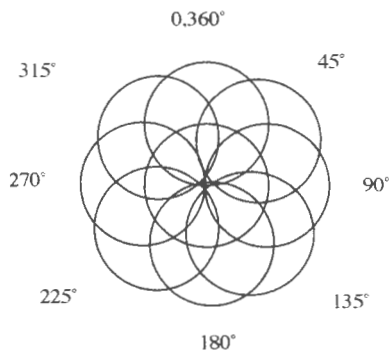
1.4 Results

The tablets used in this study were manufactured by direct compression. This is the simplest tablet production method and has several advantages over wet granulation methods. It is an economical method, since few processing steps are involved in comparison to wet granulation. No moisture is involved in the preparation of the blends for direct compression, thus the tablets made from this process tend to be more stable than those produced by wet granulation[5]. However there are several disadvantages to direct compression methods. There are relatively few crystalline substances that may be directly compressed. Also, many products contain a low effective dose of the active drug, which may be difficult to adequately distribute throughout the tablet matrix. Another disadvantage of direct compression is that a limited amount of active ingredient may be incorporated into the matrix (usually no more than 30%). This is a major limitation when formulating high dose products.

A relationship between NIR signal and tablet hardness or compaction force was established for four tablet formulations containing active drugs, and for one placebo formulation. The same excipient matrix was used for the entire study.

1.4.1 Results of Physical Testing of Tablets

Results of tablet evaluations for hydrochlorothiazide 15% (HCTZ), chlorpheniramine maleate 2% (CTM) and placebo blends were previously reported in Manuscript II. Tables 2 and 3 summarize the results of physical testing of HCTZ 20 % and CTM 6 %, respectively. Tablet weights for all batches were very consistent, with a relative standard deviation of less than 0.6 %. Friability was observed to increase in response to a decrease in tablet hardness. The properties of all batches fell within acceptable performance guidelines.

The mean values for tablet hardness were generally lower than the target hardness value for each batch (Table 4). An exception to this occurred with the placebo blend, where batches in the 4, 6, and 8 kg range were higher than the target values. One other

Table 2. Summary of hydrochlorothiazide 20% tablet evaluation.

Lot Number	Mean Hardness (kg) n=20	Mean Weight (g) n=20	Mean Thickness (mm) n=5	Friability % loss
KM65 (h=2kg)	1.26 ± 0.13 (rsd=10.1%)	0.3324 ± 0.00078 (rsd=0.24 %)	-	-
KM67 (h=4kg)	2.66 ± 0.25 (rsd=9.52%)	0.333 ± 0.001 (rsd=0.20%)	4.06	0.80
KM69 (h=6kg)	4.38 ± 0.31 (rsd=7.1%)	0.3323 ± 0.00067 (rsd=0.20%)	3.71	0.80
KM71 (h=9kg)	6.93 ± 0.52 (rsd=7.5%)	0.3313 ± 0.00064 (rsd=0.19%)	3.43	0.25
KM73 (h=12kg)	8.06 ± 0.51 (rsd=6.36%)	0.3310 ± 0.00107 (rsd=0.32%)	3.43	0.09

Table 3. Summary of chlorpheniramine maleate 6% tablet evaluation.

Lot Number	Mean Hardness (kg) n=20	Mean Weight (g) n=20	Mean Thickness (mm) n=5	Friability % loss
KM77 (h=12kg)	8.26 ± 0.28 (rsd=3.33 %)	0.339 ± 0.001 (rsd=0.28 %)	3.84	0.02
KM79 (h=10kg)	7.61 ± 0.29 (rsd=3.76 %)	0.3296 ± 0.0007 (rsd=0.20 %)	3.91	0.01
KM81 (h=8kg)	5.16 ± 0.26 (rsd=5.04 %)	0.3324 ± 0.001 (rsd=0.31 %)	4.09	0.14
KM83 (h=6kg)	4.41 ± 0.23 (rsd=5.29 %)	0.3293 ± 0.0007 (rsd=0.22 %)	4.39	0.24
KM85 (h=4kg)	2.74 ± 0.22 (rsd=8.1 %)	0.3312 ± 0.0011 (rsd=0.33 %)	4.65	0.57
KM87 (h=2kg)	1.31 ± 0.16 (rsd=12.2 %)	0.3303 ± 0.0012 (rsd=0.37 %)	5.18	2.02

Table 4. Comparison of mean tablet hardness with target hardness.

Product	Mean hardness (kg)	Target hardness (kg)	% Difference
Placebo	9.625	12	19.79
	8.14	8	-1.75
	6.11	6	-1.83
	4.66	4	-16.50
	2.09	2	-4.50
HCTZ 15%	10.09	12	15.92
	8.96	9	0.44
	4.85	6	19.17
	3.46	4	13.50
	1.61	2	19.50
CTM 2%	11.2	12	6.67
	9.49	9.5	0.11
	6.31	6	-5.17
	4.1	4	-2.50
	2.38	2	-19.00
	7.58	8	5.25
HCTZ 20%	1.26	2	37.00
	2.66	4	33.50
	4.38	6	27.00
	6.93	9	23.00
	8.06	12	32.83
CTM 6%	8.26	12	31.17
	7.61	10	23.90
	5.16	8	35.50
	4.41	6	26.50
	2.74	4	31.50
	1.31	2	34.50

exception was in the CTM 2% batches having target hardnesses of 2, 4, and 6. These differences may have been due to environmental conditions, since all the hardness data was not collected on the same day as the tablet manufacture. HCTZ 20% and CTM 6% tablets were manufactured during the months of April and May, when ambient humidity is generally higher. The other three formulations were manufactured during the months of January and February, when ambient conditions are relatively dry. Although all batches were stored in tightly closed plastic containers, ambient conditions in the laboratory change frequently and may have resulted in increased uptake of moisture by the samples. No relationship was found between the deviation from target values and the "age" of the samples on the day of testing.

Overall, the relative standard deviation (RSD) for lab hardness values ranged from 3.23 to 13.24%. For each formulation, the RSD was found to increase as the average hardness decreased. The RSD for hardness was plotted against the age of the tablet, relative to the time that hardness data was collected (Figure 2). No relationship was found between RSD for hardness and the age of the sample. However, when the age of the product was plotted (Figure 3) against the percentage difference from the target hardness, there was a linear relationship ($r^2 = 0.586$). In Figure 4, the data was plotted and regression was performed by product. No correlation between age and percentage difference from the target hardness was found for the single products HCTZ 20% ($r^2 = 0.047$) or CTM 2% ($r^2 = 0.00$). In Figure 5, we find similar behavior between both HCTZ products and CTM 6%. The overall r^2 for both HCTZ products was 0.82, and 0.83 for CTM 6% alone. Similar slope values resulted when both HCTZ products (slope = 0.446) were compared with the CTM 6% (slope = 0.531) formulation. Although inconsistent between products, this evidence suggests that tablet hardness may change over time, and hardness data should be collected immediately after tablet manufacture for the most accurate results.

Figure 2. Product age versus percent standard deviation in hardness.
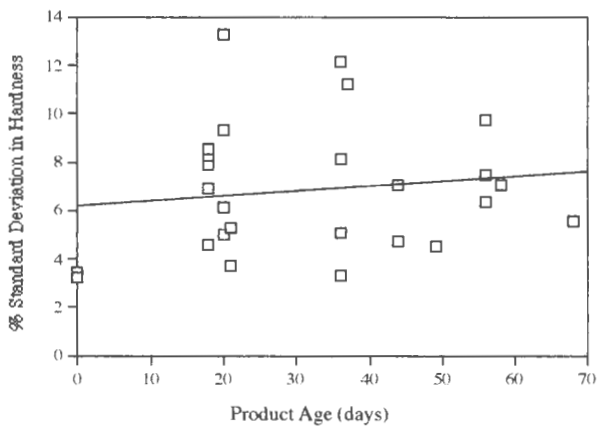
□   All Data $y = 0.021x + 6.190$ $r^2 = 0.019$

Figure 3. Product age versus deviation from target hardness (data from all four formulations included).
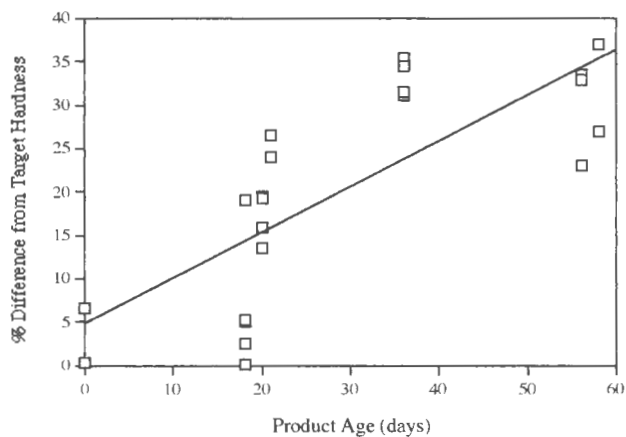
AllData   y = 0.526x + 4.851 r^2 = 0.586

Figure 4. Product age versus deviation from target hardness: data separated by product to determine individual regression coefficients.
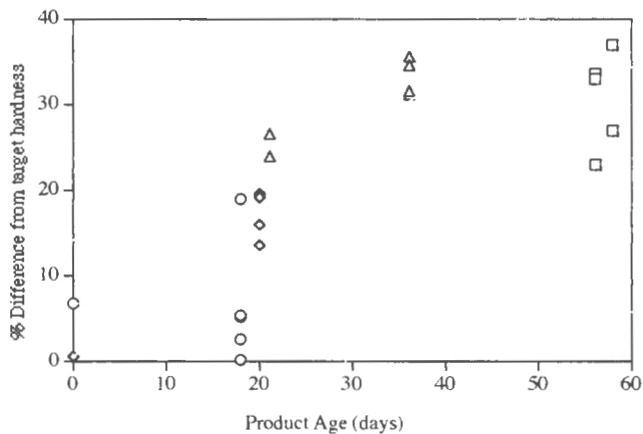
□	hctz 20%	$y = 1.112x - 32.477$	$r^2 = 0.047$
◇	hctz 15%	$y = 0.829x + 0.440$	$r^2 = 0.900$
○	ctm 2%	$y = -0.015x + 6.670$	$r^2 = 0.000$
△	ctm 6%	$y = 0.531x + 14.045$	$r^2 = 0.830$

Figure 5. Product age versus deviation from target hardness: HCTZ data grouped together for regression and compared to CTM 6% regression.
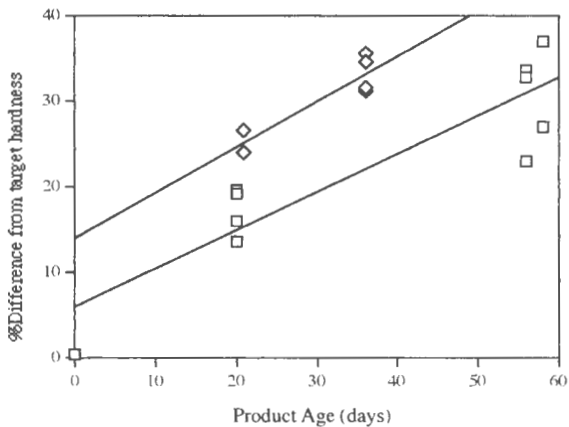
□	All HCTZ	$y = 0.446x + 5.955$ $r^2 = 0.820$
◇	CTM 6%	$y = 0.531x + 14.045$ $r^2 = 0.830$

A linear relationship was observed between tablet hardness and calculated density values for each batch. Table 5 summarizes the regression and correlation coefficients for each batch. (Detailed calibration results are given in Appendix C.) Hardness versus density values for the CTM 2% and 6% tablets were plotted in Figures 6 and 7. The regression equations ($r^2 = 0.980$ and 0.956, respectively) were similar, but when plotted together (Figure 8) the correlation was reduced to 0.65. A similar trend was observed with the HCTZ 15% and 20% data, shown in Figures 9 and 10. The correlation between density and hardness for HCTZ 15% and 20% was $r^2 = 0.962$ and 0.938, respectively. When all of the HCTZ data was plotted together as in Figure 11, the r^2 dropped to 0.729. Figure 12 is a plot of density and hardness values for all four formulations. When from all four formulations were plotted together, the r^2 was 0.45. As a linear relationship was demonstrated between density and tablet hardness for these products, I concluded that it would be feasible to develop NIR calibration models for density as well as hardness.

1.4.2 Results of NIR Spectral Analysis

The raw spectra of CTM 6% and HCTZ 20% are illustrated in Figures 13 and 14. The corresponding second derivative spectra are displayed in Figures 15 and 16. The overall shapes of the spectra are similar between the two formulations, due to the fact that the major portion of each formulation was composed of the same matrix. It may be observed from the spectra in Figures 15 and 16 that the baseline at 1100 nm starts out quite close for all hardness levels, then begins to diverge after about 1500 nm.

The raw and second derivative spectra of CTM 2% and HCTZ 15% were given in Manuscript II. The second derivative spectra of all four products at a hardness level of 2 kilograms is shown in Figure 17. The spectral differences between the formulations are more obvious in this plot. Each spectrum represents the average spectra of twenty single tablets.

Table 5. Linear relationship between tablet hardness and calculated density.

Formulation	Slope	Y-Intercept	r^2
CTM 2%	0.031	0.720	0.980
CTM 6%	0.042	0.779	0.956
CTM 2% and 6%	0.029	0.790	0.651
HCTZ 15%	0.038	0.837	0.962
HCTZ 20%	0.035	0.969	0.938
HCTZ 15% and 20%	0.036	0.899	0.729
all 4 formulations	0.031	0.843	0.450

Figure 6. CTM 2% hardness versus density (n=20).

$y = 0.031x + 0.720 \quad r^2 = 0.980$

Mean density (g/ml) vs Mean hardness (kg)
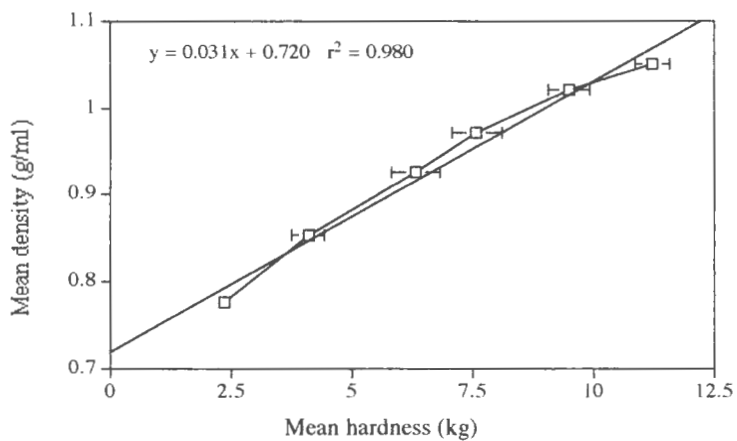
Figure 7. CTM 6% hardness versus density (n=20).

$$y = 0.042x + 0.779 \quad r^2 = 0.956$$

Mean density (g/ml)

Mean hardness (kg)
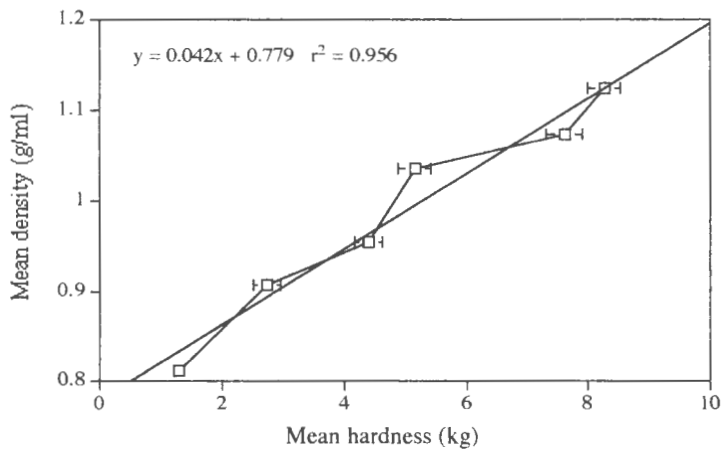
Figure 8. CTM 2% and 6% combined data: hardness versus density (n=20).
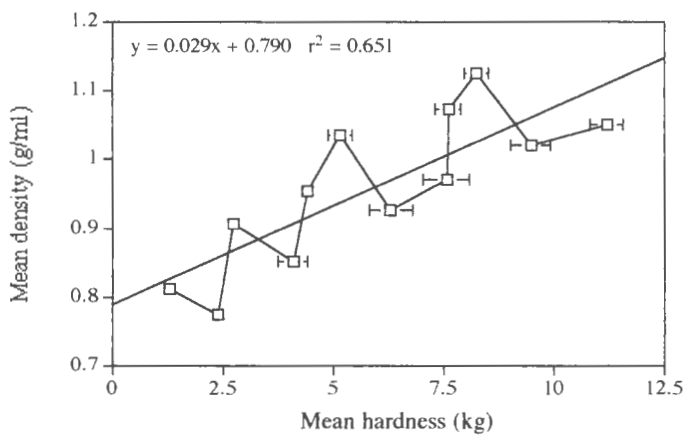
Figure 9. HCTZ 15% hardness versus density (n=20).

$y = 0.038x + 0.837 \quad r^2 = 0.962$

Mean density (g/ml)

Mean hardness (kg)
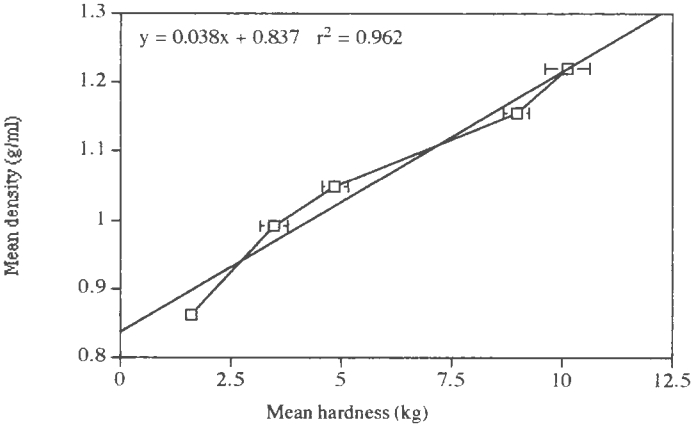
Figure 10. HCTZ 20% hardness versus density (n=20).
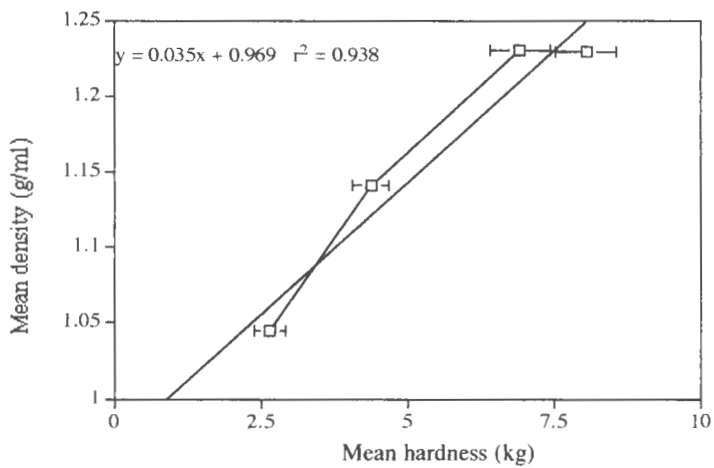
Figure 11. HCTZ 15% and 20% combined data hardness vsersus density.

$y = 0.036x + 0.899 \quad r^2 = 0.729$

mean density (g/ml)

mean hardness (kg)
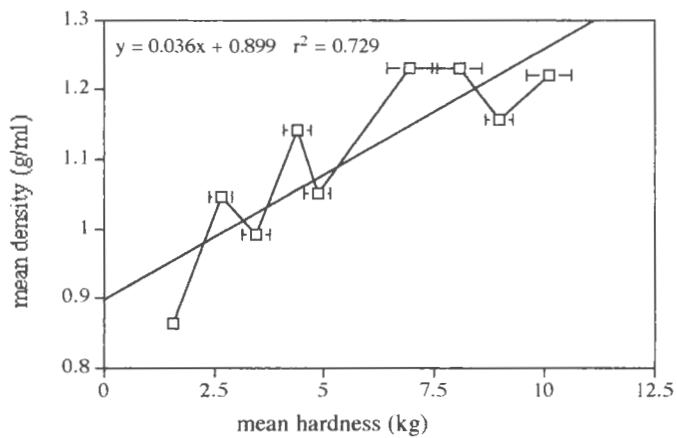
Figure 12. All CTM and HCTZ data: hardness versus density.

$y = 0.031x + 0.843 \quad r^2 = 0.450$

Mean density (g/ml)

Mean hardness (kg)
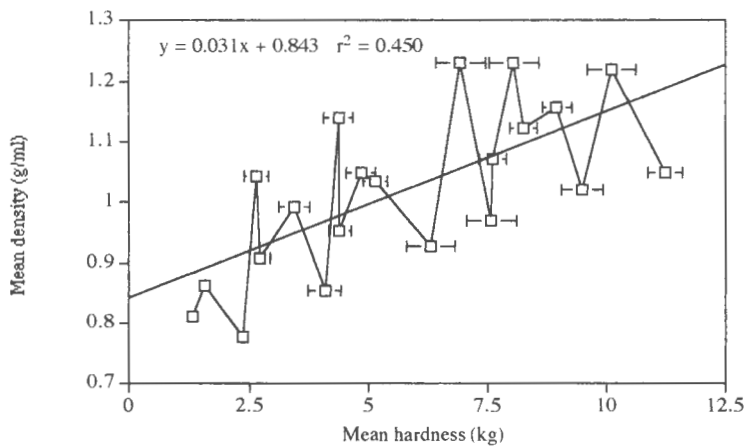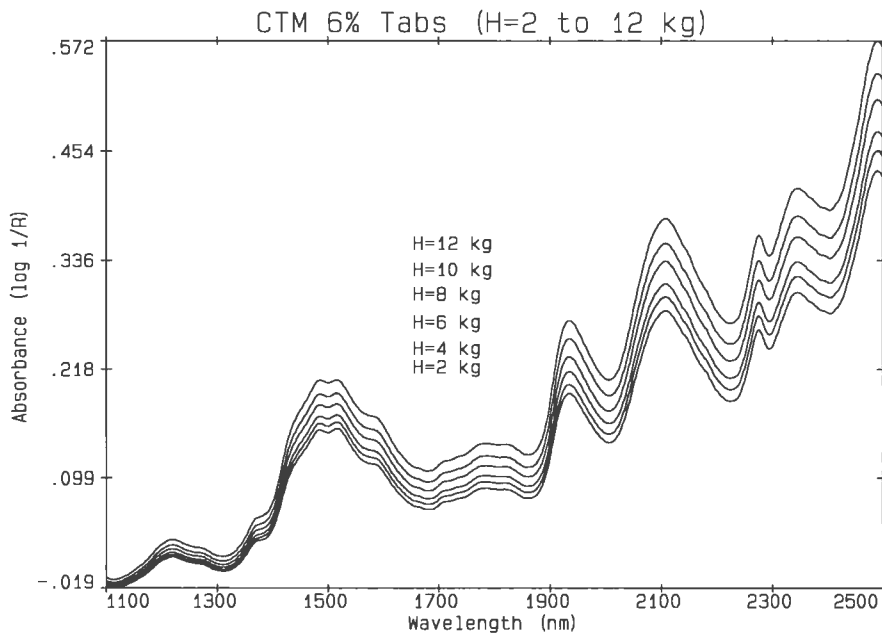
Figure 13. Raw NIR spectra of CTM 6% tablets at six hardness levels.
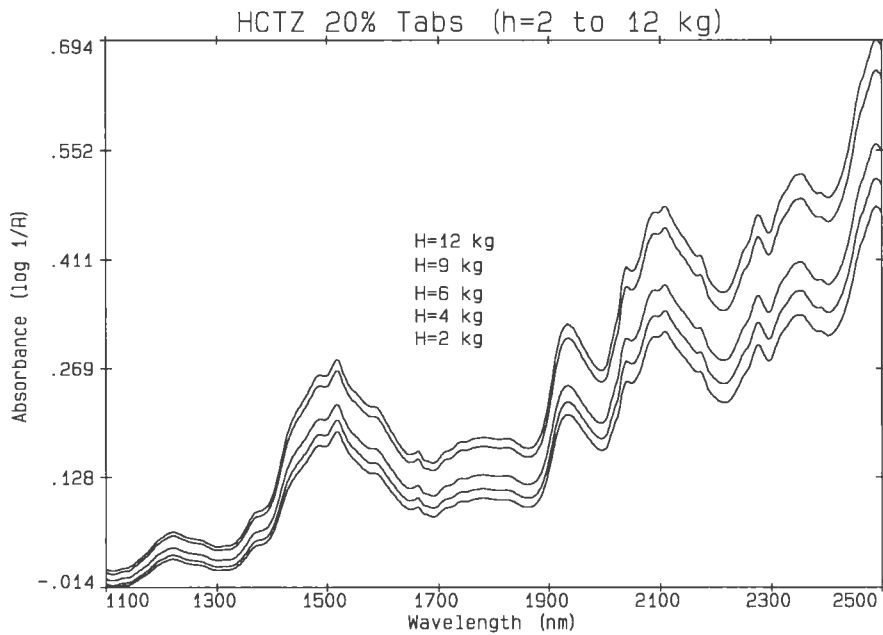
Figure 14. Raw NIR spectra of HCTZ 20% tablets at five hardness levels.
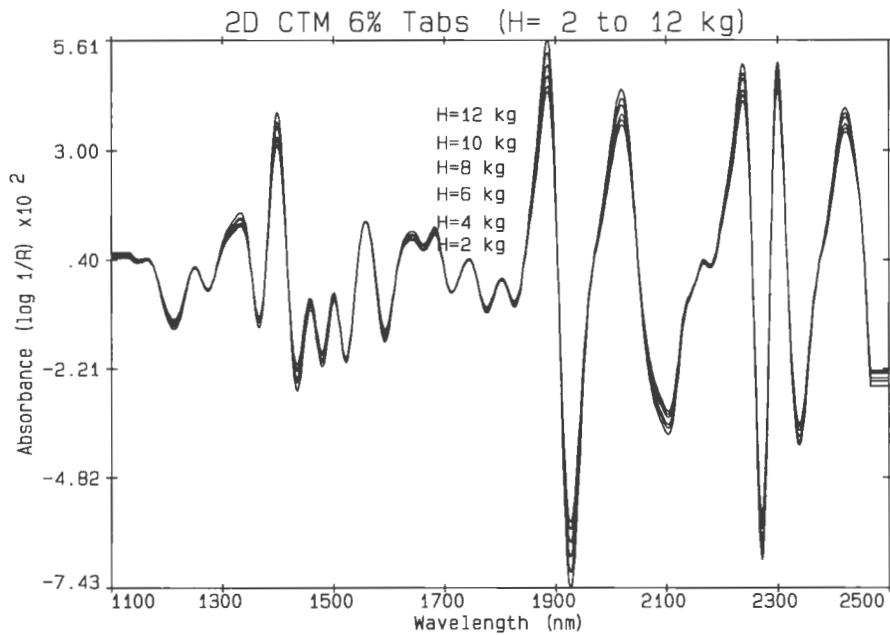
Figure 15. Second derivative NIR spectra of CTM 6% tablets.
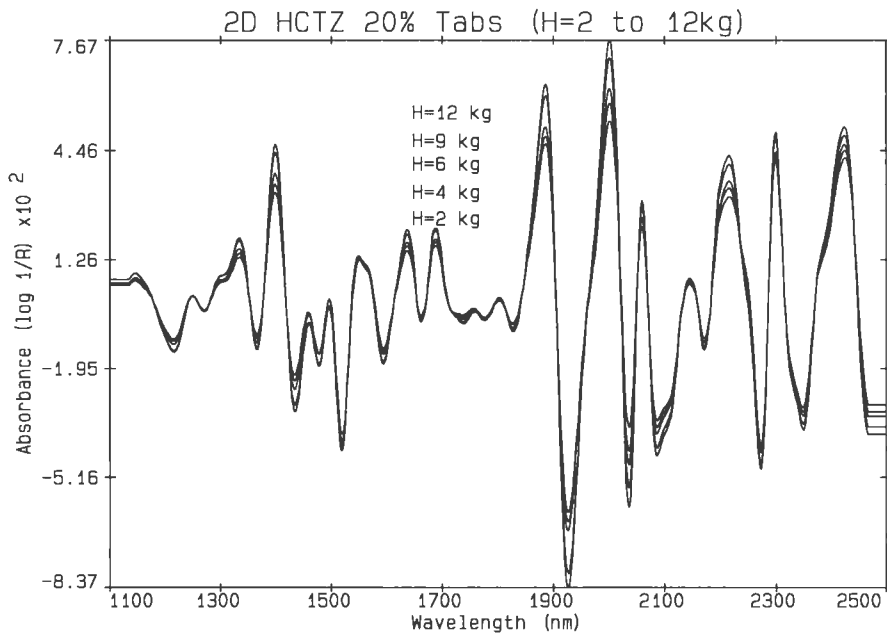
Figure 16. Second derivative NIR spectra of HCTZ 20% tablets .
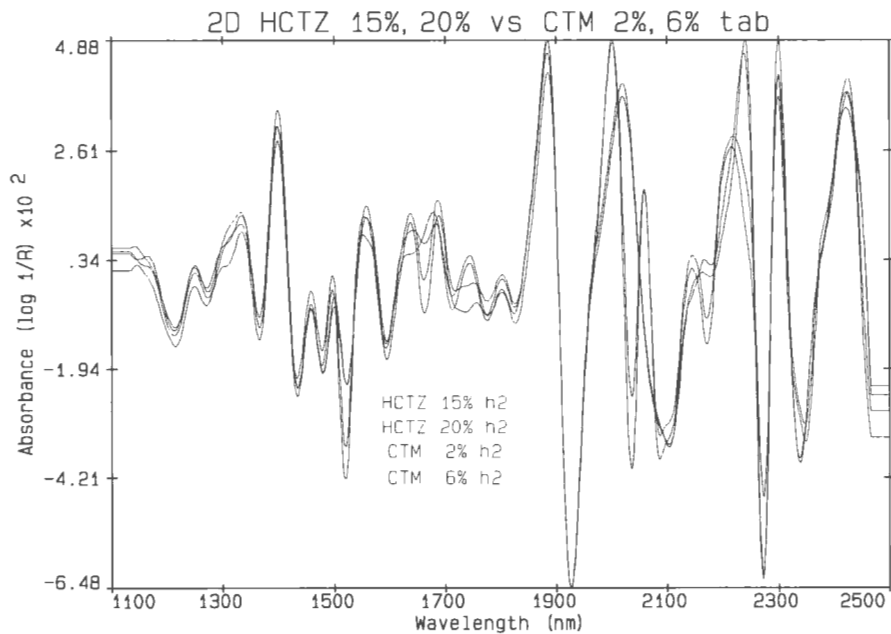
Figure 17. Second derivative NIR spectra of HCTZ 15%, HCTZ 20%, CTM 2% and CTM 6% tablets at a hardness of approximately 2 kg.

Figure 18 illustrates the effect of various sampling positions on the NIR spectra of one tablet. The resulting spectra cover nearly a four-fold range in absorbance. Without the use of the iris to position the sample, even the spectra of the two replicates at 12:00 were shifted from one another. The sample scanned in the center position was closest to the actual baseline. The remaining samples were grossly shifted upward in relation to the center sample. Samples positioned at 180° and 225° were nearly superimposed, as were samples at 45° and 270°. It is interesting to note that the second derivative treatment (Figure 19) reduced the baseline offset of the samples so that they were almost superimposed upon each other. The region from 1476 nm to 1594 nm contained a significant amount of variation, as is evident from the plot. The standard deviation spectrum of these samples appears in Figure 20, where the highest amount of variation appears around 1500 nm. It is likely that a loss of spectral information occurs when the sample is not reproducibly and accurately positioned.

There was no significant difference between the raw spectral plots of one tablet scanned twenty times (Figure 21) versus twenty tablets scanned once (Figure 22). These spectra appear to be one solid line of varying thickness at specific wavelength regions. The iris was used on both sets of samples, thus the shapes of the spectra are the same. Figure 23 and Figure 24 further illustrate the similarity between these two sets of samples. These are the standard deviation spectra of the respective sample sets. When superimposed, they differ slightly in absorbance, but not in "peak" position. This portion of the study demonstrates the precision of the NIR method. Multiple scans of the same sample yielded nearly the same results as a single scan of several samples. Overall, using the iris to center the tablet dramatically reduced the error due to sample positioning.
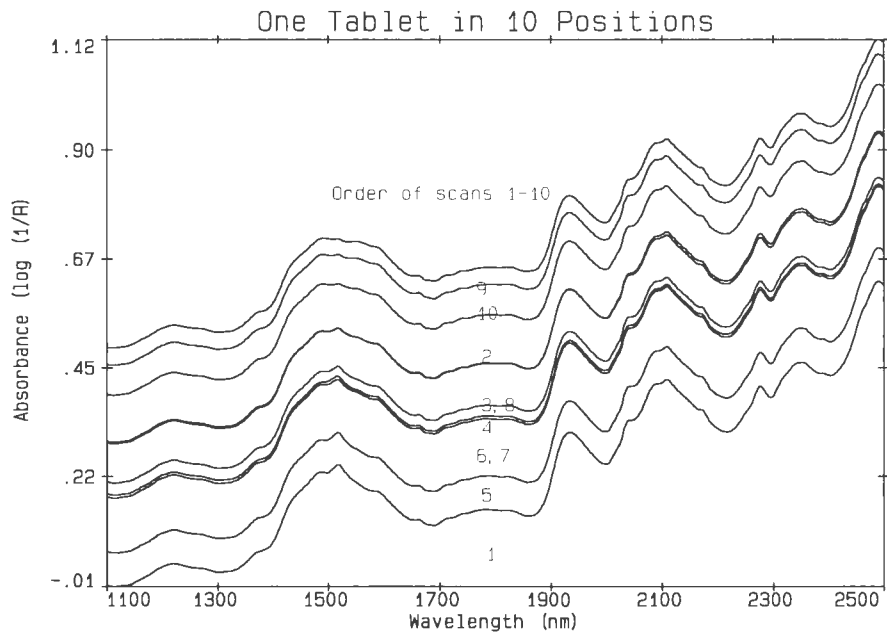
Figure 18. Raw NIR spectra of one tablet scanned in ten positions.
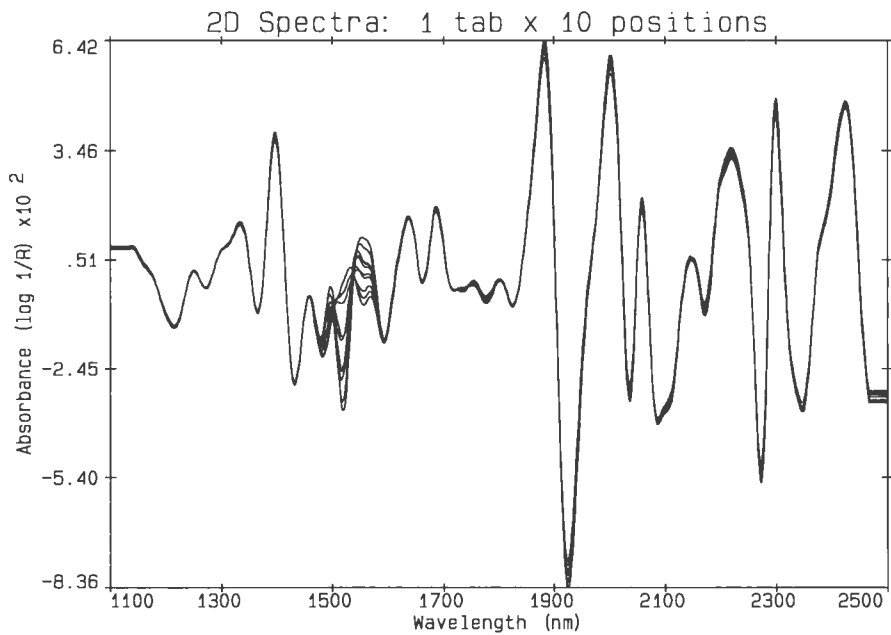
Figure 19. Second derivative NIR spectra of one tablet in ten positions.
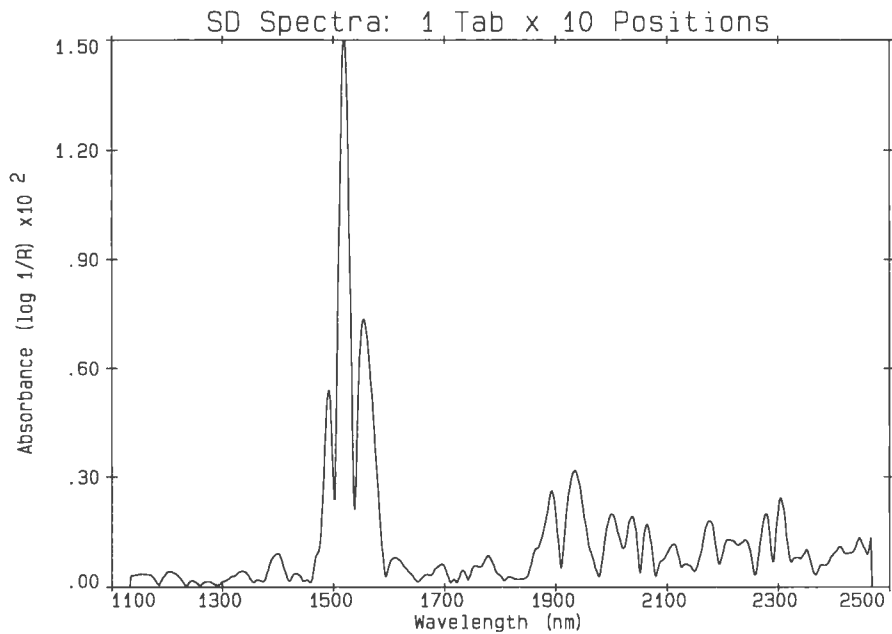
Figure 20. Standard deviation spectra of one tablet scanned in ten positions
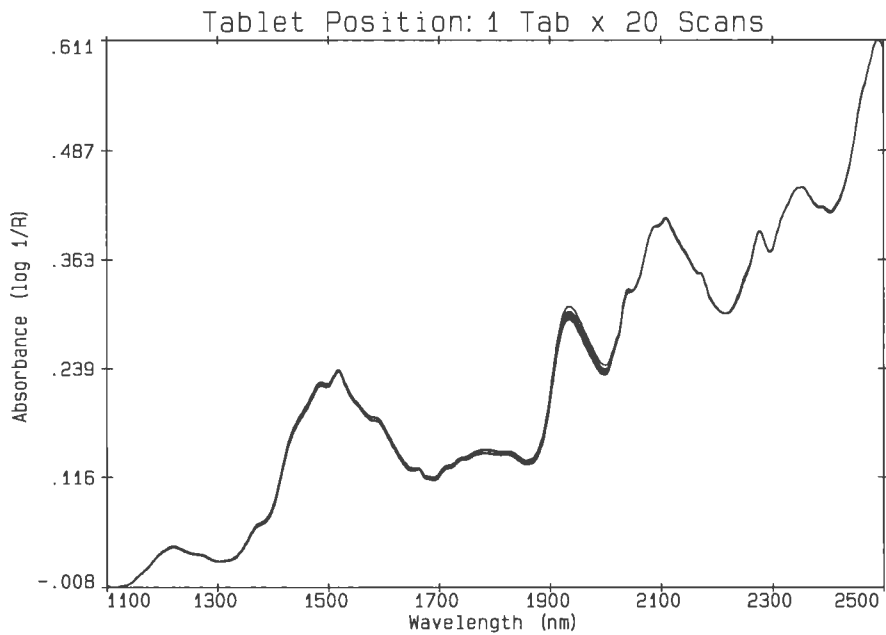
Figure 21. Raw NIR spectra of one tablet scanned twenty times.
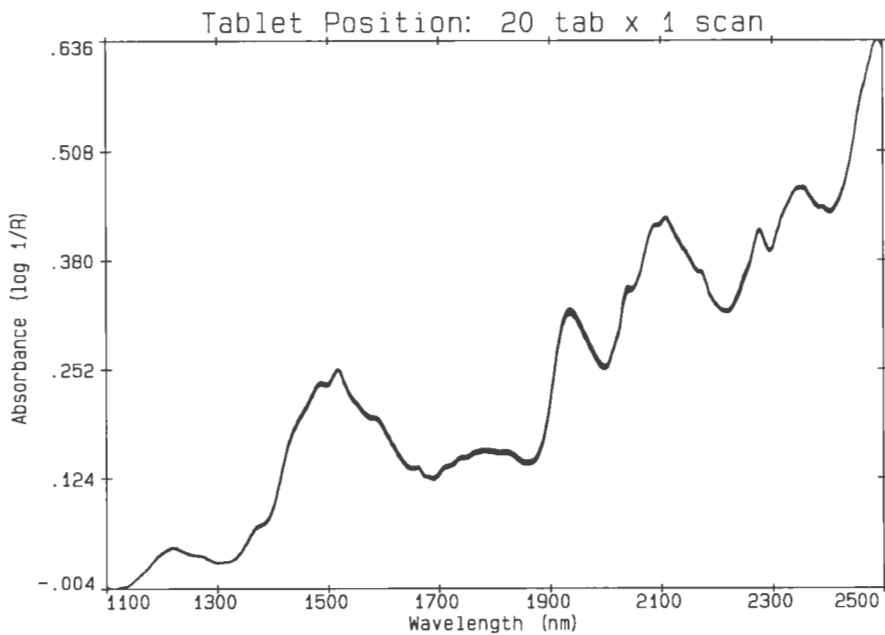
Figure 22. Raw NIR spectra of twenty tablets scanned once each.
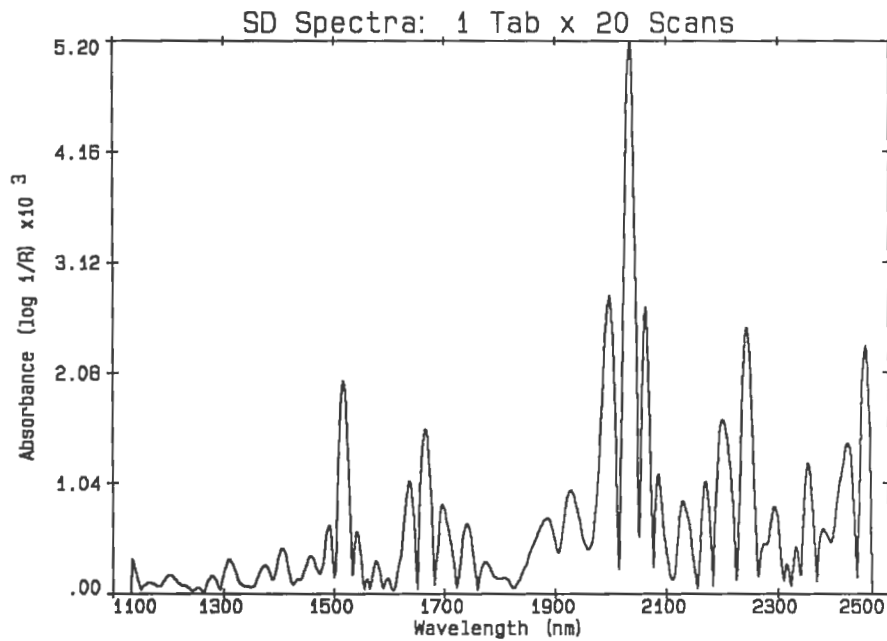
Figure 23. Standard deviation spectra of one tablet scanned twenty times.
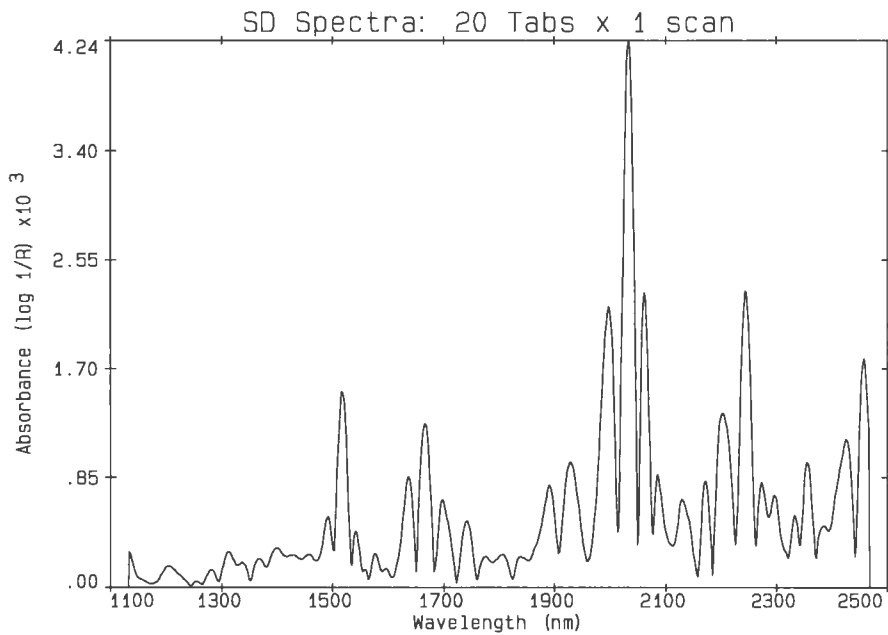
Figure 24. Standard deviation spectra of twenty tablets scanned once.

1.4.4 Results of Calibration Development

Once a suitable set of calibration models was developed, they were applied to a set of validation samples that were part of the original population but not included in the calibration set. The choice of the best calibration models was made by comparing statistical parameters that were calculated by the NSAS™ software. First, since a NIRS method cannot be more sensitive than its primary analytical method[6], it is important that the standard error of estimation (SEE) of the NIR method be as at least as good as that of the primary analytical method. The SEE indicates whether the answers provided by the calibration equation will be sufficiently accurate for the purposes for which they are being generated. The laboratory standard error on the Erweka Hardness Tester was calculated to be 0.32 kg. Readings may be subjective if the value falls between the 0.25 kg markings on the hardness tester.

The NIR standard error was calculated for each MLR calibration along with the slope (k1), intercept (k0) and correlation coefficient (r^2). A better correlation coefficient and standard error of estimation (SEE) were usually obtained by using more than one analytical wavelength in the calibration. Calibration coefficients (slope terms) should be in the same range relative to one another, and their values should be under 5000[7]. If there is a large change in the x value for the calibration set with a relatively large change in absorbance (y), the regression coefficients tend to stay small, indicating a large sensitivity and signal-to-noise ratio. On the other hand, a large change in x with a small change in absorbance results in large regression coefficients and may indicate low sensitivity and low signal-to-noise[8].

The validation process involved the calculation of various statistical parameters that measure goodness of fit. These parameters (defined in Appendix 1) include the ratio of bias to standard error of the bias (bias/SEB) and the ratio of standard deviation of the difference to root mean square (SDD/RMS). The RMS is close to the standard error of prediction (is not n-1); it is the non-bias corrected standard error. Standard deviation of the

difference (SDD) is the bias-corrected standard error. The desirable ratio between these parameters is 0.9 to 1.0. A rule of thumb for goodness of fit using these parameters is that bias/SEB should equal no more than 3.0. and the ratio SDD/RMS should be close to 1.0. It is desirable to have the bias and the SEB close to zero. It is also important that the value for slope adjustment be close to 1.0 as well, since this indicates linearity. Note that it is unacceptable to change the slope[9], as this indicates that the model does not fit the sample population.

When using PLS, large MSECV (mean square error of cross validation) values indicate differences between spectra. The choice of the number of factors to use is based on the number of variables present in the formulation. Since we are measuring a physical property, rather than a chemical property, choosing the number of factors is not as straight forward. The usual practice is to select a model that uses no more than twice the number of variables in the formulation. The formulations in this study were composed of one active and two excipients, and varied in the level of hardness used in the manufacturing process. Therefore, eight factors were chosen as the maximum number allowed in the regression. The "mixed" calibrations required more factors, since they included the addition of drug concentration as a variable.

As the current study was extensive in the development of various calibration models, only the summary results will appear in the text of this manuscript. The reader is directed to Appendix 2 for more detailed calibration results, which include wavelength and calibration coefficient information for each formulation.

1.4.4.1   Results of HCTZ Calibrations

Tables 6 and 7 summarize the calibration of HCTZ 15% tablets and HCTZ 20% tablets, respectively. Different MLR wavelengths were selected by the computer for calibrating each HCTZ formulation. Although it might be expected that the calibration wavelengths would be the same for a given drug, it must be reiterated that the equations are developed through chemometric methods using the wavelengths having the greatest

Table 6. Results of HCTZ 15% hardness calibration/prediction.

Calibration					Prediction		
Cal.file	Math	n	r^2	SEE	n	r^2	SEP
10hc15ca	MLR	65	0.991	0.393	25	0.994	0.332
2hc15cal	MLR	65	-0.983	0.541	25	0.987	0.535
3h15c3	MLR	65	0.996	0.295	25	0.994	0.318
5hc15cal	MLR	62	0.989	0.445	25	0.992	0.405
8hc15cal	MLR	65	0.990	0.417	25	0.990	0.419
*hct15c2	MLR	65	0.944	1.010	25	0.964	7.410
*hc20cal4	MLR	61	0.991	0.354	36	0.888	3.100
7hc15pls	PLS	63	0.994	0.341	36	0.991	0.399
pls4hc15	PLS	62	0.995	0.294	36	0.990	0.403
plshct15	PLS	65	0.995	0.310	25	0.994	0.326

*Calibration model from HCTZ 20% formulation

Table 7. Results of HCTZ 20% hardness calibration/prediction.

	Calibration				Prediction		
Cal.file	Math	n	r^2	SEE	n	r^2	SEP
5hc20cal	MLR	65	0.980	0.446	25	0.985	0.479
6hc20cal	MLR	65	0.981	0.442	25	0.986	0.460
hc20cal3	MLR	64	0.989	0.385	35	0.992	0.366
hc20cal4	MLR	61	0.991	0.354	35	0.992	0.367
pls2hc20	PLS	65	0.988	0.414	25	0.985	0.477
pls3h20	PLS	63	0.990	0.374	25	0.985	0.486
plshct20	PLS	75	0.991	0.359	25	0.984	0.529
*plshct15	PLS	65	0.995	0.310	25	0.987	3.720

*Calibration model from HCTZ 15% formulation.

variation in absorbance. It was possible to preselect the regression wavelengths, but in this experiment, the resulting predictions were not generally as good. Calibrations that were designed for HCTZ 15% did not fit data sets from HCTZ 20% samples.

Table 8 contains a series of HCTZ 15% calibrations at 2076 nm. The calibration sets used to generate these models differed in the manner of sample selection and exclusion of outliers. (An outlier is a data point that falls well outside the main population.) The first model (hct15cal) was generated from a sample set that was not randomly selected. The first thirteen spectra from each of the five hardness levels were selected for the calibration sample set. The next two models were generated from a calibration set that was randomly selected. These two models differ in the number of wavelengths used to perform the regression. The addition of another wavelength to the model resulted in an improved SEE and correlation coefficient. The next set of three models in Table 8 demonstrates the effect of deleting outliers from the data set during the calibration process. Again, the SEE was improved by the addition of other wavelengths to the model.

It was not possible to develop acceptable calibrations by combining data from two concentrations of the same drug. The models themselves (Table 9) had acceptable correlation coefficients, but did not pass the validation process. For example, calibrations constructed from HCTZ 15% and 20% data resulted in a high bias value when applied to validation sets containing either concentration of drug. Equations developed for HCTZ 15% were applicable to HCTZ 20% samples (and vice versa) only if an adjustment was made to the "bias/slope" value of the calibration. Equations developed for an HCTZ formulation did not fit a CTM validation set (and vice versa), unless an adjustment to the slope or bias was made. The NSAS™ software was capable of making this adjustment, which resulted in a shift of the plot of lab hardness values versus NIR predicted values. In practice, this type of adjustment would not be acceptable, as it indicates that the model does not fit the sample population (i.e., the samples are outside the calibration set).

Table 8.   NIR calibration models for HCTZ 15% tablets, where
             Hardness = $k_0 + k_1(Abs_{\lambda 1}) + k_2(Abs_{\lambda 2}) + k_3(Abs_{\lambda 3})$

MLR Calibration

Cal.file	k_0	k_1	k_2	k_3	λ nm	mult r	SEE
hct15c2#	-21.81	511.34	0	0	1998	0.944	1.010
6hc15cal	21.54	-139.21	0	0	1572/1998	-0.985	0.513
4hc15cal	-9.21	235.44	-2027.65	0	1998+1578	-0.959	0.441
hct15cal#	-31.17	-1399.01	0	0	2076	-0.984	0.547
2hc15cal	-29.89	-1345.28	0	0	2076	-0.983	0.541
5hc15cal	-27.78	-992.81	771.80	0	2076+1316	0.989	0.445
3h15c1*	-29.37	-1323.68	0	0	2076	-0.991	0.412
3h15c2*	-26.25	-896.24	-1232.31	0	2076+1822	0.994	0.330
3h15c3	-22.25	-479.63	-2172.43	292.36	2076+1822+1902	0.996	0.295
7hc15cal	-2.11	-955.78	0	0	1360+2262	0.990	0.502
9hc15cal	71.97	-51.69	0	0	1580/1676	-0.989	0.430
8hc15cal	-25.11	-1372.35	908.01	0	2320+1328	0.990	0.417
10hc15ca	-12.16	-631.55	-3582.01	0	1520+1576	0.991	0.393

PLS Calibration

Cal. file	#factors	MSECV	λ range nm	(min)	mult r	SEE
pls2hc15*	4	0.03	1100-2500	1.13	0.995	0.301
pls4hc15	4	0.03	1300-2350	1.18	0.995	0.294
7hc15pls	6	0.04	1100-2500	1.21	0.994	0.341
plshct15	6	0.04	1100-2500	1.01	0.995	0.310
3h15p1	4	0.06	1100-2500	1.12	0.996	0.289

*outliers deleted

#nonrandom sample selection

Table 9. Results of HCTZ 15% and 20% (combined) hardness calibration/prediction.

Calibration					Prediction			
Cal.file	Math	n	r^2	SEE	n	Val.Set	r^2	SEP
hcAcal1	MLR	65	-0.971	0.665	25	HCTZ 15%	0.977	0.713
hcAcal1	MLR	65	-0.971	0.665	35	HCTZ 20%	0.983	0.508
hcAcal3	MLR	57	-0.979	0.551	36	HCTZ 15%	0.964	0.822
hcAcal3	MLR	57	-0.979	0.551	35	HCTZ 20%	0.983	0.476
hcAcal5	MLR	52	-0.984	0.464	36	HCTZ 15%	0.909	1.340
hcAcal5	MLR	52	-0.984	0.464	35	HCTZ 20%	0.985	0.464
pls4hcA	PLS	59	0.991	0.350	36	HCTZ 15%	0.834	1.600
pls4hcA	PLS	59	0.991	0.350	35	HCTZ 20%	0.989	0.394

Calibration models for CTM 2% and CTM 6% are summarized in Tables 10 and 11, respectively. Numerous equations were developed at multiple wavelengths for each formulation. The computer selected different wavelengths for the two different drug concentrations. In general, the addition of wavelengths to the calibration resulted in a higher correlation coefficient and a better SEE. However, better predictions (validations) resulted from the models that used fewer wavelengths in the multiple regression of both CTM 2% and CTM 6% tablets. PLS performed somewhat better than MLR.

Validation of CTM 2% models resulted in higher (ten-fold) bias values than the CTM 6% predictions. This may be a reflection of the higher variability in the laboratory hardness data.

All of the MLR models that were developed for CTM 6% tablets successfully predicted their corresponding validation sets. It is evident from Tables 10 and 11 that the model with the best SEE may not yield the best prediction results. The best models consisted of three or four terms, but the same equations did not yield the best validation results. Overall, PLS performed slightly better than MLR for CTM 6% samples.

Equations developed for combined CTM 2% and 6% samples followed the same rule as the combined HCTZ formulations (Table 12). The computer selected wavelengths for the combined formulations that were different from those forCTM 2% or CTM 6%.

1.4.4.3   *Results of "Mixed" Calibrations*

"Mixed" calibrations were developed by performing regression on combined data from the four tablet formulations (Table 13). In the process of developing these calibration equations, the software defined a significant number of data points as outliers. The majority of the outlying points originated from the CTM 2% data. One PLS calibration was developed using the data from all four formulations (Table 14). This model only marginally fit both sets of HCTZ validation data and the CTM 6% data. None of the developed models fit the CTM 2% data. The best performance was obtained from the

Table 10. Results of CTM 2% hardness calibration/prediction.

Calibration					Prediction		
Cal.file	Math	n	r^2	SEE	n	r^2	SEP
ct2cal2	MLR	90	0.991	0.423	42	0.985	0.548
ct2cal3	MLR	88	0.991	0.411	42	0.985	0.563
ct2cal4	MLR	88	-0.988	0.482	42	0.980	0.638
ct2cal5	MLR	88	0.993	0.372	42	0.985	0.552
pls2ctm2	PLS	88	0.987	0.490	30	0.981	0.650
pls3ctm2	PLS	88	0.987	0.486	30	0.980	0.658
pls5ctm2	PLS	75	0.991	0.431	42	0.984	0.552
pls6ctm2	PLS	75	0.991	0.417	42	0.981	0.623

Table 11. Results of CTM 6% hardness calibration/validation.

Calibration					Prediction		
Cal.file	**Math**	**n**	**r²**	**SEE**	**n**	**r²**	**SEP**
c6sscal1	MLR	78	-0.989	0.365	42	0.986	0.439
c6sscal2	MLR	78	-0.992	0.318	42	0.990	0.370
c6sscal3	MLR	78	0.993	0.298	42	0.992	0.336
c6sscal5	MLR	78	0.994	0.271	42	0.991	0.340
c6sscal7	MLR	78	0.994	0.285	42	0.994	0.287
c6sscal9	MLR	78	0.993	0.291	42	0.994	0.288
*ctm2cal	MLR	90	-0.986	0.510	30	0.979	4.000
pls1ctm6	PLS	78	0.997	0.204	30	0.991	0.365
pls2ctm6	PLS	77	0.996	0.224	30	0.991	0.360
pls3ctm6	PLS	77	0.994	0.272	42	0.991	0.356
*plsctm2	PLS	90	0.988	0.474	30	0.978	5.380

* Calibration model from CTM 2% formulation

113

Table 12. Results of CTM 2% and 6% (combined) hardness calibration/prediction.

Calibration					Prediction			
Cal.file	Math	n	r^2	SEE	Val. set	n	r^2	SEP
ct26cal3	MLR	78	0.954	0.887	CTM 6%	42	0.955	0.834
ct26cal3	MLR	78	0.954	0.887	CTM 2%	42	0.967	0.929
ct26cal4	MLR	78	0.971	0.710	CTM 6%	42	0.945	0.862
ct26cal4	MLR	78	0.971	0.710	CTM 2%	42	0.980	0.659
ct26cal4	MLR	78	0.971	0.710	both	84	0.967	0.762
ct26cal5	MLR	78	0.944	0.982	both	84	0.941	1.010
ctm26cal	MLR	78	0.968	0.746	CTM 6%	42	0.948	0.833
ctm26cal	MLR	78	0.968	0.746	CTM 2%	42	0.976	0.705
c26pls1	PLS	78	0.991	0.412	CTM 6%	42	0.979	0.683
c26pls1	PLS	78	0.991	0.412	CTM 2%	42	0.985	0.451

Table 13. Results of "mixed" hardness calibration/prediction.

Calibration					Prediction			
Cal.file	Math	n	r^2	SEE	n	Val.File	r^2	SEP
mix2pls1	PLS	199	0.991	0.3686	42	CTM 6%	0.989	0.416
mix2pls1	PLS	199	0.991	0.3686	42	CTM 2%	0.827	2.770
mix2pls1	PLS	199	0.991	0.3686	25	HCTZ 15%	0.992	0.379
mix2pls1	PLS	199	0.991	0.3686	25	HCTZ 20%	0.984	0.485
mix2cal1	MLR	208	-0.95	0.832	42	CTM 6%	0.978	0.817
mix2cal1	MLR	208	-0.95	0.832	25	HCTZ 15%	0.934	1.080
mix2cal1	MLR	208	-0.95	0.832	25	HCTZ 20%	0.971	0.755
mix2cal2	MLR	199	-0.963	0.709	42	CTM 6%	0.978	0.844
mix2cal2	MLR	199	-0.963	0.709	25	HCTZ 20%	0.971	0.731
mix2cal3	MLR	199	-0.938	0.637	42	CTM 6%	0.981	0.723
mix2cal3	MLR	199	-0.938	0.637	25	HCTZ 15%	0.953	0.920
mix2cal3	MLR	199	-0.938	0.637	25	HCTZ 20%	0.983	0.589

Table 14. "Mixed" hardness calibration models developed using the indicated products.

MLR

CTM 2,6 and HCTZ 15,20

Cal.file	k(0)	k(1)	k(2)	λ nm	mult r	SEE
1 not saved	-18.73	-2111.33	0	1586	-0.877	1.39
2 not saved*	-22.48	-4567.17	0	1820	-0.903	1.17

*deleted outliers (CTM 2% 12kg)

CTM 6 and HCTZ 15, 20

Cal.file	k(0)	k(1)	k(2)	λ nm	mult r	SEE
mix2cal1	-22.24	-4550.70	0	1820	-0.950	0.832
mix2cal2*	-21.90	-4489.33	0	1820	-0.963	0.709
mix2cal3	-28.12	-3104.72	-436.49	1820+2344	-0.938	0.637

CTM 2, 6 only

Cal.file	k(0)	k(1)	k(2)	λ nm	mult r	SEE
ctm26cal1	-33.12	-5821.95	0	1824	-0.951	0.912
ctm26cal2	-20.65	-9243.32	1510.45	1824+2324	0.968	0.746

PLS

CTM 2,6 and HCTZ 15,20

Cal. file	# factors	MSECV	(min)	λ range nm	mult r	SEE
mix2pls1	13	0.05	1.19	1100-2500	0.991	0.369

CTM 2, 6 only

Cal. file	# factors	MSECV	(min)	λ range nm	mult r	SEE
c26pls1	11	0.06	1.18	1100-2500	0.991	0.412

HCTZ 15% data, which resulted in a SEE of 0.379 when predicted with the PLS model. For practical purposes, the use of this type of mixed calibration is not viable due to the relatively high standard errors; the majority of these calibrations have SEE's which are higher than the reference SE for the Erweka hardness tester.

In theory, it might be expected that mixed calibrations would work on a global scale since there is no analytical wavelength for hardness. The effect of changing hardness is seen as an overall spectral effect. The instrument selects the wavelength(s) having the highest correlation coefficient in the wavelength region selected. Other factors, such as sensitivity plots and loadings aid in the selection of the appropriate wavelength(s) in a case where the computer chooses a wavelength that is unrelated to the constituent of interest. The instrument evaluates the overall spectral variation- changing the hardness in a specific formulation has an overall effect on the spectra, which may vary between formulations.

Although the present study did not find a universal calibration equation for hardness, it was found that the NIR signal responded in the same way to a change in hardness, regardless of the drug. A change in hardness caused a shift in the spectra at several common wavelengths for each formulation. Upon observation of the average second derivative spectra of each batch of tablets, it was noted that all four formulations demonstrated a shift in the spectra at 1330, 1366, 1396, 1432, 1882 and 1926 nm. The spectral bands at 1432 nm and 1926 nm are characteristic of the water content in the sample. Absorbance changes at these wavelengths suggest changes in moisture content due to changes in tablet compaction forces. Since all four formulations were composed of the same excipient matrix, similarities in the general peak shape would be expected.

1.4.4.4   Results of Placebo Calibrations

The results of MLR and PLS calibrations and validations for the placebo tablets are summarized in Table 15. Several multiple term models were developed using MLR. The best MLR model utilized three wavelengths and resulted in multiple correlation coefficient

117

Table 15. NIR hardness calibration/validation of placebo tablets.

	Calibration				Prediction			
Cal.file	Math	n	r^2	SEE	n	Val.Set	r^2	SEP
pl3c1	MLR	52	0.990	0.400	28	placebo	0.974	0.676
pl3c1	MLR	52	0.990	0.400	26	placebo*	0.986	0.537
pl3c2	MLR	49	0.993	0.338	28	placebo	0.975	0.669
pl3c2	MLR	49	0.993	0.338	26	placebo*	0.986	0.493
pl3c2	MLR	49	0.993	0.338	25	placebo*	0.988	0.438
pl4c1	MLR	49	0.991	0.383	28	placebo	0.978	0.627
pl4c1	MLR	49	0.991	0.383	24	placebo*	0.991	0.398
pl4c1	MLR	49	0.991	0.383	30	CTM 2%	0.887	3.860
pl4c1	MLR	49	0.991	0.383	35	HCTZ 20%	0.928	2.330
pl2p2	PLS	47	0.994	0.314	28	placebo*	0.988	0.495
pl2p3	PLS	47	0.992	0.345	28	placebo	0.964	0.840
pl2p3	PLS	47	0.992	0.345	25	placebo*	0.987	0.528
pl2p4	PLS	47	0.991	0.359	28	placebo	0.986	0.536
pl2p5	PLS	45	0.994	0.301	28	placebo	0.987	0.533
pl2p6	PLS	45	0.993	0.329	28	placebo	0.985	0.557
pl2p7	PLS	42	0.994	0.295	28	placebo	0.986	0.546
pl2p8	PLS	42	0.989	0.382	28	placebo	0.984	0.561

Legend:

*	outliers deleted from validation set
PLS	Partial Least Squares
MLR	Multiple Linear Regression

of 0.993 and a SEE of 0.338. PLS produced slightly better SEE values. Validation of both types of models resulted in marginally acceptable predictions. Overall, linearity was not as good as it was for other formulations. Calibrations of the placebo formulations were constructed from only four levels of hardness. Better performance could likely be achieved by including more data in the models.

1.4.4.5 *Results of Density/NIR Calibration*

Calibrations were also developed for the four formulations using the calculated tablet density versus NIR signal. The models themselves were much better than those developed using hardness data. One factor that might be expected to contribute to this improvement is the degree of variability in the laboratory measurements. Relative standard deviations (Table 16) in laboratory hardness measurements were 3 to 13% compared with errors in density of only 0.2 to 1.0%. In evaluating the laboratory hardness data, a trend was observed in the percentage standard deviation: as hardness was decreased, percentage variation increased. This effect was not observed with the calculated tablet density data.

In order to evaluate the performance of the NIR determination of density, the NIR values were compared to the reference SE for density, i.e., the laboratory values. The overall reference SE for density was 6.67×10^{-3} (g/ml). The calculation of the SE for density is dependent on the precision of the weight and thickness measurements. These measurements are generally very good, due to the quality of the tablet press tooling and the accuracy of the balance.

Numerous one and two-term density calibration models were developed for each of the four products and are summarized in Tables 17 to 20. In general, the SEE's were three to four times greater than the reference SE for density measurement. PLS models were slightly better in terms of linearity and SEE. CTM 2% calibrations developed using MLR had only slightly higher SEE values (0.018) in comparison to the reference SE value of 0.013. PLS models for CTM 2% resulted in SEE values of approximately 0.011.

119

Table 16. Comparison of % standard deviation between tablet hardness data and density calculations.

Product		Density SD%	Hardness SD%
hct20	4kg	0.298	9.77
hct20	6kg	0.201	7.06
hct20	9.5kg	0.311	7.51
hct20	12kg	0.438	6.35
	mean	0.312	7.67
hct15	2kg	0.370	13.24
hct15	4kg	0.510	9.31
hct15	6kg	0.625	6.12
hct15	9kg	0.466	3.42
hct15	12kg	0.450	4.98
	mean	0.484	7.41
ctm2	12kg	1.000	3.23
ctm2	9.5kg	0.470	4.60
ctm2	6kg	0.690	7.90
ctm2	4kg	0.370	8.29
ctm2	2kg	0.930	8.57
ctm2	8kg	0.510	6.92
	mean	0.662	6.59
ctm6	12kg	0.284	3.33
ctm6	10kg	0.262	3.76
ctm6	8kg	0.310	5.04
ctm6	6kg	0.220	5.29
ctm6	4kg	0.330	8.10
ctm6	2kg	0.370	12.17
	mean	0.296	6.28

Table 17. NIR density calibration/prediction results for HCTZ 15% tablets.

Calibration					Prediction		
Cal.file	Math	n	r^2	SEE	n	r^2	SEP
c1	MLR	65	-0.985	0.0217	36	0.967	0.0335
c3	MLR	65	-0.994	0.0135	36	0.981	0.0263
c2	MLR	65	0.995	0.0127	36	0.980	0.0266
p1	PLS	65	0.997	0.0109	36	0.981	0.0252
p2	PLS	63	0.997	0.0098	36	0.981	0.0252

Table 18. NIR density calibration/prediction results for HCTZ 20% tablets.

Cal.file	Math	n	Calibration r^2	SEE	n	Prediction r^2	SEP
c1	MLR	52	-0.974	0.0178	28	0.960	0.0220
c2	MLR	52	0.989	0.0119	28	0.980	0.0156
c3	MLR	52	0.968	0.0197	28	0.966	0.0203
c4	MLR	52	0.983	0.0144	28	0.978	0.0167
p1	PLS	52	0.997	0.0062	28	0.994	0.0083

Table 19 NIR density calibration/prediction results for CTM 2% tablets.

		Calibration			Prediction		
Cal.file	Math	n	r^2	SEE	n	r^2	SEP
c1	MLR	78	0.978	0.0204	42	0.976	0.021
c2	MLR	78	0.987	0.0159	42	0.983	0.018
c3	MLR	78	0.982	0.0182	42	0.982	0.018
c4	MLR	78	-0.982	0.0187	42	0.978	0.020
p1	PLS	78	0.994	0.0112	42	0.990	0.014
p2	PLS	77	0.993	0.0118	42	0.988	0.015

Table 20. NIR density calibration/prediction results for CTM 6% tablets.

	Calibration				Prediction		
Cal.file	Math	n	r^2	SEE	n	r^2	SEP
c1	MLR	78	-0.978	0.0224	42	0.978	0.022
c2	MLR	78	0.983	0.0200	42	0.983	0.020
c3	MLR	78	0.983	0.0195	42	0.978	0.022
c4	MLR	78	0.986	0.0179	42	0.991	0.015
p1	PLS	78	0.996	0.0104	42	1.000	0.011
p2	PLS	76	0.996	0.0100	42	0.994	0.012

Overall, PLS models also performed better in the validation process. Although the laboratory density values were less variable than the laboratory hardness values, calibrations produced from hardness data were more rugged than the density models, and were better at predicting hardness. In other words, the models based on hardness contained built-in variability which contributed to the good prediction ability of the hardness calibrations.

1.5   Conclusions

This work presents a viable and non-destructive alternative to hardness testing of tablets. A method was developed which offers the potential of 100% quality control testing for tablet hardness. There is a correlation between the hardness or compression force of a tablet and its NIR spectra. As tablet hardness increased, an upward shift in the raw NIR spectra was observed. This relationship was modeled by the development of formulation specific calibration equations for the determination of hardness via NIRS. The NIR method of hardness testing did not suffer from subjective differences in reading the results. Because the method is non-destructive, the samples can be further tested or even packaged for sale after NIR testing. The use of the iris was important to maintain accurate and reproducible sampling technique.

Equations based on tablet density produced statistically improved models for NIR density determination. Predictions based on tablet density had slightly lower multiple correlation coefficients than predictions based on tablet hardness.

In applying multivariate regression techniques, we are assuming that there is an equation that will best fit all the data in a set. We also assume that a perfect fit of any model to all the data cannot be made because of random errors in the data. Thus, we end up with a list of potential equations that fit our criteria (none of them a perfect fit). Each time we select a different wavelength, or include additional wavelengths in the model, different calibration coefficients result. This reflects the different values of the molar absorptivity

(extinction coefficient) at different wavelengths. The calculation for each calibration coefficient contains a contribution from each constituent at each wavelength[10].

It may not be possible, or desirable to develop a single, global equation for the evaluation of hardness. Since hardness is a physical property for which there is no single analytical wavelength, PLS may be a more reliable approach to calibration. PLS models the entire spectra, not just data at specific wavelengths. The goal in developing a global calibration is "...to cover as broad a range of samples as possible while maintaining acceptable accuracy".[11] Unique equations that are developed for a particular product can secondarily act to identify or qualify the product. In the agricultural industry, a global calibration is one that is designed to analyze 90 to 95% of samples of a given product[12]. Specific calibrations based on a small range of samples typically perform better than general calibrations, provided the samples to be analyzed are represented in the calibration set.

1.6   Considerations for future work

The calibrations developed in this study covered a hardness range of 2 to 12 kg. In a manufacturing setting, a more realistic range of acceptable hardness values would be +/- 20%, at most. In this situation, a slightly different approach to calibration would be required. Rather than manufacturing tablets covering a broad range of hardness values, spectral data from several lots of a product would be collected over a period of time. An acceptable range of hardness would be identified for the product, and a calibration would be developed using the collected data.

In order to fully characterize the potential of NIRS as an alternative to conventional hardness testing, several tablet matrices should be evaluated. A comparison of tablets produced by direct compression versus wet granulation would be useful in the determination of the extent of NIRS utility for hardness testing.

In the current study, second derivative data was used to develop the calibration models. Derivative spectroscopy is a powerful technique for magnifying the fine structure of spectral curves. The result is an enhancement of structure that is offset by a decrease in

126

the signal-to-noise (S/N) ratio. The major advantage is an increase in resolution, which may be very useful for resolving bands that are too close to be resolved in their absorption spectrum. In the case of a physical property, such as tablet hardness, the use of the second derivative spectra may not be desirable since taking derivatives minimizes non-chemical composition effects, such as particle size. Since we are interested in a physical property, it seems logical to include such influences by using the untreated (raw) spectra.

Acknowledgments

References

1) American Society for Testing and Materials, "Standard Practices for Infrared, Multivariate, Quantitative Analysis", Official ASTM Publication No. E1655, pp. 1-25 (1995).

2) Gemperline, P. J. and Boyer, N. R., *Anal. Chem.*, 67(1) pp 160-166 (1995).

3) United States Pharmacopoeia XXIII/National Formulary XVIII, USP Convention, Inc., Rockville, MD, printed by Rand McNally, Taunton, Massachusetts, pp. 1680 (1995).

4) Mark, H., "Data Analysis: Multilinear Regression and Principal Component Analysis", in Handbook of Near-Infrared Analysis, ed. D. A. Burns and E. W. Ciurczak, Marcel Dekker, Inc., New York, NY, pp. 107-158 (1992).

5) Gunsel, W. C., et al, "Tablets", in The Theory and Practice of Industrial Pharmacy, L. Lachman, H. A. Lieberman, and Kanig, J. L., editors, Lea & Febiger, Philadelphia, pp. 305-345 (1970).

6) Reference Manual for Near Infrared Spectral Analysis Software (NSAS) Version 3.30a, NIRSystems, Inc./Perstorp Analytical Co., Silver Spring, MD, pp.3-53 (1995).

7) ibid.

8) Workman, J. J., "NIR Spectroscopy Calibration Basics", in Handbook of Near-Infrared Analysis, ed. D. A. Burns and E. W. Ciurczak, Marcel Dekker, Inc., New York, NY, pp. 247-280 (1992).

9) Workman, J., and Brown, J., *Spectroscopy* 11(2), 48-51 (1996).

10) Mark, H., "Data Analysis: Multilinear Regression and Principal Component Analysis", in Handbook of Near-Infrared Analysis, ed. D. A. Burns and E. W. Ciurczak, Marcel Dekker, Inc., New York, NY, pp. 107-158 (1992).

11) Abrams, S. M., et al, *J. Dairy Sci.* 70, 806-813 (1987).

12) Shenk, J. S., J. J. Workman, Jr., and M. O. Westerhaus, "Applications of NIR Spectroscopy to Agricultural Products", in Handbook of Near-Infrared Analysis. D. A. Burns and E. W. Ciurczak, editors, Marcel Dekker, Inc., New York, pp. 383-431 (1992).

1.1 Abstract

The purpose of this study was to evaluate the effect of matrix and geometry on the determination of tablet hardness via near-infrared reflectance spectroscopy (NIRS). A secondary objective was to evaluate any differences in NIR response due to scoring of a tablet. Flat-faced and convex (scored on one side) tablets were manufactured at five levels of compression force, using two excipient matrices. Blend #1 consisted of chlorpheniramine maleate 6%, magnesium stearate 0.5% and microcrystalline cellulose. Blend #2 contained chlorpheniramine maleate 6%, magnesium stearate 0.5% and dibasic calcium phosphate dihydrate.

Multiple linear regression and partial least squares were used to develop calibration models using NIR spectral data and tablet hardness. Differences in these models enabled comparisons of matrix and geometry, as well as scoring. NIR absorbance data at several individual wavelengths were subject to linear regression and one-way analysis of variance in order to assess the potential of hardness prediction at one wavelength.

Formulation specific calibration models were developed for two tablet matrices and two geometries. NIRS calibration models successfully predicted tablet hardness for both matrices and both geometries. Absorbance (log 1/R) values were higher for convex tablets than flat tablets. Scored tablets produced slightly more variable results than nonscored tablets. Tablets containing dibasic calcium phosphate dihydrate produced more variable hardness and spectral results than those containing microcrystalline cellulose. Models developed for one formulation could not be used to predict hardness in other formulations.

Models developed for flat tablets could not be used to predict hardness for convex tablets. The previously established hardness/NIR relationship was valid for other formulations.

1.2 Introduction

Powdered drugs are generally combined with a number of excipients when formulating solid dosage forms, and then processed into convenient forms for drug administration. It is important to characterize their fundamental powder and processing properties since, in principle, all factors influencing the final compact depend upon them[1].

Consolidation of a particulate solid into a compact or tablet is affected by the way the material behaves under an applied pressure. For example, microcrystalline cellulose is primarily a deforming material, dicalcium phosphate dihydrate fragments and lactose is an intermediate of the two[2]. Once the particles have been brought sufficiently close together, they undergo some form of bonding, such as solid bridge formation, intermolecular forces and mechanical interlocking.

Compressed tablets are characterized by several specifications, including weight, hardness, thickness, shape and diameter. The diameter and shape are defined by the tooling selected for use in the tablet press. Tablets may be of numerous shapes and their surfaces may be flat, concave or convex to varying degrees. Concave punches are used to prepare convex tablets. Tablets may also be scored to facilitate breakage into smaller doses. These characteristics make the tablets distinctive and identifiable with the manufacturer's product[3].

In Manuscript III, near-infrared reflectance spectroscopy (NIRS) was used to develop calibration models capable of predicting tablet hardness. These models were based upon flat faced tablets having no scoring or indentations on their surfaces, and utilized tablets made from only one excipient matrix. It is suspected that a convex surface may produce a different NIR spectrum in response to changes in compression force. It is also suspected that scoring may also affect on the NIR response to hardness, as the surface integrity would be different from an nonscored tablet. The effect of matrix on NIR

calibration was shown by Corti, et al[4], in the comparison of a powder with a gel formulation containing ketoprofen. There are no known studies that examine the effect of tablet matrix on NIR calibration efforts. The current study was undertaken to investigate the effect of tablet geometry, scoring and excipient matrix on the NIR/compression force relationship.

1.3   Experimental

1.3.1   Tablet Manufacture

Flat faced (FF) round and standard round convex (SRC), half-inch diameter tablets were manufactured by direct compression using a Korsch Type PH106-DMS, six-station tablet press, interfaced with Korsch Compression Research System Instrumentation KWS 506A (courtesy of Pfizer Central Research, Pharmaceutical R & D, Groton, Connecticut.). The FF tablets were made first, then the tooling was changed and the SRC tablets were made. The SRC tablets were scored on one side only.

Two formulations were used, differing only in the type of diluent (Table 1). The first blend contained 93.5 % Emcompress® (dicalcium phosphate dihydrate, Edward Mendell Company) and the second contained 93.5% Avicel® PH102 (microcrystalline cellulose, FMC Corporation). Chlorpheniramine maleate (CTM) 6% was the active component and each blend was lubricated with 0.5% magnesium stearate (Fisher Scientific). The basis for selection of the matrices was the behavior of the diluent when compressed. Microcrystalline cellulose compresses due to plastic deformation while dicalcium phosphate dihydrate is known to fracture upon compaction. Each blend was mixed for ten minutes in a 16-quart, twin shell dry blender (Patterson-Kelley). The Emcompress®/CTM blend was screened (20 mesh) after mixing, to reduce lumps of CTM. The CTM for the Avicel®/CTM blend was screened (20 mesh) prior to mixing.

The target weight for the CTM/Emcompress®/magnesium stearate tablets was 800 mg. The target weight for the CTM/Avicel®/magnesium stearate tablets was 540 mg.

After adjusting the tablet press for correct target weight, the hardness level was adjusted to achieve five different levels for each blend.

Target hardnesses of 2, 4, 6, 9, and 12 kg (as monitored by a Heberlein, vector-type Hardness Tester) were used for each combination of blend and geometry for a total of 20 different batches of tablets. The tablet press was adjusted to the desired hardness level, beginning with the lowest level, and monitored for constant tablet hardness. After achieving a constant hardness level, the next ten tablets were collected from each batch, in order, and stored in labeled Whirl-top® plastic bags. The instrumented tablet press recorded compression force data for the first six tablets of the ten collected from each batch. Upper and lower compression forces (in kN, or kilonewtons) and ejection force data were recorded for each batch. This compression data was correlated to the first six reserved tablet samples, for later calibration with NIR data. The tablet press was allowed to continue compressing until approximately 200 tablets per batch were manufactured. The same process was repeated for the next hardness level.

Each batch of tablets was labeled according to geometry, matrix and hardness (low to high) level. Flat-faced Avicel®/CTM tablets were labeled AF1 through AF5. Convex Avicel®/CTM tablets were labeled AC1 through AC5. Flat-faced Emcompress®/CTM were labeled EF1 through EF5, and convex Emcompress®/CTM tablets were labeled EC1 through EC5.

1.3.2 Near-Infrared Spectroscopic Analysis

A Perstorp Analytical/NIRSystems Rapid Content Analyzer® Model 5000 was used for the analyses of tablet samples. This instrument and corresponding setup was described in Manuscript II.

NIR reflectance parameters were set at 32 scans per sample in the range of 1100 to 2500 nm. A ceramic (Coor's Standard) reference scan was taken before each set of samples. Near-infrared reflectance measurements were made on the ten reserved tablets from each batch. The sample to be measured was placed directly above the detector surface

and centered with the iris. Before positioning each sample, the detector surface was gently cleaned of debris. Flat faced (FF) tablets were scanned once on each side. Standard round convex tablets (SRC) were measured twice, alternately, on each side, and given spectral sample names corresponding to score and replicate number.

1.3.3 Tablet Evaluation

After completion of the NIR scans, the ten reserved tablets from each batch were subjected to weight, thickness and hardness testing using a Vector Systems-3 hardness tester, which was interfaced with a Mettler balance, Model AM50. The tablets were manually added to the hardness tester without regard to the orientation of the scoring on the SRC tablets. The order in which the instrument performed these tests was thickness, weight, and then tablet hardness.

The laboratory hardness and compression data were analyzed using Minitab® Statistical Software (Version 8, Student Edition) to test the means. Two-sided t-tests were performed between batches and on consecutive hardness levels to test for equal means.

The individual hardness data was entered into the near-infrared software, NSAS, as constituent number one, hardness. The corresponding upper compression force data was entered into NSAS as constituent number two, upper kN. Lower compression force data was entered into NSAS as constituent number three, lower kN. Thus, there were three constituents for each NIR spectrum: hardness (n=10), upper punch force (n=6), lower punch force (n=6).

1.3.4 Effect of Sample Position of SRC Tablets on the NIR Spectra

Reproducibility of sample position is an important factor in NIR analysis. Flat faced, round tablets can be reproducibly positioned on the detector surface (this experiment was described in Manuscript III) using the iris. However, one might suspect that SRC tablets may be subject to more variation in position since the point of contact between the tablet and the detector surface is so much smaller than that of a flat faced tablet. Scoring of

Table 1. Summary of formulations used in tablet manufacture.

Formulation 1.

		Theoretical	Actual
Chlorpheniramine maleate (CTM)	6.0 %	240.0 g	240.0 g
Emcompress®	93.5 %	3740.0 g	3740.36 g
Magnesium stearate	0.5 %	20.0 g	20.0 g
Total	100.0 %	4000.0 g	4000.36 g

Formulation 2.

		Theoretical	Actual
CTM	6.0 %	240.0 g	240.0 g
Avicel® PH102	93.5 %	3740.0 g	3740.31 g
Magnesium stearate	0.5 %	20.0 g	20.0 g
Total	100.0 %	4000.0 g	4000.31 g

tablets introduces another variable. The SRC tablets manufactured for this study were scored on one side only, enabling the testing of scored versus nonscored samples. A validation study was performed to evaluate the effect of sample position on the NIR spectra of SRC tablets. The effect of scoring on reproducible sample positioning was also examined in this study.

Emcompress®/CTM 6%/magnesium stearate SRC tablets (6 kg hardness) were chosen for this portion of the study. One tablet was placed in the center sampling position using the iris and scanned ten times on each side, removing and flipping the tablet over between scans. First the nonscored side of the tablet was scanned, and then the scored side was scanned. During the analysis of the scored side, an attempt was made to align the score at the same point for each scan.

Next, one tablet was placed in the center position using the iris, and scanned ten times on each side without removing it from the detector surface. The nonscored side was run first, followed by the scored side. In the third phase of the study, ten tablets were scanned once on each side in the center position, using the iris.

Finally, one tablet was scanned in ten positions on the detector surface. The methods for this study were previously described and illustrated in Manuscript III (Figure 1 in section 1.3.4). Beginning with the center position, the tablet was moved to the 12:00 (twelve o'clock) position, then rotated to a position 45° from the previous spot. At each rotation, one edge of the tablet was touching the center position. The 12:00 position was repeated, as position number ten. The resulting spectra were entered into spectral libraries, where the mean and standard deviation spectra were extracted for each condition. Standard deviation spectra were plotted and compared.

1.3.5   Near-Infrared Calibration of Hardness and Compression Force

Table 2 summarizes the numerous spectral data sets that were created for the calibration process. FF tablet spectral data for the general calibration was the average of two replicates per tablet. SRC data was treated in three separate ways: 1) all four replicates

per sample were averaged (two scored replicates and two nonscored replicates from each tablet), 2) data from the scored sides (n=2) of the samples were averaged, and 3) data from the non-scored sides (n=2) were averaged. The subsets of scored and nonscored data were used for separate calibrations.

Constituent #1, hardness, was calibrated first. Calibration sets were created from the averaged spectra by using the Sample Select function of NSAS™, which selected six spectra from each level of hardness, based on a "boxcar" distribution. The software selects the spectra having the most variation in the set. Thus, the calibration set AF contained hardness and spectral data from six tablets at each of five hardness levels of flat tablets of the Avicel® / chlorpheniramine/ magnesium stearate blend, for a total of 30 calibration samples. The calibration set AC was composed of SRC tablets at five hardness levels, containing Avicel® /chlorpheniramine/ magnesium stearate blend. The calibration set EF was comprised of flat tablets at five hardness levels, containing Emcompress®/CTM/ magnesium stearate blend. The calibration set EC was composed of SRC tablets at five hardness levels, containing Emcompress®/CTM/ magnesium stearate.

A separate calibration set was needed to test the second and third constituents, upper and lower compression force. This was because compression data was available for only six tablets from each batch. The same sample selection process was followed, except four spectra per batch were selected by the computer from the samples having associated compression data, and the remaining two spectra from each batch were used in the validation (prediction) set.

Each subset of spectral data was converted to the second derivative. Standard multiple linear regression (MLR) and partial least squares regression (PLS) were performed on each calibration set. One to three wavelengths were used for each MLR model. PLS regression was limited to eight factors and the wavelength range was 1100 to 2500 nm. Equations were developed from second derivative and "raw" (untreated) spectral data.

Table 2. Summary of spectral data sets for hardness calibration (H-Cal.) and compression force (C-Cal.)

Matrix	Cal. group	Cal. file name	n per hardness level	n per H-Cal. Set	n per C-Cal. Set
Avicel	general	AC	4	30	-
	SRC- scored	ACS	2	30	-
	SRC-nonscored	ACN	2	30	-
	Flat	AF	2	30	20
Emcompress	General	EC	4	30	-
	SRC- scored	ECS	2	30	-
	SRC-nonscored	ECN	2	30	-
	Flat	EF	2	30	20

Validation sets for hardness were created using the remaining four spectra from each batch of tablets (for a total of 20 validation samples per formulation). Validation of the models was performed using the Percent Predict function of NSAS™. Equations that were developed for one calibration set were applied to the corresponding validation set (of the same math treatment), as well as validation sets from other blends, to test their fit.

The subsets of scored and nonscored data were compared chemometrically to detect spectral differences. Mean and standard deviation spectra for each subset were calculated using the $IQ^{2™}$ function of NSAS. Standard deviation spectra of raw and second derivative data were compared to evaluate differences between scored and nonscored sides of the samples. Calibration equations for hardness were also developed for the scored and nonscored data, as described above.

1.4 Results

1.4.1 Results of Tablet Evaluation

The results of the evaluation of physical tablet parameters for Avicel®/CTM FF and SRC tablets are summarized in Tables 3 and 4. Emcompress® /CTM FF and SRC tablet data are summarized in Tables 5 and 6. All hardness, thickness and weight evaluations were completed within one week of the date of tablet manufacture. Good reproducibility was achieved in all batches for tablet weight and thickness. Avicel® /CTM tablet weights varied from 0.54% to 1.84% (relative standard deviation, RSD) and thickness varied from 0.59% to 1.42%. Emcompress® /CTM tablet weights varied from 0.30% to 0.49% and thickness varied from 1.07% to 2.10%.

It was generally noted in all formulations that an increase in tablet hardness was associated with an increase in variability (RSD). Hardness values for the Avicel® /CTM batches varied from 3.3% to 11.2%. Variation in Emcompress® /CTM tablets ranged from 1.70% to 10.7%. In the Emcompress® /CTM formulations, data from the two highest hardness levels contained several extremely low values which were eliminated from the data set (summary table does not include the deleted values). These were: SRC level 4

(n=2), SRC level 5 (n=5), FF level 4 (n=1) and FF level 5 (n=4). No outliers were initially detected in the Avicel® /CTM hardness data. Hardness testing of scored tablets may occasionally result in a false value if the score is aligned with the applied crushing force. Orientation of scoring on SRC tablets during hardness testing may have contributed to the variability in the hardness data.

Calculation of the reference standard error for hardness is summarized in Table 7. Deletion of outlying hardness values for Emcompress® /CTM FF tablets resulted in a SE of 0.39 (kg), the same value as Avicel® /CTM FF tablets. The SE for EC tablets was 0.58, and for AC it was 0.68. The matrix SE was 0.49 for all Emcompress® /CTM tablets, and 0.54 for all Avicel®/CTM tablets. The geometry SE for all SRC tablets was 0.63, and 0.39 for all flat tablets. The overall SE for all tablets analyzed in the experiment was 0.51 kg.

Hardness data from two batches of the Emcompress®/CTM SRC tablets were found to have equal means. Hardness level 4 (9.41 ± 0.97 kg) was determined to be not significantly different (p= 0.05) from hardness level 5 (9.86 ± 1.29 kg). In contrast to this finding, the corresponding upper and lower compression force data did not follow the same pattern. The five levels of upper and lower compression force were found to be significantly different (p= 0.05) from one another in these batches.

A comparison of average hardness data was made between FF and SRC tablets at each hardness level for both formulations (Table 8). In other words, EF data at hardness level 1 was compared to EC hardness level 1, AF data at hardness level 1 was compared to AC hardness level 1, etc. Emcompress/CTM means were equal for hardness levels 1 through 4. Avicel/CTM means were equal only at hardness level 5. (This was an important piece of information for later spectral comparisons. It might not be useful to compare, for example, spectra of EF tablets at hardness level 2 to EC tablets at hardness level 2 if the actual hardness means were not equal).

Table 3.   Summary of weight, thickness and hardness data for Avicel/CTM 6%
/magnesium stearate flat 1/2" round tablets (AF).

Product	Weight (g) ± St.Dev. (RSD%)	Thick (cm) ± St.Dev. (RSD%)	Hardness (kg) ± St.Dev. (RSD%)
AF1	0.539 ± 0.009 (1.666)	0.552 ± 0.005 (0.841)	2.30 ± 0.26 (11.23)
AF2	0.551 ± 0.005 (0.970)	0.503 ± 0.004 (0.888)	4.23 ± 0.23 (5.35)
AF3	0.550 ± 0.004 (0.696)	0.453 ± 0.003 (0.591)	6.93 ± 0.29 (4.20)
AF4	0.545 ± 0.003 (0.546)	0.410 ± 0.003 (0.752)	9.87 ± 0.33 (3.34)
AF5	0.545 ± 0.008 (1.544)	0.380 ± 0.004 (1.096)	13.81 ± 0.84 (6.10)

Table 4.   Summary of weight, thickness and hardness data for Avicel/CTM 6%
            /magnesium stearate SRC 1/2" round tablets (AC).

Product	Weight (g) ± St.Dev. (RSD%)	Thick (cm) ± St.Dev. (RSD%)	Hardness (kg) ± St.Dev. (RSD%)
ACH1	0.540 ± 0.005 (0.900)	0.626 ± 0.008 (1.220)	3.00 ± 0.25 (8.31)
ACH2	0.540 ± 0.005 (0.890)	0.552 ± 0.007 (1.348)	6.37 ± 0.26 (4.06)
ACH3	0.544 ± 0.009 (1.612)	0.523 ± 0.006 (1.126)	8.59 ± 0.78 (9.04)
ACH4	0.545 ± 0.008 (1.410)	0.490 ± 0.007 (1.339)	12.06 ± 0.84 (6.99)
ACH5	0.542 ± 0.010 (1.835)	0.472 ± 0.007 (1.421)	14.25 ± 1.27 (8.90)

Table 5.   Summary of weight, hardness and thickness data for CTM 6%
            /Emcompress/Magnesium Stearate flat 1/2" round tablets (EF).

Product	Weight (g) ± St. Dev. (RSD%)	Thick (cm) ± St. Dev. (RSD%)	Hardness (kg) ± St. Dev. (RSD%)
EFH1	0.790 ± 0.003 (0.327)	0.347 ± 0.007 (2.104)	3.37 ± 0.21 (6.23)
EFH2	0.795 ± 0.002 (0.295)	0.333 ± 0.005 (1.544)	5.89 ± 0.25 (4.24)
EFH3	0.791 ± 0.004 (0.489)	0.325 ± 0.005 (1.619)	8.25 ± 0.14 (1.70)
EFH4	0.796 ± 0.004 (0.473)	0.321 ± 0.005 (1.405)	11.01 ± 0.49 (4.45)
EFH5	0.799 ± 0.003 (0.396)	0.307 ± 0.004 (1.208)	14.53 ± 0.85 (5.85)

Table 6.   Summary of weight, thickness and hardness data for Emcompress/CTM 6%
             /magnesium stearate SRC 1/2" round tablets.

Product	Weight (g) ± St.Dev.(RSD%)	Thick (cm) ± St.Dev.(RSD%)	Hardness (kg) ± St.Dev.(RSD%)
ECH1	0.809 ± .002 (0.290)	0.442 ± 0.008 (1.74)	3.28 ± 0.14 (4.27)
ECH2	0.803 ± 0.004 (0.458)	0.424 ± 0.005 (1.257)	6.11 ± 0.21 (3.44)
ECH3	0.806 ± 0.002 (0.301)	0.417 ± 0.005 (1.259)	7.94 ± 0.29 (3.60)
ECH4	0.809 ± 0.003 (0.392)	0.413 ± 0.004 (1.074)	9.41 ± 0.97 (10.31)
ECH5	0.811 ± 0.003 (0.377)	0.406 ± 0.005 (1.337)	9.86 ± 1.29 (13.1)

Table 7. Calculation of Standard Error (SE) for Pfizer Hardness Tester. Results are in kilograms (kg).

Hardness Level	EF sd	EC sd	AF sd	AC sd
1	0.21	0.14	0.26	0.25
2	0.25	0.21	0.23	0.26
3	0.14	0.29	0.29	0.78
4	0.49	0.97	0.33	0.84
5	0.85	1.29	0.84	1.27
SE-product	0.39	0.58	0.39	0.68
SE- Emcompress	0.49		SE-Avicel	0.54
SE flat	0.39		SE SRC	0.63
		Overall SEE= 0.51		

KEY: EF   Emcompress/CTM flat faced tablets

               EC   Emcompress/CTM SRC tablets

               AF   Avicel/CTM flat faced tablets

               AC   Avicel/CTM SRC tablets

Table 8. Comparison of hardness means between EF versus EC and AF versus AC tablets (as determined by two-sided t-test).

EF Hardness (kg) mean ± St.Dev. (RSD)	EC Hardness (kg) mean ± St.Dev. (RSD)	Equal Means?	p
3.37 ± 0.21 (6.2%)	3.28 ± 0.14 (4.3%)	=	0.27
5.89 ± 0.25 (4.2%)	6.11 ± 0.21 (3.4 %)	=	0.05
8.25 ± 0.14 (1.7%)	7.94 ± 0.29 (3.6 %)	=	0.0099
11.01 ± 0.49 (4.5%)	9.41 ± 0.97 (10.3%)	=	0.0018
14.53 ± 0.85 (5.9%)	9.86 ± 1.29 (13.1%)	≠	-

AF Hardness (kg) mean ± St.Dev. (RSD)	AC Hardness (kg) mean ± St.Dev. (RSD)	Equal Means?	p
2.30 ± 0.26 (11.2%)	3.0 ± 0.25 (8.3%)	≠	-
4.23 ± 0.23 (5.4%)	6.37 ± 0.26 (4.1%)	≠	-
6.93 ± 0.29 (4.2%)	8.59 ± 0.78 (9.0%)	≠	-
9.87 ± 0.33 (3.3%)	12.06 ± 0.84 (7.0%)	≠	-
13.81 ± 0.84 (6.1%)	14.25 ± 1.27 (8.9%)	=	0.24

A comparison of average hardness means was also made between formulations of the same geometry and hardness level (Table 9). The purpose of these comparisons was to evaluate the spectral differences between excipients (matrices) at one hardness level. Mean hardness values for AC and EC were found to be equal at hardness levels 1, 2 and 3. Mean hardness for AF at level 5 was found to be equal to EF at level 5 ($p = 0.13$).

Avicel®/CTM upper (UC) and lower (LC) compression force data is summarized in Table 10. Variability (% RSD) in compression data was generally from 2 to 5.7%. UC and LC data for Emcompress®/CTM tablets are summarized in Table 11. Emcompress®/CTM compression data was less variable than Avicel®/CTM data (0.73 to 2.5%) with the exception of EF5, which varied by over 25%.

In order to achieve the desired levels of tablet hardness, significantly greater compression forces were required to compress tablets containing Emcompress®. UC forces required for Avicel®/CTM batches ranged from 1.8 to 5.1 kN, while those for Emcompress®/CTM tablets ranged from 6.7 to 22.7 kN. This was partially due to the fact that Emcompress® has a higher bulk density than Avicel®. Particle size distributions also differ between the two excipients. Emcompress® bulk tapped density was reported to be 0.99 g/ml (per the manufacturer's certificate of analysis). Its density is 2.89 g/cm³. The average particle size is 120 to 150 μm. Emcompress® is a crystalline solid or powder, consisting of granules of which over 95% are less than 425 μm and less than 15% are under 75 μm. It is not known to be hygroscopic[5]. Compaction of dibasic calcium phosphate takes place primarily by brittle fracture. Due to its abrasive nature, it is important to include a lubricant in the tablet formulation.

Avicel® PH102 (microcrystalline cellulose) is a crystalline powder composed of porous particles. Its bulk density is 0.3 g/ml³ and its density is 1.55 g/cm³. Typical mean particle size is 20 to 200 μm. Particle size distribution consists of less than 8% of particles greater than 250 μm and over 45% of particles greater than 75μm. The moisture content of Avicel® is less than 5.0% but it is known to be hygroscopic[6].

147

Table 9.   Comparison of hardness means between AF versus EF and AC versus EC tablets (as determined by two-sided t-test).

AF Hardness (kg) mean ± St.Dev. (RSD)	EF Hardness (kg) mean ± St.Dev. (RSD)	Equal Means?	p
2.30 ± 0.26 (11.2%)	3.37 ± 0.21 (6.2%)	≠	-
4.23 ± 0.23 (5.4%)	5.89 ± 0.25 (4.2%)	≠	-
6.93 ± 0.29 (4.2%)	8.25 ± 0.14 (1.7%)	≠	-
9.87 ± 0.33 (3.3%)	11.01 ± 0.49 (4.5%)	≠	-
13.81 ± 0.84 (6.1%)	14.53 ± 0.85 (5.9%)	=	0.13

AC Hardness (kg) mean ± St.Dev. (RSD)	EC Hardness (kg) mean ± St.Dev. (RSD)	Equal Means?	p
3.0 ± 0.25 (8.3%)	3.28 ± 0.14 (4.3%)	=	0.0079
6.37 ± 0.26 (4.1%)	6.11 ± 0.21 (3.4 %)	=	0.025
8.59 ± 0.78 (9.0%)	7.94 ± 0.29 (3.6 %)	=	0.030
12.06 ± 0.84 (7.0%)	9.41 ± 0.97 (10.3%)	≠	-
14.25 ± 1.27 (8.9%)	9.86 ± 1.29 (13.1%)	≠	-

Table 10.   Avicel/CTM Compression Data Summary (AF= flat faced tablets; AC = SRC tablets at hardness levels H1 to H5).

	Upper, kN			Lower, kN		
	Mean	St. Dev.	% RSD	Mean	St. Dev.	% RSD
AF-H1	1.789	0.036	2.04	1.066	0.025	2.367
AF-H2	2.218	0.047	2.109	1.413	0.033	2.344
AF-H3	2.835	0.060	2.113	1.924	0.041	2.117
AF-H4	3.520	0.133	3.774	2.491	0.099	3.977
AF-H5	4.260	0.220	5.162	3.072	0.177	5.755
AC-H1	1.912	0.054	2.834	1.145	0.035	3.093
AC-H2	2.886	0.115	3.977	1.906	0.075	3.952
AC-H3	3.465	0.152	4.386	2.368	0.102	4.301
AC-H4	4.335	0.173	3.982	3.062	0.129	4.212
AC-H5	5.075	0.190	3.736	3.674	0.147	4.007

Table 11.   Emcompress/CTM Compression Data Summary (EF= flat faced tablets;
              EC= SRC tablets at hardness levels H1 to H5).

	Upper, kN			Lower, kN		
	Mean	St. Dev.	% RSD	Mean	St. Dev.	% RSD
EC-H1	6.755	0.133	1.963	4.935	0.064	1.294
EC-H2	11.633	0.206	1.774	8.417	0.099	1.172
EC-H3	14.811	0.185	1.249	10.771	0.089	0.823
EC-H4	17.535	0.210	1.197	12.848	0.102	0.793
EC-H5	22.661	0.241	1.065	16.779	0.122	0.730
EF-H1	6.690	0.159	2.377	4.911	0.125	2.542
EF-H2	10.624	0.201	1.894	7.709	0.112	1.458
EF-H3	14.148	0.247	1.743	10.219	0.152	1.487
EF-H4	17.600	0.297	1.690	12.801	0.176	1.378
EF-H5	21.487	5.482	25.512	15.733	4.060	25.806

It must be noted that the formulations chosen for this study were composed of a minimum number of components, and thus were not optimized. The goal was to create a comparison between blends containing the same concentrations of active and lubricant, so as not to introduce additional variables. In practice, it would be unlikely for a tablet to be manufactured using over 90% of one major excipient. This factor may be responsible for some of the variability in the Emcompress®/CTM hardness data.

UC force varied from 2.04% to 5.16% for all Avicel®/CTM batches. Emcompress®/CTM compression force data was considerably more variable than the Avicel®/CTM data. The highest level of compression force for the flat Emcompress®/CTM tablets was responsible for a 25.5% variation: the lower four levels of flat-faced tablets ranged from 1.69% to 2.38%. Compression force for Emcompress®/CTM SRC tablets varied from 1.07% to 1.96%.

1.4.2 Results of NIR Spectral Analysis

The effect of blending Emcompress® with CTM and magnesium stearate is demonstrated in Figure 1. This plot compares the raw NIR spectrum of Emcompress® powder (alone) with that of the blended formulation. The spectra have similar shapes except for the two small peaks between 2100 and 2300 nm on the blend spectrum.

In Figure 2, the raw spectrum of the Emcompress®/CTM/magnesium stearate blend is plotted with the average spectrum of the FF tablets (n=10) at each of five hardness levels. (Note: unless otherwise indicated, all spectral plots represent the average of 10 tablets). This plot demonstrates the effect of varying the compression force on the blend. As the hardness (compression force) was increased, the absorbance value also increased. The spectrum of the uncompressed powder blend shifted slightly between the spectra of the second and third hardness levels.

Figure 3 is the raw spectrum of the Emcompress®/CTM/magnesium stearate blend plotted with the spectra of the SRC tablets at each of five hardness levels. The spectrum of the powder blend was in close proximity to the lower level hardness tablets. The powder

151
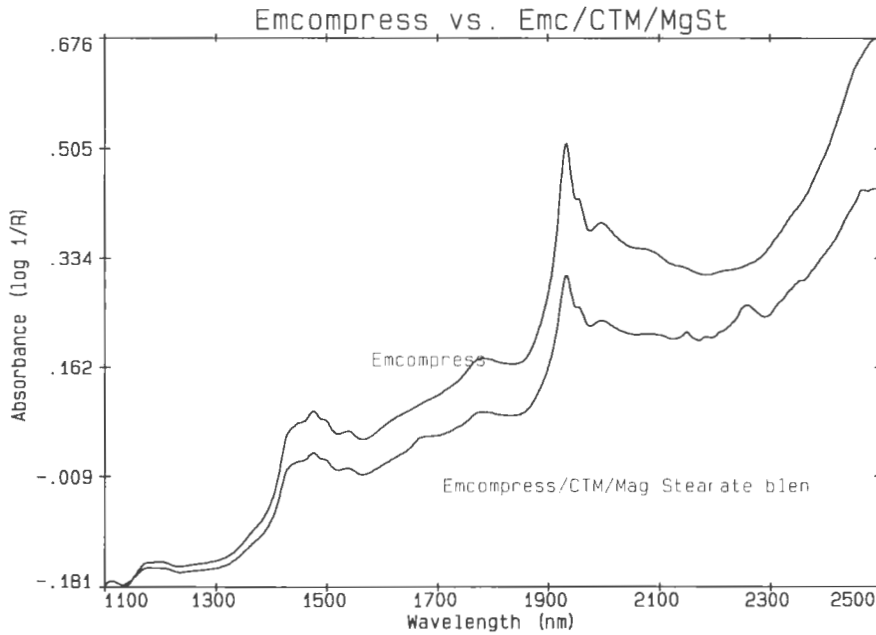
Figure 1. Raw spectral plot of Emcompress® versus Emcompress®/ CTM/magnesium stearate blend.
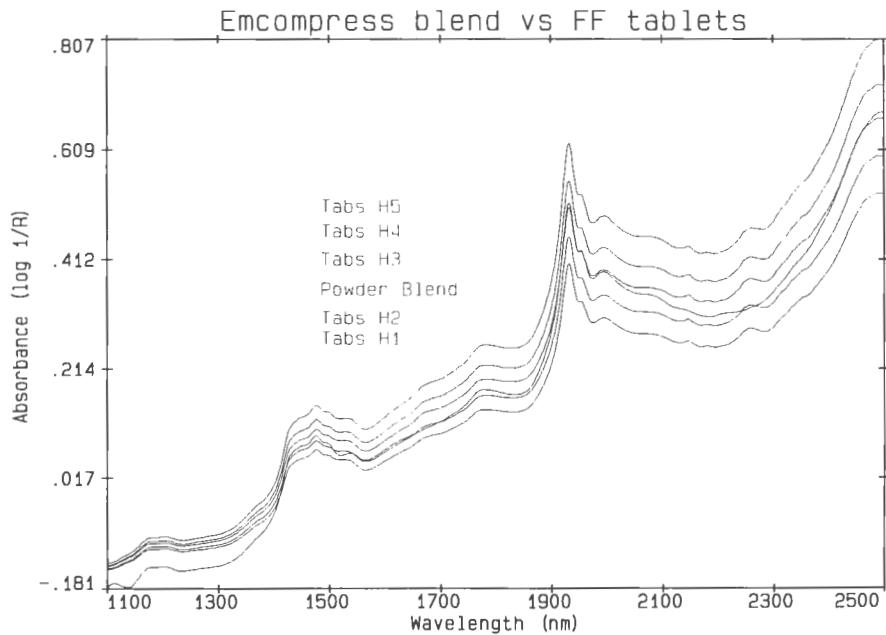
Figure 2. Raw spectral plot of Emcompress ®/CTM/magnesium stearate FF tablets versus blend.
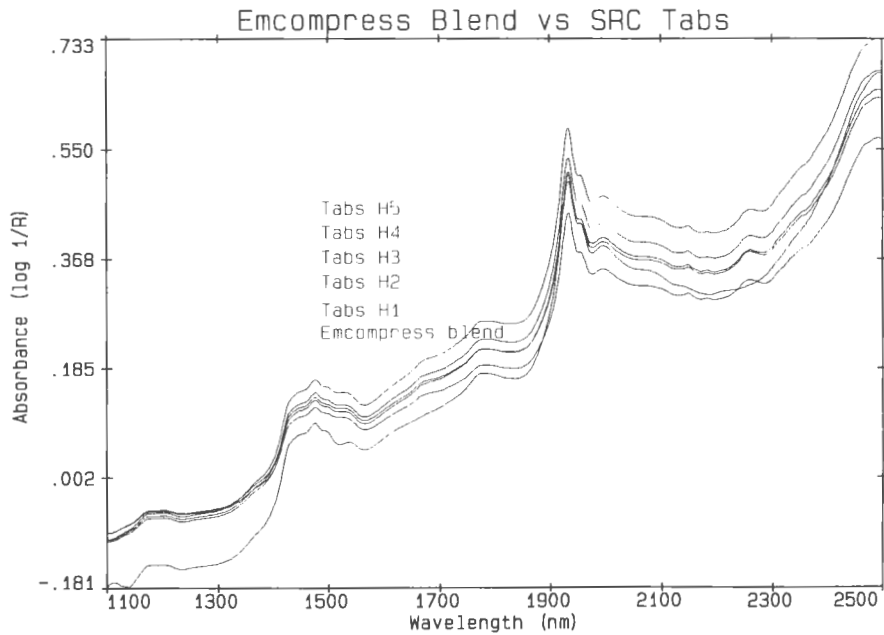
Figure 3. Raw spectral plot of Emcompress®/CTM/magnesium stearate SRC tablets versus blend.

blend spectrum deviates most from the tablet spectrum in the region of 1100 nm to approximately 1900 nm.

The difference between the flat and SRC Emcompress®/CTM tablets is shown in Figure 4. Here, the high and low hardness level tablets of each geometry type were plotted together. The two upper spectra compare flat to SRC tablets at hardness level 5. At hardness level 5, the mean hardness value for the SRC tablets was 9.86 ± 1.29 kg, while that of the FF tablets was 14.5 ± 0.85 kg. Thus, due to the large difference in the hardness data at this level, a direct comparison of the spectra based on hardness at this level is not possible. The plot at hardness level 5 shows a higher absorbance for the FF tablets in comparison to the SRC tablets. At hardness level 1, absorbance values are higher for the SRC tablets (hardness means were equal at level 1).

Figure 4 also demonstrates the large increase in absorbance for both tablet shapes when the compression force was increased. Hardness level 1 represents an applied upper compression force of 6.76 ($\pm$ 0.13) kN for both types of tablet geometry. The upper compression force at hardness level 5 was 22.66 ($\pm$ 0.24) kN.

Observation of the pattern of the spectra in Figure 4 reveals striking similarities between FF and SRC tablets. The chemical composition of the sample is responsible for the unique spectrum of the formulation. We can see that tablet hardness and geometry do not affect this uniqueness; instead, these physical changes are responsible for the drifting baseline and "peak" shifts in the spectra.

Figures 5 and 6 are the second derivative spectra of FF Emcompress®/CTM tablets at five hardness levels in two different wavelength ranges. Each plot illustrates the change in absorbance as the tablet hardness is increased. At numerous maxima and minima, there appeared to be the same degree of increase in absorbance in response to increasing hardness.
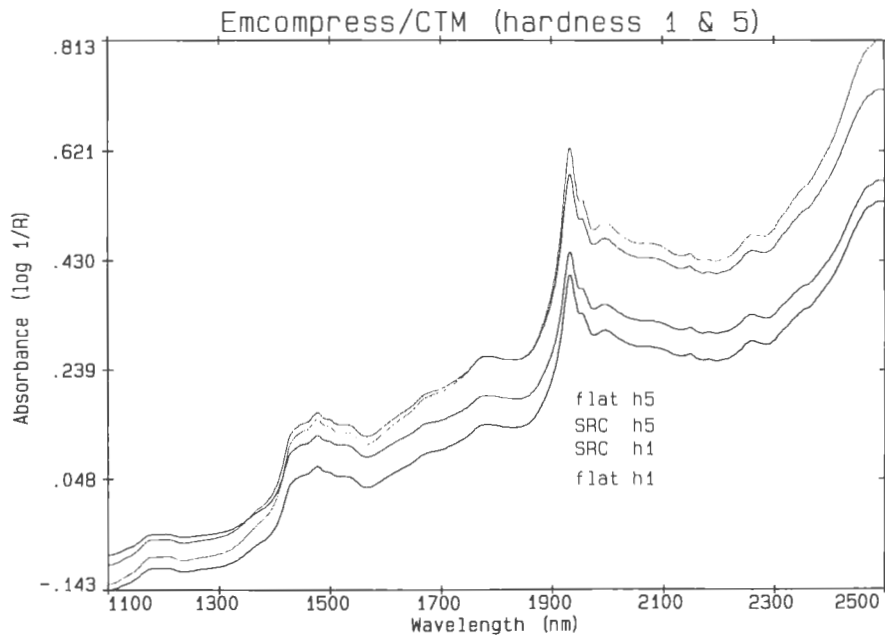
Figure 4. Raw spectral plot of Emcompress[tt]/CTM/magnesium stearate hardness 1 versus hardness 5 (SRC versus FF)
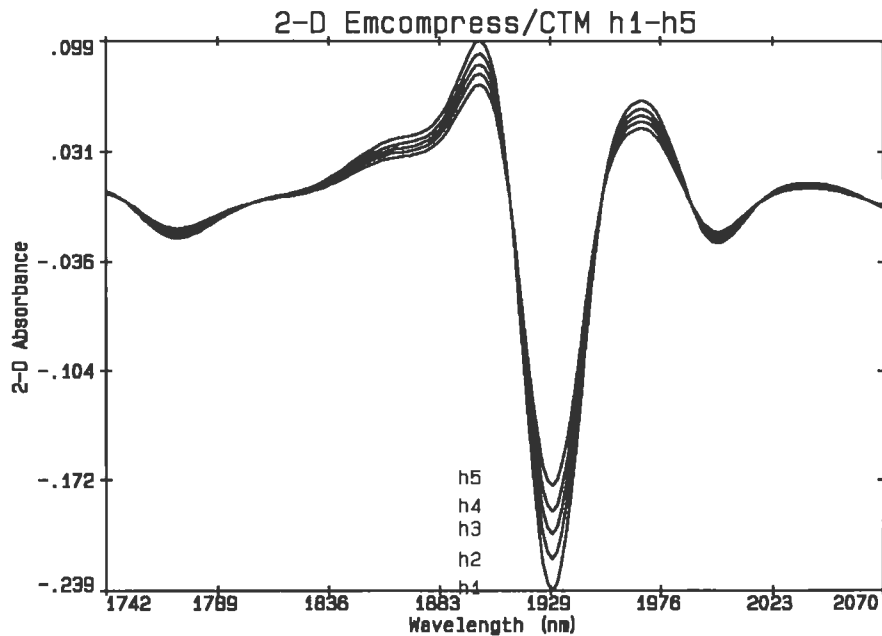
Figure 5. Second derivative plot of Emcompress®/CTM/magnesium stearate tablets at hardness level 1 versus level 5 in 1742 nm to 2070 nm.
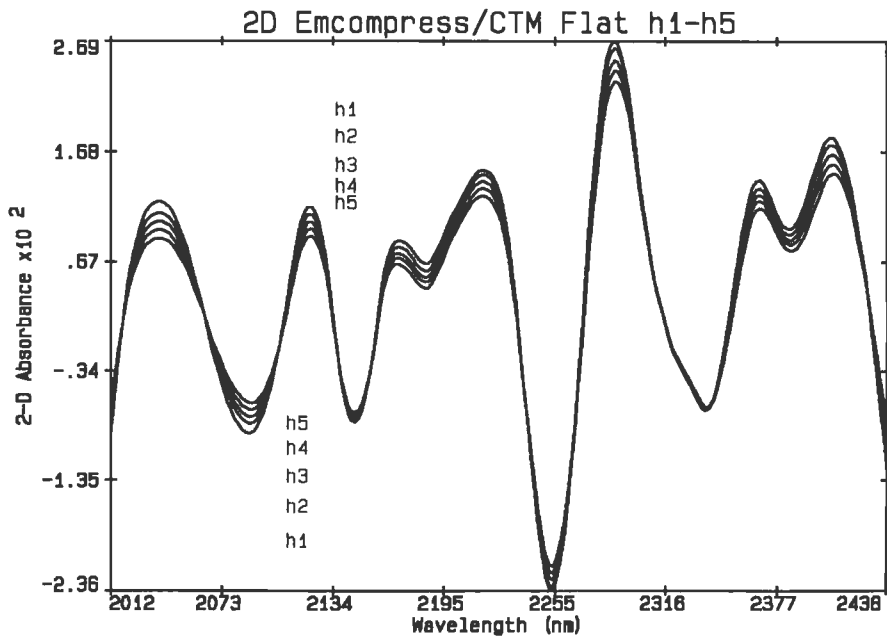
Figure 6. Second derivative plot of Emcompress®/CTM/magnesium stearate tablets at hardness level 1 versus level 5 in 2012 nm to 2438 nm.

Figures 7 through 11 compare the raw spectra of FF versus SRC Emcompress®/ CTM tablets at each hardness level. Reference to the data in Table 8 will be useful for reviewing Figures 7 through 11. As discussed earlier, the mean values for hardness for Emcompress®/ CTM tablets were equal for hardness levels 1, 2, 3 and 4, and so direct comparisons could be made about the effect of tablet geometry. In each of these four plots, the absorbance of the SRC tablets was higher in comparison to the FF tablets. It is also noted that the FF and SRC spectra partially overlap in the 1900 nm region (water band). It would be expected to find the same concentration of water in the two batches, since they originated from the same blend. However, the maximum absorbance at about 1930 nm was higher in the SRC tablets for all but hardness level 3 spectra. In Figure 11, a direct comparison could not be made since the mean hardness values at level 5 were not equivalent.

Figure 12 is the raw spectrum of Avicel® /CTM/magnesium stearate powder blend plotted with that of the FF Avicel® /CTM/magnesium stearate tablets (n=10) at five hardness levels. In the region of 1100 nm to approximately 2100 nm, the absorbance of the powder blend spectrum is much lower than the absorbance of the FF compressed tablets. From 2100 nm to 2500 nm, the powder blend spectrum falls much closer to the tablet spectrum. In Figure 13, a similar comparison is made between the powder blend and the compressed SRC tablets at five hardness levels. Again, the greatest amount of difference is seen from 1100 nm to about 2100 nm, where the powder blend spectrum is closer to the tablet spectrum.

In contrast to the observation of the deviation of powder blends from the tablet spectrum (deviation on the left side of the plots), the tablet spectra behaved in the opposite fashion. The tablet response to increasing compression force was greatest on the right side of the plots. In each of the plots comparing tablet spectra, the raw spectra were often indistinguishable in the 1100 nm to 1500 nm region. Increases in absorbance due to increasing compression force were not noted until 1500 nm.
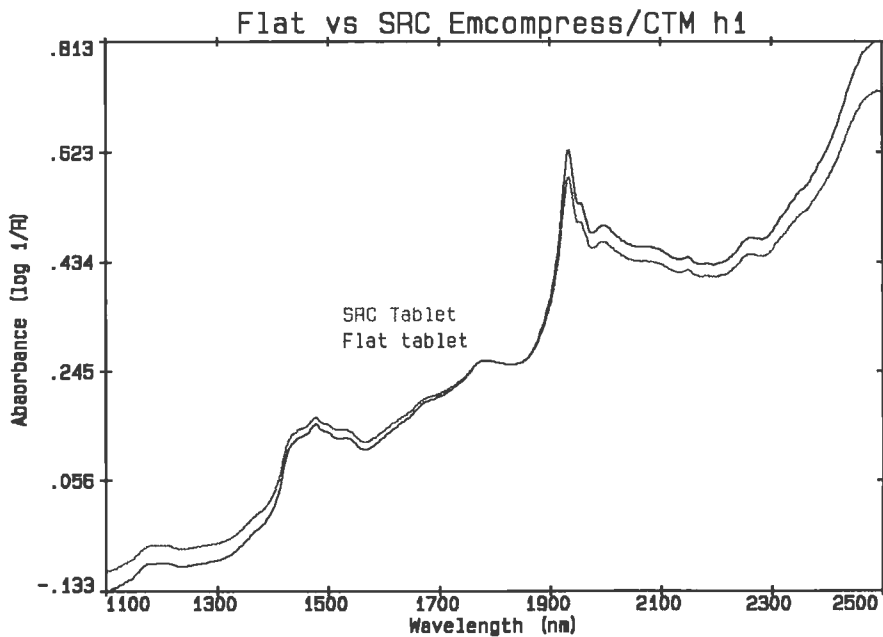
Figure 7. Raw spectral plot of Emcompress®/CTM/magnesium stearate FF versus SRC tablets at hardness level 1.
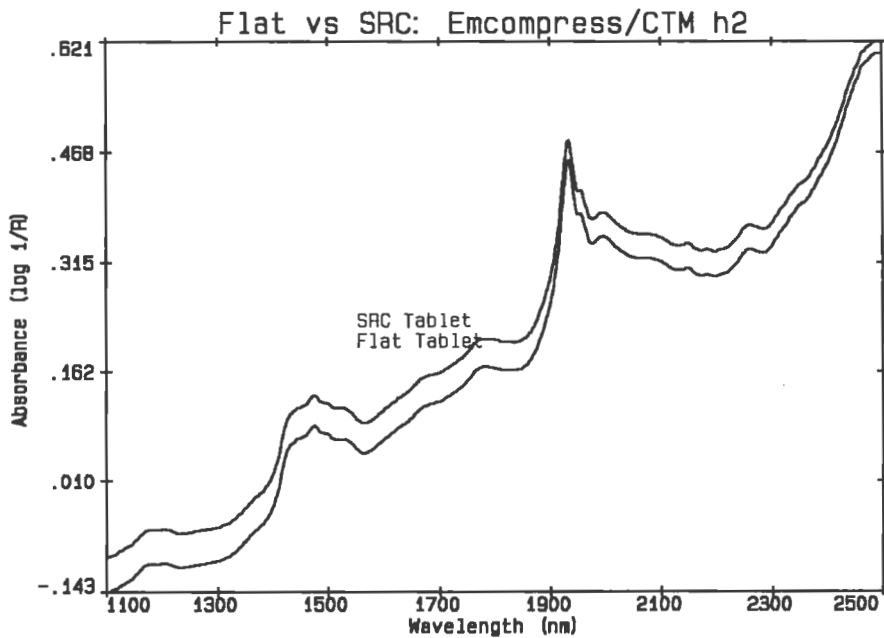
Figure 8. Raw spectral plot of Emcompress®/CTM/magnesium stearate FF versus SRC tablets at hardness level 2.
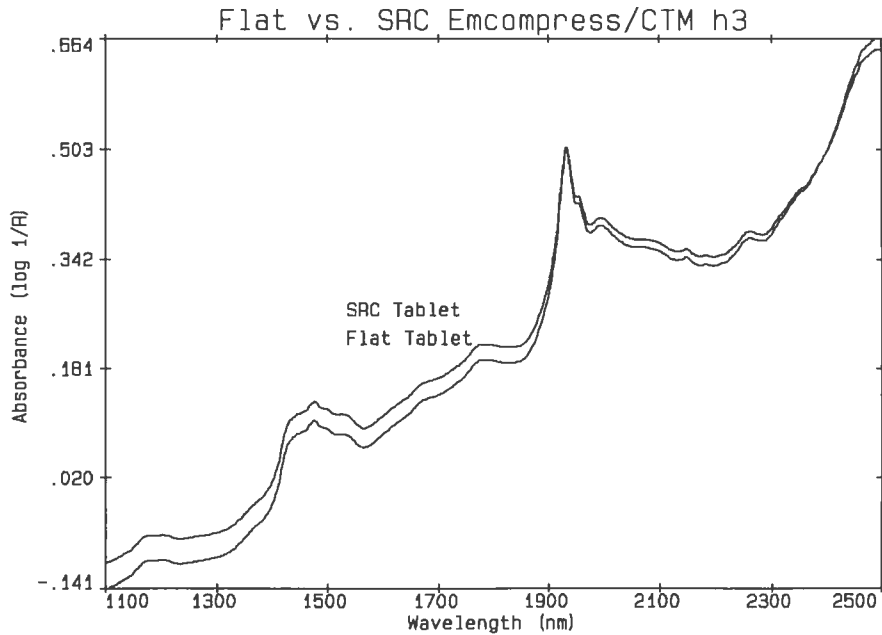
Figure 9. Raw spectral plot of Emcompress®/CTM/magnesium stearate FF versus SRC tablets at hardness level 3.
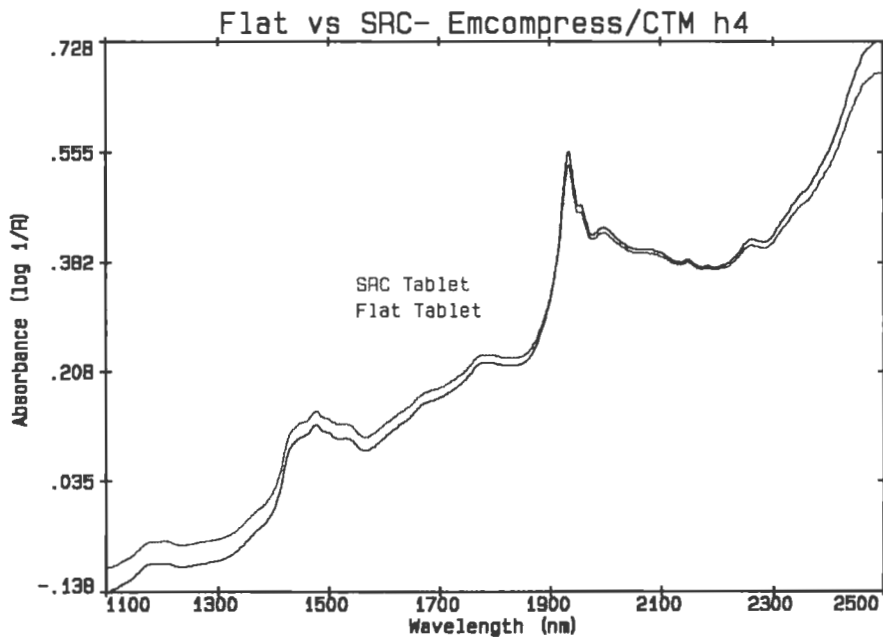
Figure 10. Raw spectral plot of Emcompress®/CTM/magnesium stearate FF versus SRC tablets at hardness level 4.
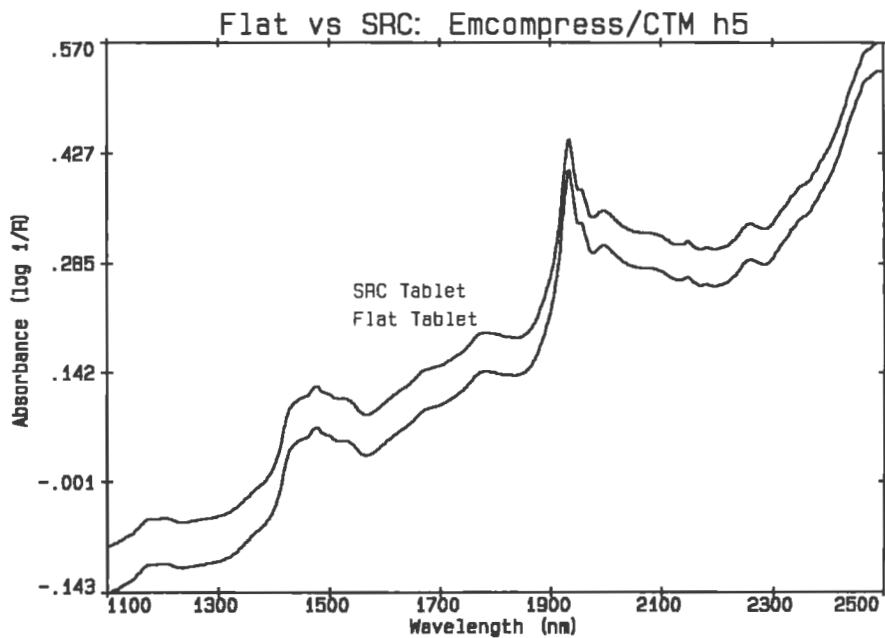
Figure 11. Raw spectral plot of Emcompress®/CTM/magnesium stearate FF versus SRC tablets at hardness level 5.
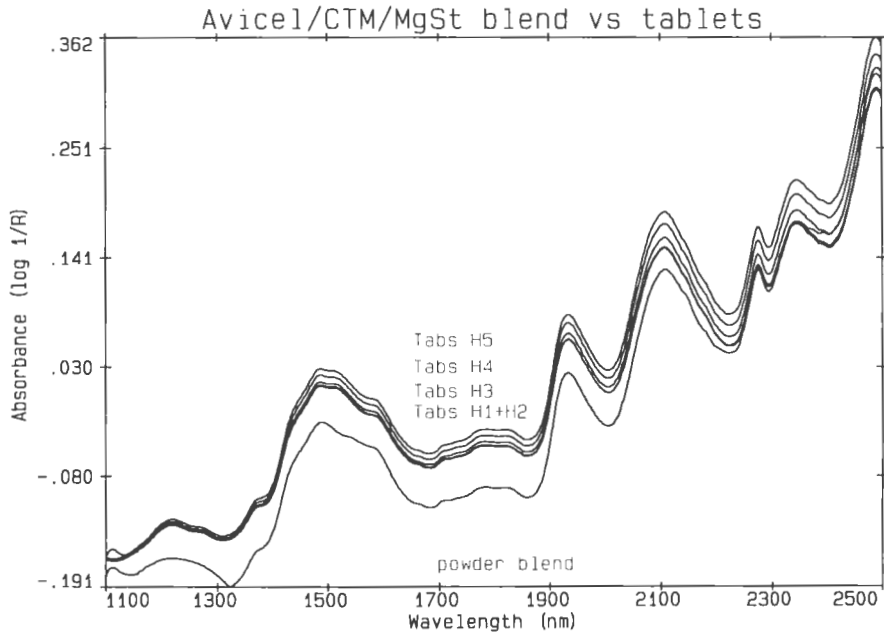
Figure 12. Raw spectral plot of Avicel[®]/CTM/magnesium stearate flat-faced tablets versus blend.
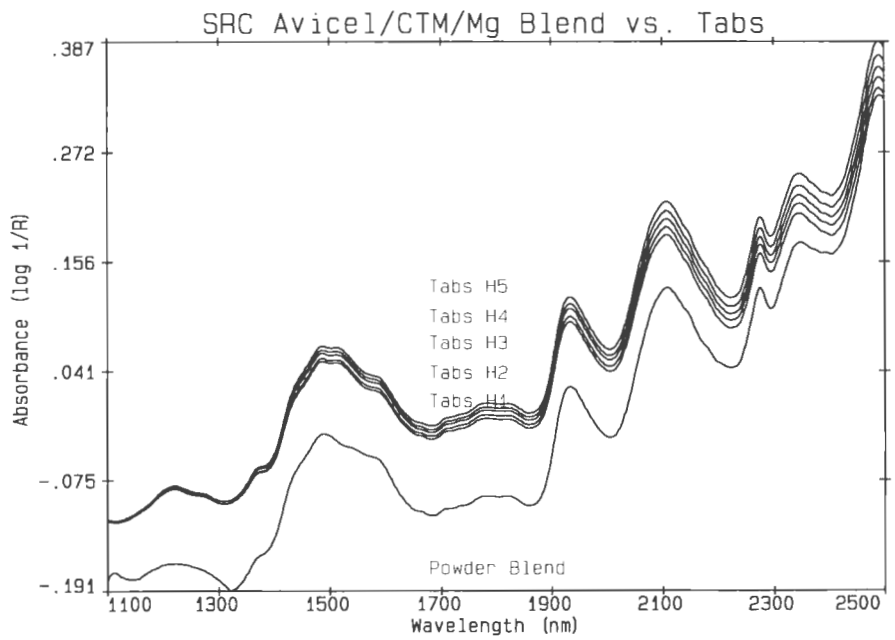
Figure 13. Raw spectral plot of Avicel[r]/CTM/magnesium stearate SRC tablets versus blend.

The raw spectra of FF and SRC Avicel® /CTM/magnesium stearate tablets are compared in Figure 14. The spectra of five hardness levels of SRC tablets were plotted against the spectra of five hardness levels of FF tablets. In the region from 1100 nm to 1500 nm, each set of samples was practically overlayed. From approximately 1475 nm, the effects of increasing compression force are manifested in the spectra. The maximum absorbance of the SRC tablets was greater than that of the FF tablets.

Figure 15 is a second derivative plot comparing the FF and SRC tablets at the highest and lowest hardness levels. The absorbance of the Avicel®/CTM SRC tablets was slightly greater than that of the FF tablets. The difference between Avicel®/CTM FF and SRC tablets was small in comparison to that seen with the Emcompress®/CTM tablets. This expanded view (in the region from 1414 nm to 1646 nm) of the derivitized spectrum further illustrates the effect of increasing hardness on the NIR spectrum. As previously mentioned, derivative treatment of spectral data enhances spectral features, but may decrease the signal to noise (S/N) ratio.

1.4.3 Results of Sample Position Study

Emcompress®/CTM 6%/magnesium stearate SRC tablets (6 kg hardness) were used to evaluate the effect of various sampling positions on the NIR spectra. Examination of the raw spectra of each condition does not initially appear to reveal much information. Figures 16 and 17 are equally unexciting in their comparison of scanning a sample with replacement versus not moving it between scans. There does not appear to be a difference in the two conditions for either scored or nonscored sides of tablets.
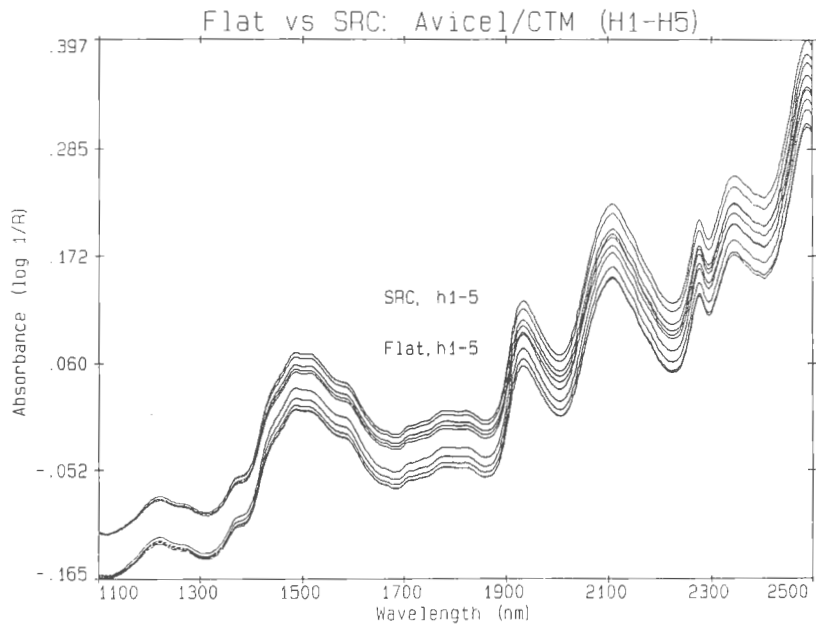
Figure 14. Raw spectra of FF and SRC Avicel® /CTM/magnesium stearate tablets.
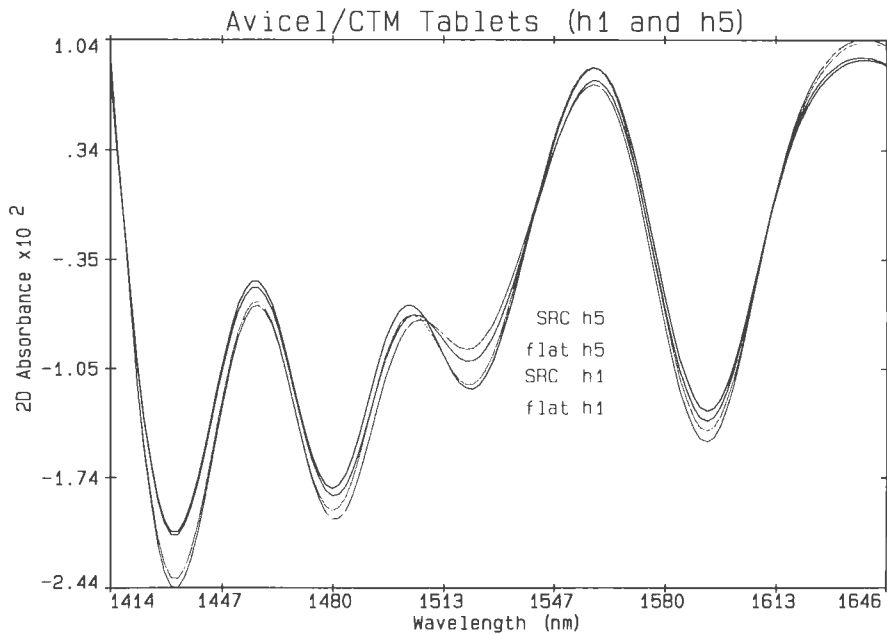
Figure 15. Second derivative plot of Avicel⊕ versus Avicel⊕/CTM/ magnesium stearate FF versus SRC tablets at hardness level 1 and level 5.
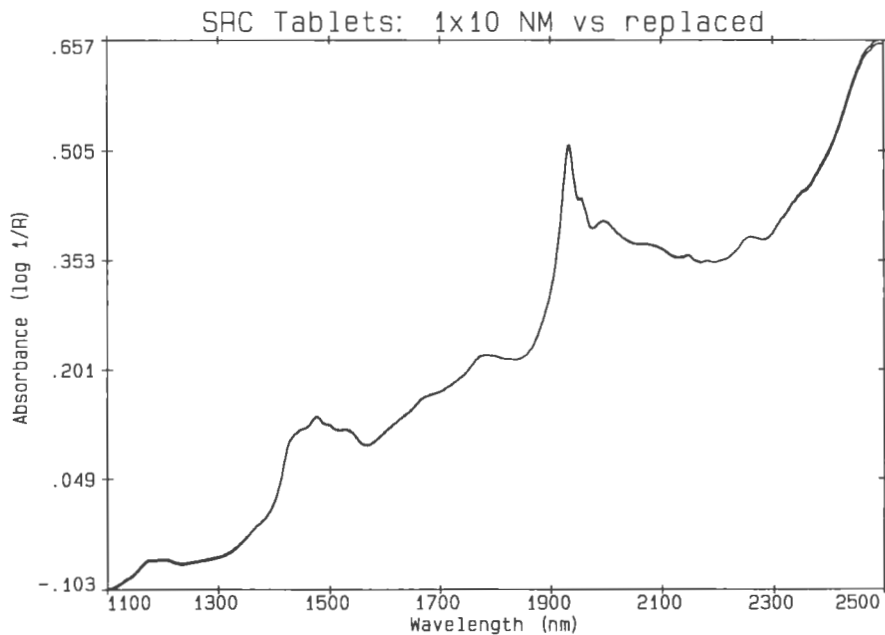
Figure 16. Raw NIR spectra of Emcompress®/CTM scored tablets: 1 tablet scanned 10 times with replacement versus not moving between scans.
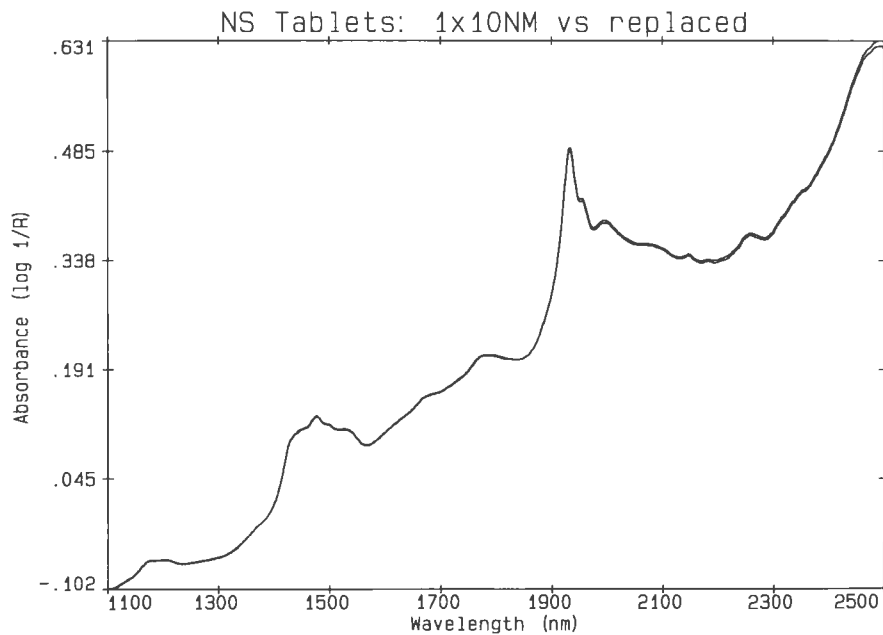
Figure 17. Raw NIR spectra of Emcompress®/CTM nonscored tablets 1 tablet scanned 10 times with replacement versus not moving it between scans.

Figure 18 compares the reflectance spectra (raw data) of one tablet scanned ten times on each side without moving it. The upper spectrum is the average of ten scans of the scored side of the tablet. The lowermost spectrum is the average of ten scans of the nonscored side of the tablet. Observation of the plot shows that the spectra were overlayed from 1100 to about 1450 nm, then began to diverge. Beyond 1900 nm, the difference between the two spectra was at its maximum. This plot demonstrates slightly higher absorbance values for the scored tablet data.

The standard deviation spectrum is a useful tool for extracting more information from the samples. When comparing second derivative data from the scored and nonscored sides of the tablet scanned ten times without moving it, there was so little difference that the computer could not create a standard deviation plot for either of these conditions. Obviously, ten replicates of this type of sample (without moving it) would not be needed in a real calibration.

Figure 19 compares the standard deviation spectrum (second derivative) of a scored versus nonscored tablet scanned ten times. There appeared to be more variation in the water band for the scored sides of the tablets; the rest of the nonscored spectra are in the same range as the scored plot.

Figure 20 compares the raw spectra of ten scans of a scored side of a tablet versus ten scans of a nonscored side of a tablet. The spectrum of the scored side had a slightly higher absorbance than that of the nonscored side.

Figure 21 compares the standard deviation spectrum of scored versus nonscored sides of ten tablets scanned once. Figure 22 displays the second derivative transformation of the same data. Again, the second derivative treatment reduced much of the apparent baseline shift caused presumably by sample placement. There was greater variability in the scored data.

Figure 23 illustrates the difference between the raw spectra of ten scored tablets scanned once and one tablet scanned ten times. The average absorbance spectrum of ten
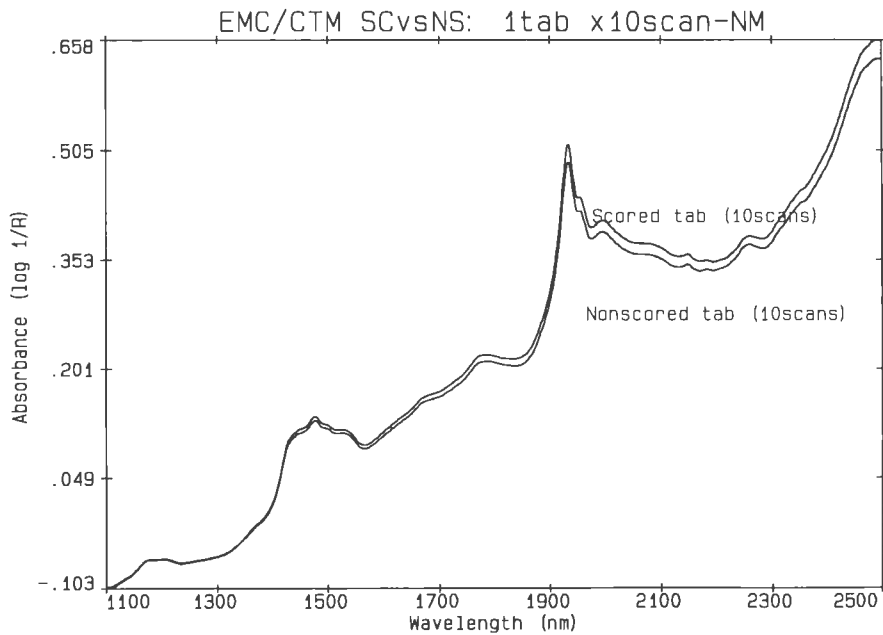
Figure 18. Raw spectra of scored versus nonscored tablets 1 tablet scanned 10 times without moving it between scans.
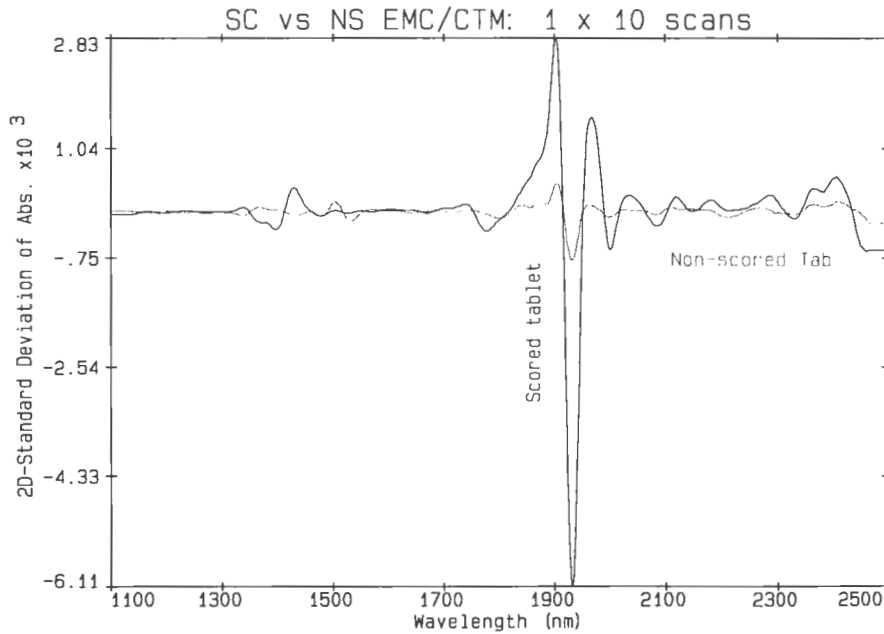
Figure 19. Standard deviation spectrum (second derivative data) of scored versus nonscored tablets: 1 tablet scanned 10 times.
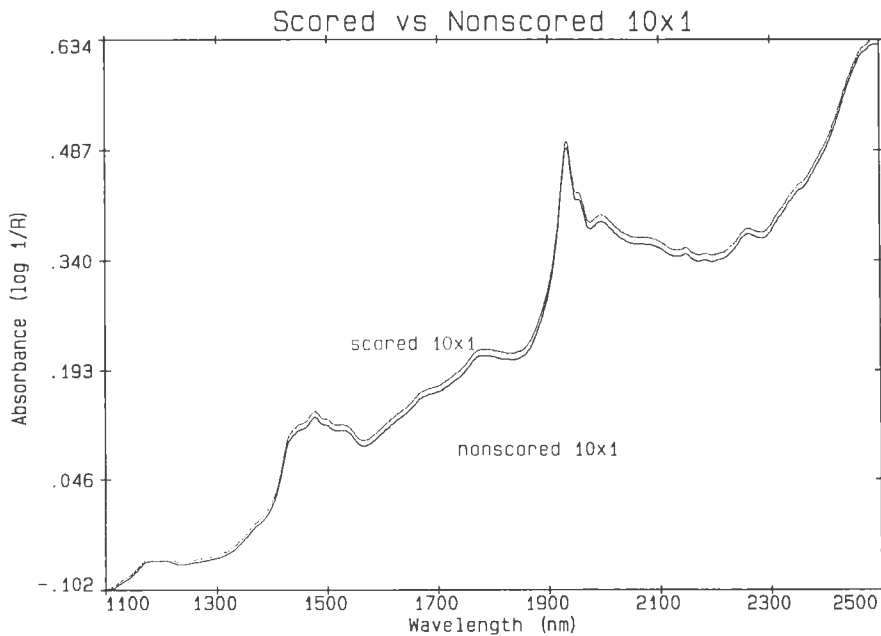
Figure 20. Raw NIR spectra of Emcompress®/CTM scored versus nonscored tablets: 10 scans of 1 tablet.
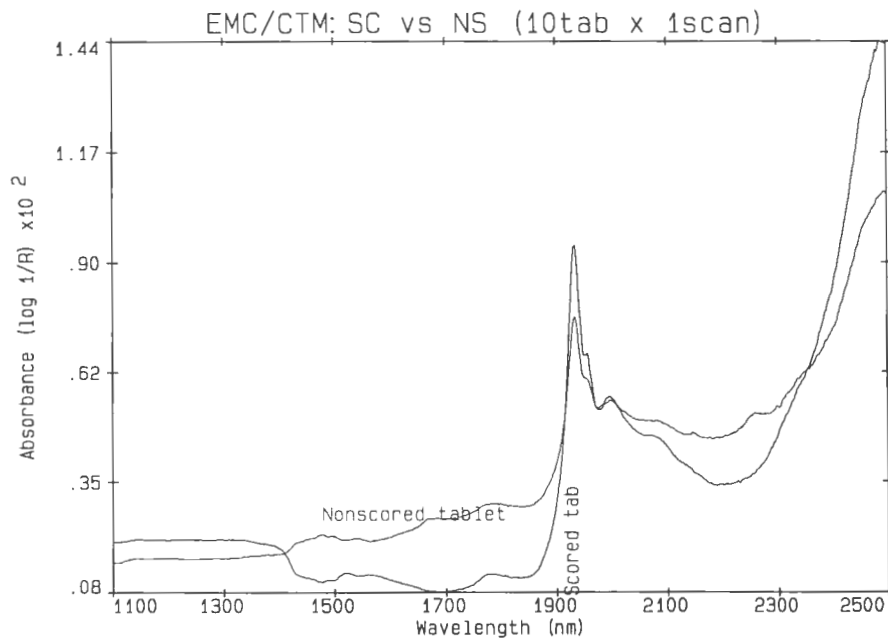
Figure 21. Standard deviation spectra (raw data) of scored versus nonscored tablets 10 tablets scanned once each.
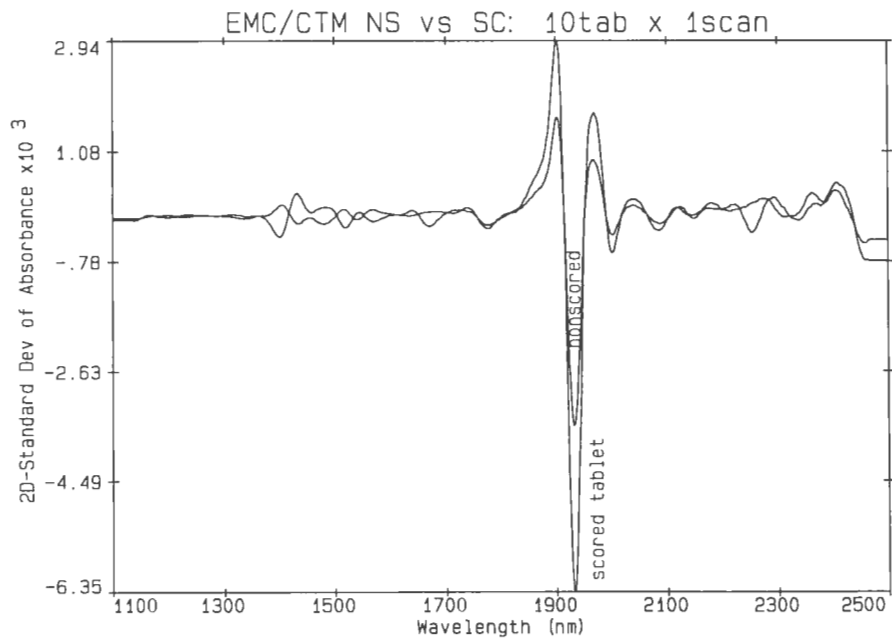
Figure 22. Standard deviation spectra (second derivative data) of scored versus nonscored tablets 10 tablets scanned once each.
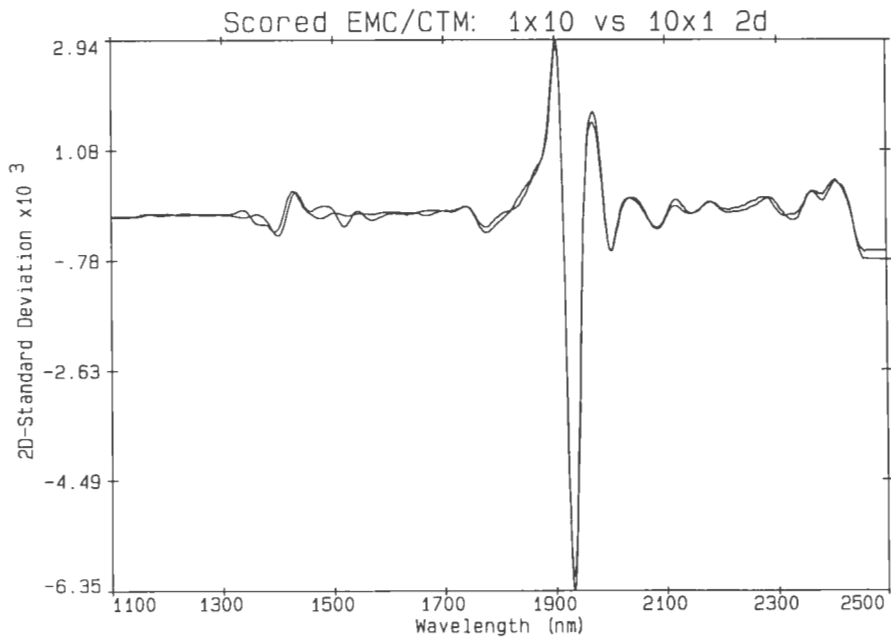
Figure 23. Raw NIR spectra of Emcompress®/CTM scored tablets 10 scans of 1 tablet versus 1 scan of each of 10 tablets.

scans of the same tablet was lower than that of ten tablets scanned once each.

Figure 24 is the second derivative of the standard deviation spectrum comparing one scored tablet scanned ten times versus ten scored tablets scanned once each. The standard deviation spectrum of the scored tablets under these sampling conditions are essentially the same.

Figure 25 shows the raw spectra of nonscored tablets, comparing one tablet scanned ten times versus ten tablets scanned once. The difference was not obvious to the naked eye. Figure 26 displays the standard deviation spectra of these conditions. Note the vastly greater difference in variation in the spectrum representing the average of ten tablets scanned once (upper spectrum). A second derivative plot of the same samples (Figure 27) shows two very different looking spectra. Overall, there was greater variability in the average spectrum of ten tablets scanned once each. There is one region of overlap of the data in the 1900 to 1930 nm range, which is due to water content.

The raw spectrum of one tablet scanned in ten positions on the detector surface is shown in Figure 28. The absorbances at 1100 nm ("origin" of the plot) range from -0.102 to 0.41, demonstrating a five-fold shift in response to a change in sample position. The naked eye cannot discern any real differences in the overall shape of the spectra. It is noteworthy that the spectra of the two replicates scanned in the 12:00 position (above the center) were quite close to each other. Also near the 12:00 spectra were the 135° and 315° samples. The spectra of the 45°, 180°, and 270° samples were close to each other, with the 225° sample not far above it. The sample from the center position was the lowermost spectrum in the plot, beginning at an absorbance of -0.102. The 90° sample originated at approximately 0.130.

The second derivative spectra of the tablet in ten positions are shown in Figure 29. Much of the baseline shift was removed by the derivitization of the spectra. The spectra appear to be completely overlayed except for the region from about 1450 nm to 1600 nm. Figure 30 is an enlarged view of this wavelength range. There are large differences in

179
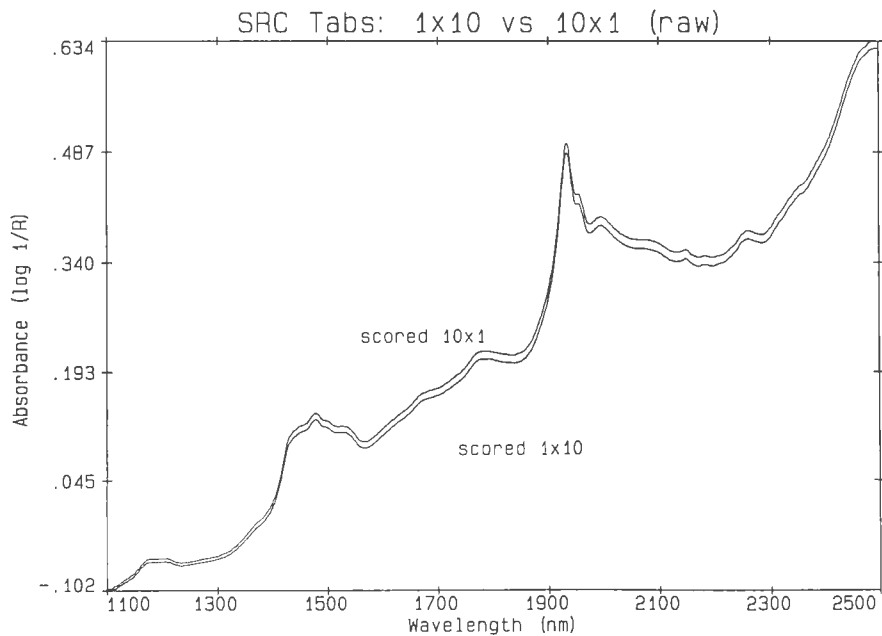
Figure 24. Standard deviation spectra (second derivative data) of scored tablets: 1 tablet scanned 10 times versus 10 tablets scanned once each.
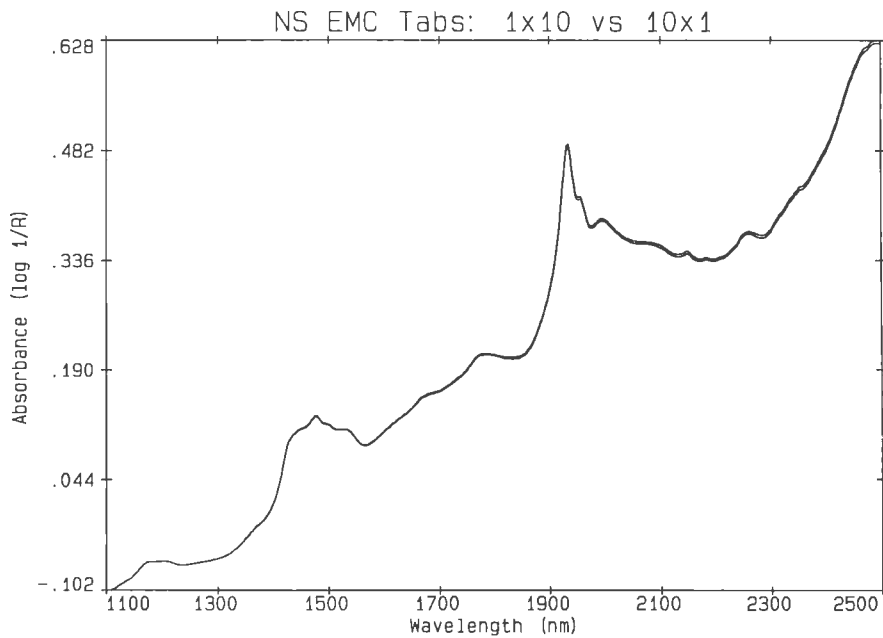
Figure 25. Raw NIR spectra of nonscored tablets: 1 tablet scanned 10 times versus ten tablets scanned once.
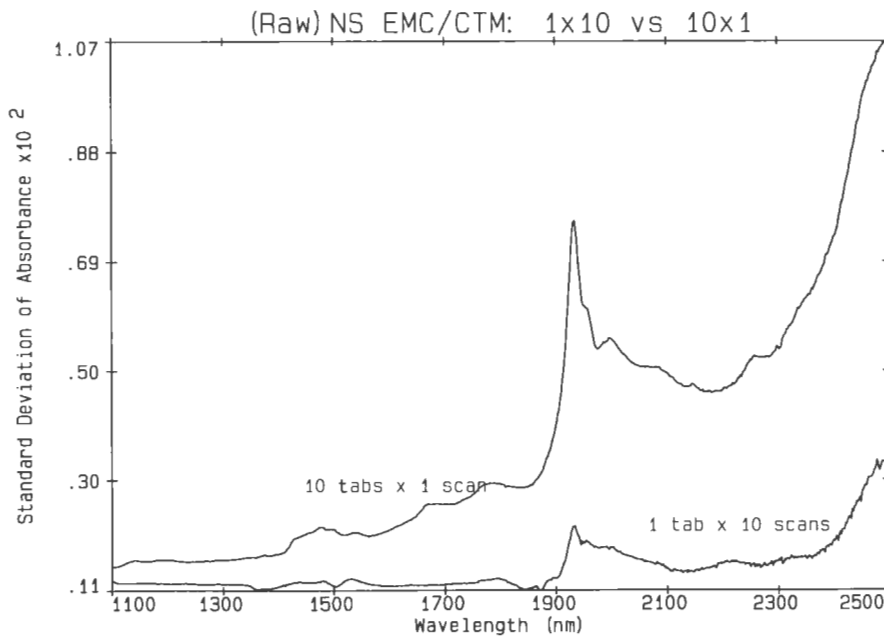
Figure 26. Standard deviation spectra (raw data) of 1 nonscored tablet scanned 10 times versus 10 tablets scanned once each.
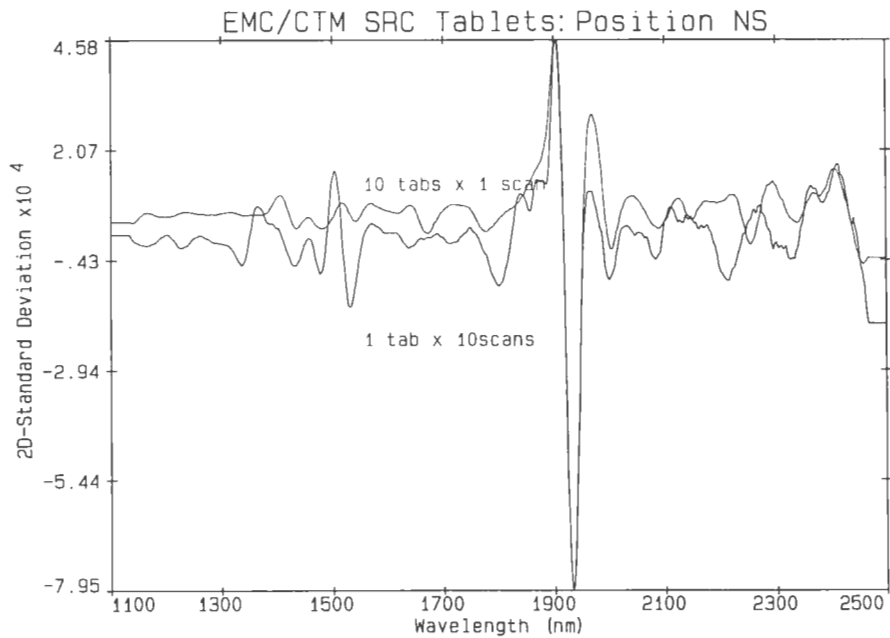
Figure 27. Standard deviation spectra (second derivative data) of 1 nonscored tablet scanned 10 times versus 10 tablets scanned once each.
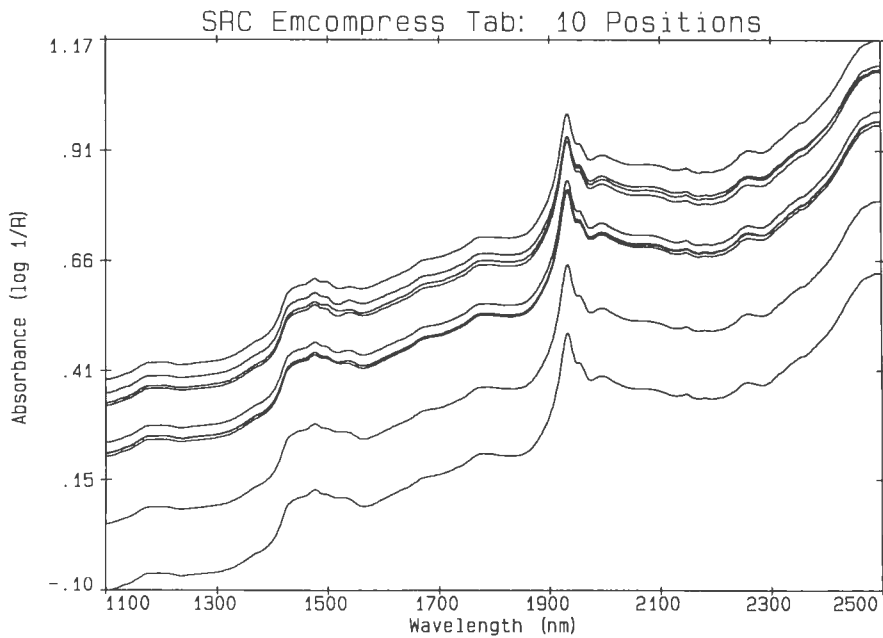
Figure 28. Raw NIR spectra of 1 nonscored tablet scanned once each at ten different positions.
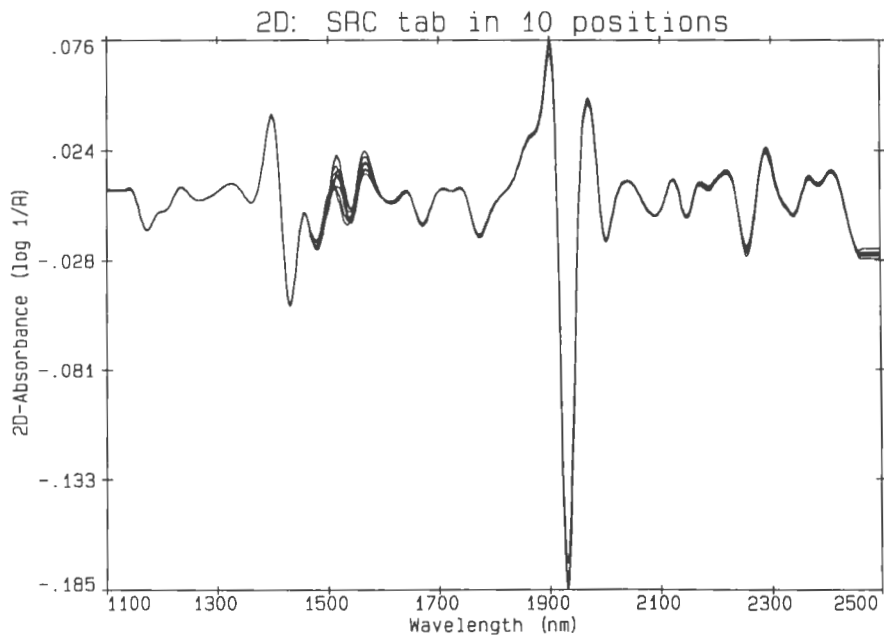
Figure 29. Second derivative NIR spectra of 1 nonscored tablet scanned 10 times.
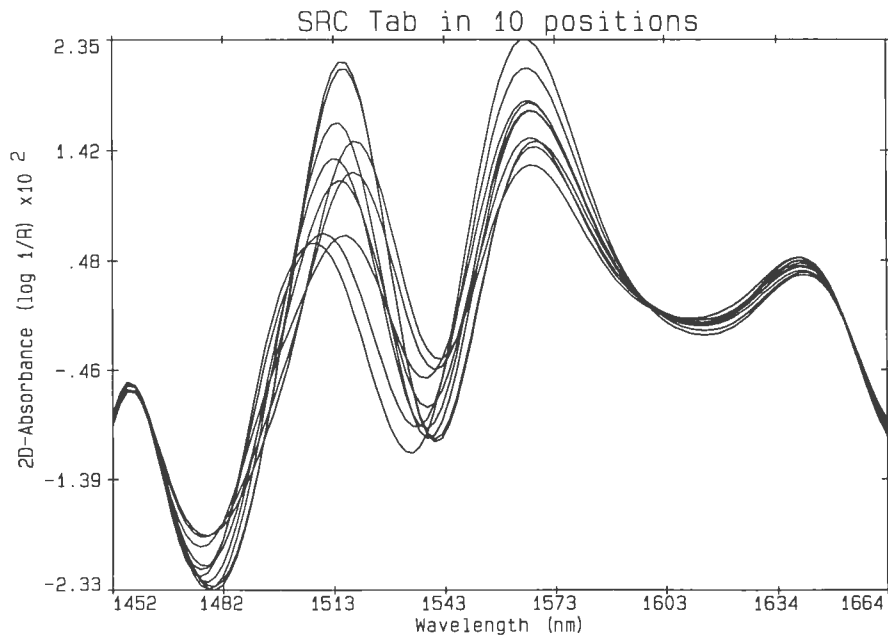
Figure 30. Enlarged view of second derivative NIR spectra of one nonscored tablet scanned ten times.

absorbance maxima at 1513 nm, 1540 nm, and 1573 nm. It is not known why this region was so highly affected by sample position in comparison to the rest of the spectrum.

The raw spectra in Figure 28 followed a similar pattern of presentation to those in Figure 4, where increases in compression force caused the spectra to shift upwards. When sample position was changed, the spectra also shifted, although not in a regular, predictable manner. Changes in sample position are known to result in this apparent "particle size" effect. The difference is that the second derivative of data from Figure 4 were not completely overlayed at the absorbance maxima, as they were in Figure 29. This indicates that the apparent "particle size" effect from changing hardness could not be entirely removed by derivitizing the spectra.

In summary, the results of the sample position study demonstrate that variability in the spectral data may be introduced through slight changes in sample placement. This variability was greater in scored than in nonscored tablet data. Much of the variation could be reduced by using a second derivative math treatment. The center position was the most reproducible sampling position due to the ability to use the iris.

1.4.4   Single wavelength regression and analysis of variance

During NIR analysis of these products, some degree of consistency was observed in the spectral response to increasing tablet hardness. For a given formulation, regular increases in second derivative absorbance values occurred at several wavelengths in response to increasing hardness. For Emcompress®/CTM tablets, these wavelengths were 1430, 1898, and 1926 nm. Avicel®/CTM tablets demonstrated regular increases in absorbance values at 1884, 1926, 2236, and 2270 nm. This portion of the study tested the theory that hardness may be measured at a single wavelength.

Second derivative absorbance values at the specified wavelengths were tabulated for each product (n=10) at all five hardness levels. Linear regression and one-way analysis of variance were applied (Minitab®) to the hardness and spectral data to assess their relationship. Cricket Graph was used to plot the data at each wavelength. Since NIR is

being used to predict tablet hardness from absorbance data, hardness becomes the dependent variable (y). Regression data are summarized in Table 12. A linear relationship was found to exist for each set of data; in most cases r^2 was better than 0.92.

Graphic representation of the data provides useful information for comparative purposes. Data for flat versus SRC Emcompress®/CTM tablets at 1430, 1898, and 1926 nm are plotted in Figures 31 through 33. EF regression lines were found to converge with EC lines, suggesting different slopes for flat versus SRC tablets at 1430 and 1898 nm.

Data for flat versus SRC Avicel®/CTM tablets at 1884, 1926, 2236, and 2270 nm are compared in Figures 34 through 37. In each case, the regression lines for flat versus SRC appeared to be parallel, indicating similar slopes. Slope and intercept data for Avicel®/CTM tablets were very similar between flat and SRC data. These data suggest that NIR response to increasing compression force is similar for flat and convex Avicel®/CTM tablets.

Figure 38 is a plot of hardness versus second derivative of absorbance for convex (SRC) Avicel®/CTM tablets and Emcompress®/CTM tablets at 1926 nm. Figure 39 shows the same conditions for the flat tablets. The same set of comparisons was made at 1430 nm and is demonstrated in Figures 40 and 41. It is obvious from these plots that the slope and intercept values between tablet matrices are quite different, supporting the theory that separate calibration models would be needed for hardness prediction of different tablet formulations.

To further investigate the single wavelength regression theory, NSAS was used to develop NIR calibrations for each product at each of the aforementioned wavelengths. Models were developed for flat, scored, nonscored and mixed (scored/nonscored) tablet surfaces. It was surprising to discover that the results of these calibrations were quite good. Table 13 summarizes the regression coefficients for Avicel®/CTM tablets. R^2 values ranged from 0.951 to 0.990. Calibration and prediction results for the

Table 12.   Summary of NIR absorbance versus hardness regression at single
            wavelengths   (Hardness = slope x absorbance + intercept).

Matrix	Geometry	λ (nm)	Slope	Intercept	r^2	F
Emcompress	flat	1926	-178.857	-25.698	0.968	1227.30
	SRC	1926	-195.908	-27.083	0.921	479.53
	flat	1898	401.831	-25.420	0.965	1116.32
	SRC	1898	495.077	-30.866	0.922	485.54
	flat	1430	-708.099	-28.579	0.975	1598.79
	SRC	1430	-604.704	-22.839	0.873	281.34

Matrix	Geometry	λ (nm)	Slope	Intercept	r^2	F
Avicel	flat	1926	-1560.251	-89.544	0.952	946.18
	SRC	1926	-1574.581	-87.26	0.972	1640.60
	flat	1884	1940.230	-82.792	0.963	1234.28
	SRC	1884	2006.831	-83.026	0.974	1807.90
	flat	2236	2449.174	-100.043	0.926	597.77
	SRC	2236	2669.498	-106.429	0.939	734.63
	flat	2270	-2164.221	-123.169	0.956	1047.55
	SRC	2270	-2419.599	-134.423	0.962	1207.58
	SRC	1430	-4001.400	-75.550	0.968	1453.27

Figure 31.   Emcompress®/CTM Flat versus SRC Tablets: Hardness versus second derivative (2D) absorbance at 1430 nm.
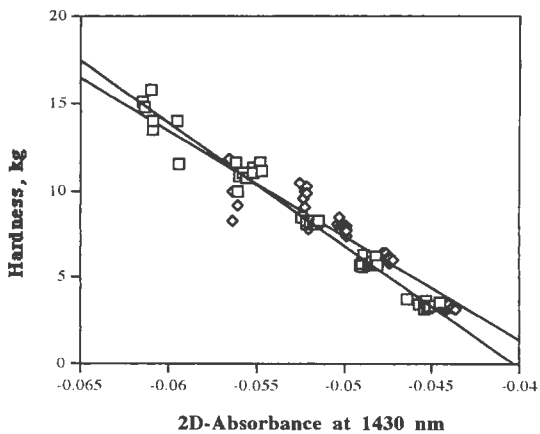
□ EF Hardness	$y = -708.099x - 28.579 \quad r^2 = 0.975$
◇ EC Hardness	$y = -604.704x - 22.839 \quad r^2 = 0.873$

Figure 32.   Emcompress®/CTM Flat versus SRC Tablets: Hardness versus second derivative (2D) absorbance at 1926 nm.
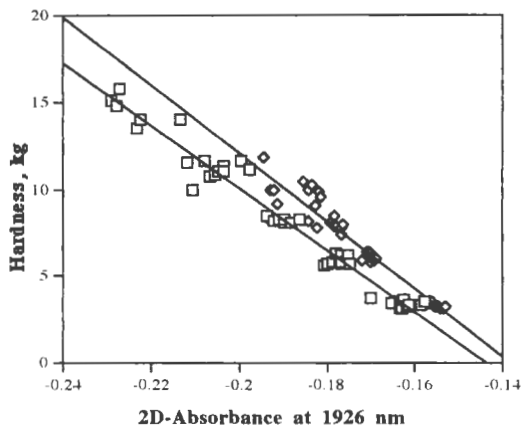
	EF Hardness	$y = -178.857x - 25.698$	$r^2 = 0.968$
◇	EC Hardness	$y = -195.908x - 27.083$	$r^2 = 0.921$

Figure 33. Emcompress®/CTM Flat versus SRC Tablets: Hardness versus second derivative (2D) absorbance at 1898 nm.
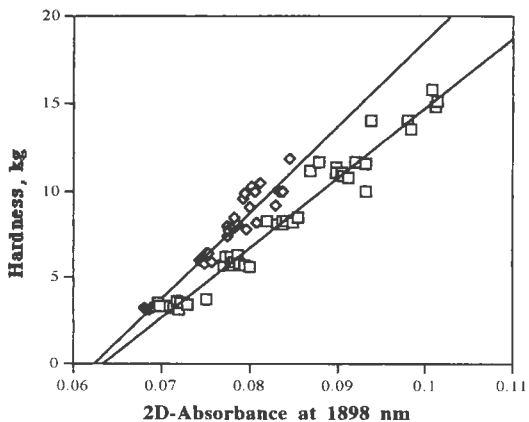
EF Hardness $y = 401.831x - 25.420$ $r^2 = 0.965$

EC Hardness $y = 495.077x - 30.866$ $r^2 = 0.922$

Figure 34. Avicel®/CTM Flat versus SRC Tablets: Hardness versus second derivative (2D) absorbance at 1884 nm.
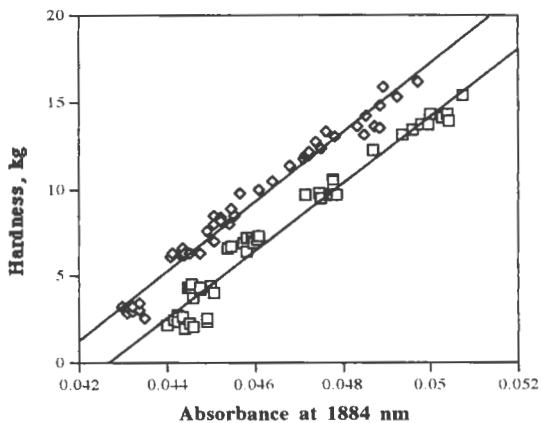
□	AF hardness	$y = 1940.230x - 82.792$	$r^2 = 0.963$
◇	AC hardness	$y = 2006.831x - 83.026$	$r^2 = 0.974$

Figure 35. Avicel®/CTM Flat versus SRC Tablets: Hardness versus second derivative (2D) absorbance at 1926 nm.
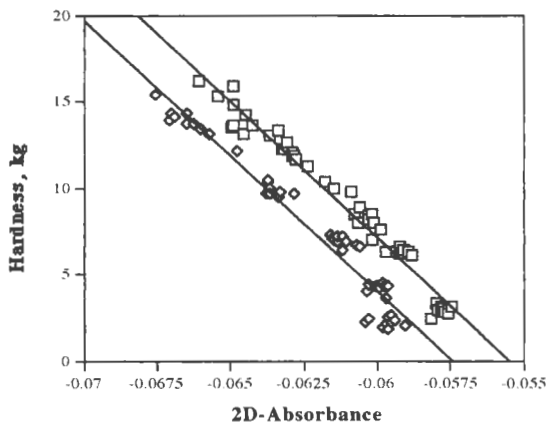
□   SRC hardness $y = -1574.581x - 87.260$ $r^2 = 0.972$

◇   AF hardness $y = -1560.251x - 89.544$ $r^2 = 0.952$

Figure 36. Avicel®/CTM Flat versus SRC Tablets: Hardness versus second derivative (2D) absorbance at 2236 nm.
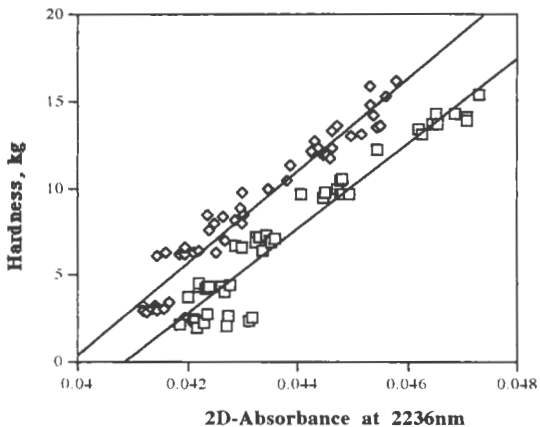
| | AF hardness | $y = 2449.174x - 100.043$ | $r^2 = 0.926$ |
| □ | AC hardness | $y = 2669.498x - 106.429$ | $r^2 = 0.939$ |

Figure 37. Avicel®/CTM Flat versus SRC Tablets: Hardness versus second derivative (2D) absorbance at 2270 nm.
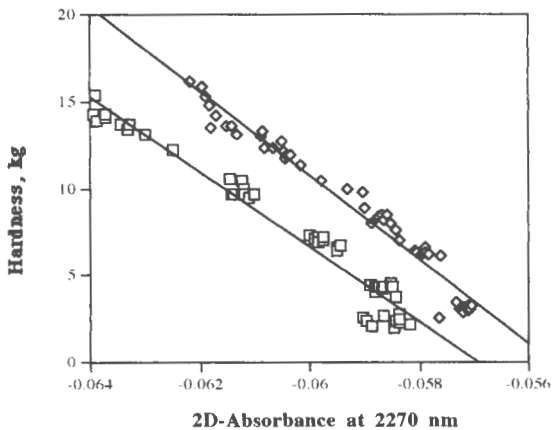
AF hardness $y = -2164.221x - 123.169$ $r^2 = 0.956$

AC hardness $y = -2419.599x - 134.423$ $r^2 = 0.962$

Figure 38.   Avicel®/CTM versus Emcompress®/CTM SRC Tablets: Hardness versus
              second derivative (2D) absorbance at 1926 nm.
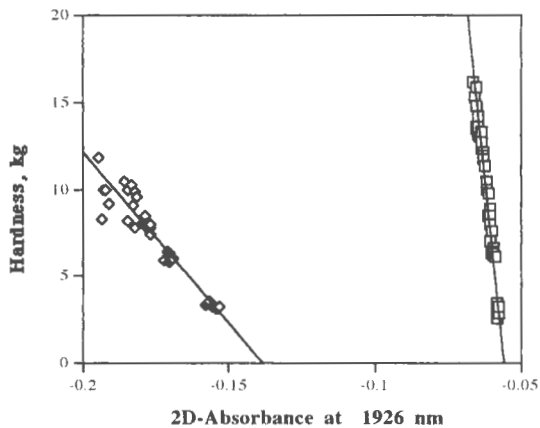
□   AC hardness $y = -1574.581x - 87.260$ $r^2 = 0.972$

◇   EC Hardness $y = -195.908x - 27.083$ $r^2 = 0.921$

Figure 39.   Avicel®/CTM versus Emcompress®/CTM Flat Tablets: Hardness versus
second derivative (2D) absorbance at 1926 nm.

2D-Absorbance at 1926 nm
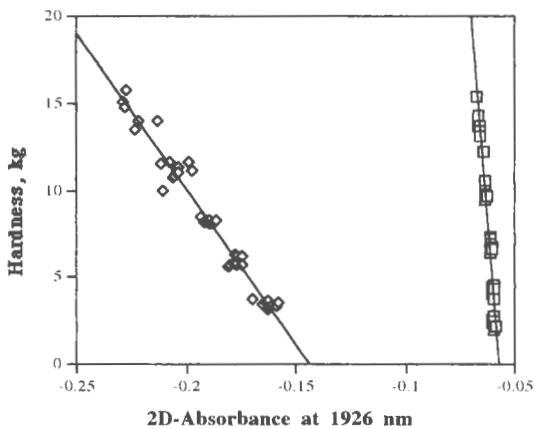
□   AF hardness $y = -1560.251x - 89.544$ $r^2 = 0.952$

◇   EF Hardness $y = -178.857x - 25.698$ $r^2 = 0.968$

Figure 40.   Avicel®/CTM versus Emcompress®/CTM SRC Tablets: Hardness versus
second derivative (2D) absorbance at 1430 nm.
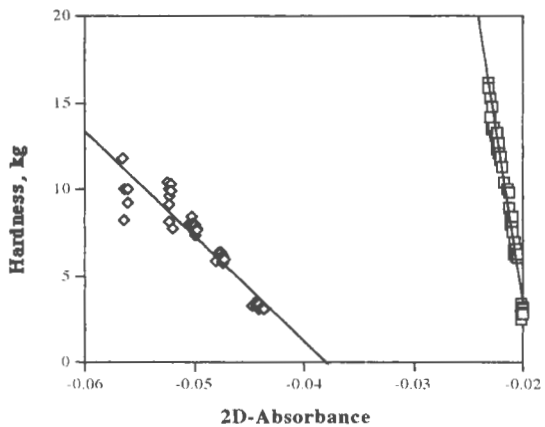
AC hardness $y = -4001.357x - 76.550$ $r^2 = 0.968$

EC Hardness $y = -604.704x - 22.839$ $r^2 = 0.873$

Figure 41.   Avicel®/CTM versus Emcompress®/CTM Flat Tablets: Hardness versus
             second derivative (2D) absorbance at 1430 nm.
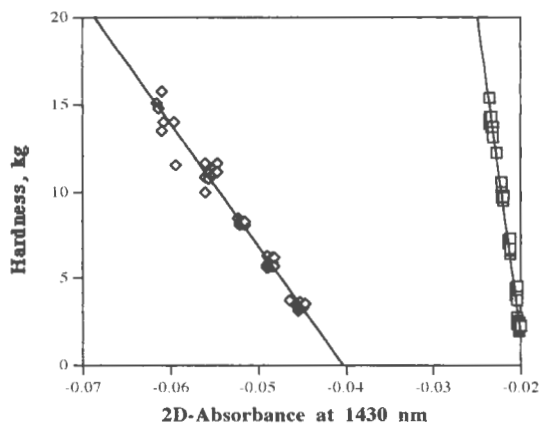
□	AF hardness	$y = -3672.603x - 71.675$ $r^2 = 0.987$
◇	EF Hardness	$y = -708.099x - 28.579$ $r^2 = 0.975$

Table 13. NSAS Avicel- Summary of nm/hardness regression

matrix	geometry	λ (nm)	slope	intercept	r2
Avicel	Flat	1884	1986.326	-84.952	0.980
	Flat	1926	-1598.096	-91.894	0.974
	Flat	2236	2495.963	-102.083	0.957
	Flat	2270	-2203.484	-125.533	0.975
	Nonscored	1884	1970.873	-80.162	0.982
	Nonscored	1926	-1541.233	-83.987	0.981
	Nonscored	2236	2629.358	-103.068	0.951
	Nonscored	2270	-2325.375	-127.233	0.970
	Nonscored	1884+1926	8755.657	-66.458	0.984
	NS/S	1884	1985.744	-81.946	0.987
	NS/S	1926	-1559.371	-86.203	0.986
	NS/S	2236	2603.937	-103.387	0.969
	NS/S	2270	-2351.095	-130.304	0.983
	Scored	1884	1993.503	-83.759	0.984
	Scored	1926	-1561.7	-87.863	0.982
	Scored	2236	2676.638	-108.485	0.960
	Scored	2270	-2502.612	-141.189	0.980
	Scored	1926+1884	8781.652	-59.469	0.990

Avicel®/CTM tablets are summarized in Table 14. Emcompress®/CTM regression coefficients are summarized in Table 15. Linearity ranged from 0.912 to 0.983. Validation results for Emcompress®/CTM tablets are given in Table 16. Comparison of the Minitab® regression results (Table 12) with NSAS results (Tables 13 and 15) reveals slight differences in regression coefficients. The primary reason for the differences was that the data sets for NSAS calibration were constructed from six spectra rather than ten (Minitab®) in order to facilitate the development of validation sets.

It should be reiterated that tablet hardness is a physical property, and thus a single wavelength cannot be assigned exclusively to hardness. The absorbance at 1926 nm is associated with water content, yet each formulation demonstrated a regular increase in absorbance at 1926 nm in response to increased hardness. Since this pattern of increased absorbance occurred at several wavelengths for each product, it may be concluded that one or more of these wavelengths could be used to calibrate tablet hardness for a particular formulation. Absorbance of interfering substances would have to be evaluated before choosing a single wavelength for this application (e.g., 1926 nm may not be a reliable single wavelength).

1.4.5 Calibration of Tablet Hardness

The yardstick for comparison of calibration equations is the set of statistics that results from the application of the equation to a validation set. The statistical parameters used to evaluate calibration models were described in Manuscript III.

The standard error (SE) of the reference method must be known before undertaking a calibration experiment. The NIR calibration is only as good as the reference values from which it was generated. In addition to the aforementioned selection criteria, the SEE of the calibration must be compared to that of the reference method. If the calibration SEE is better than the reference SE, the model may be overfitted and may not accurately predict unknown samples. For comparative purposes, the ratio of bias/standard error of the bias

Table 14. Single wavelength regression for Avicel/CTM tablets: Prediction Results

Geometry & wavelength (nm)	mult r	SEE	Val.File	bias/SEB	mult r	SEP
AC-1884+1926	0.988	0.648	NS/S	1.484	0.992	0.595
AC-1884	0.987	0.672	NS/S	2.014	0.989	0.701
AC-1926	-0.986	0.700	NS/S	2.118	0.988	0.748
AC-2236	0.969	1.030	NS/S	2.442	0.975	1.120
AC-2270	-0.983	0.765	NS/S	0.801	0.980	0.919
AN-1884	0.982	0.775	Nonscored	1.603	0.990	0.709
AN-1926	0.981	0.806	Nonscored	1.824	0.989	0.761
AN-2236	0.951	1.270	Nonscored	1.714	0.972	1.270
AN-2270	-0.970	0.995	Nonscored	1.000	0.986	0.769
AS-1926+1884	0.990	0.612	Scored	0.152	0.987	0.678
AS-1884	0.984	0.745	Scored	0.517	0.987	0.786
AS-1926	-0.982	0.793	Scored	0.595	0.985	0.854
AS-2236	0.960	1.180	Scored	0.546	0.962	1.220
AS-2270	-0.980	0.839	Scored	0.740	0.982	0.826
AF-1884	0.980	0.847	Flat	0.218	0.984	0.791
AF-1926	-0.974	0.967	Flat	0.033	0.979	0.893
AF-2236	0.957	1.250	Flat	0.158	0.972	1.000
AF-2270	-0.975	0.960	Flat	0.089	0.984	0.775

Legend:

AC	Avicel/CTM mixed nonscored/scored
AN	Avicel/CTM nonscored
AS	Avicel/CTM scored
AF	Avicel/CTM flat
NS/S	mixed nonscored/scored

Table 15. Summary of NSAS Emcompress®/CTM regression coefficients at single wavelengths.

matrix	geometry	λ (nm)	slope	intercept	r2
EMC	flat	1430	-709.667	-28.643	0.983
	flat	1898	404.347	-25.595	0.977
	flat	1926	-180.258	-25.931	0.979
	flat	1430+1926	-533.311	-28.067	0.983
	NS/S	1430	-584.592	-21.888	0.916
	NS/S	1898	489.262	-30.458	0.949
	NS/S	1926	-193.118	-26.636	0.948
	NS/S	1926+1430	-303.484	-28.492	0.953
	Nonscored	1430	-581.375	-21.502	0.912
	Nonscored	1898	440.558	-26.879	0.947
	Nonscored	1926	-177.071	-23.924	0.946
	Nonscored	1898+1926	709.504	-28.669	0.947
	Nonscored	1926+1430	-418.038	-25.383	0.963
	Scored	1430	-601.056	-22.962	0.929
	Scored	1898	507.493	-31.808	0.939
	Scored	1926	-200.179	-27.869	0.943
	Scored	1430+1926	-102.358	-27.253	0.943

Table 16. Single wavelength regression for Emcompress/CTM tablets-
Prediction Results

Geometry & wavelength (nm)	mult r	SEE	Validation File	bias/SEB	mult r	SEP
EC-1926+1430	0.953	0.771	NS/S	0.625	0.973	0.606
EC-1430	-0.916	1.000	NS/S	0.544	0.962	0.742
EC-1898	0.949	0.789	NS/S	0.643	0.976	0.569
EC-1926	-0.948	0.793	NS/S	0.686	0.976	0.572
EN-1898+1926	0.963	0.641	Nonscored	2.118	0.959	0.935
EN-1926+1430	0.947	0.770	Nonscored	2.153	0.971	0.790
EN-1430	-0.912	0.960	Nonscored	0.018	0.976	0.559
EN-1898	0.947	0.754	Nonscored	2.102	0.971	0.783
EN-1926	-0.946	0.757	Nonscored	1.981	0.970	0.777
ES-1430+1926	0.943	0.870	Scored	0.045	0.976	0.559
ES-1430	-0.929	0.952	Scored	0.308	0.956	0.747
ES-1898	0.939	0.882	Scored	0.198	0.974	0.586
ES-1926	-0.943	0.856	Scored	0.018	0.976	0.559
EF-1430+1926	0.983	0.738	Flat	0.643	0.995	0.380
EF-1430	-0.983	0.733	Flat	0.579	0.996	0.364
EF-1898	0.977	0.845	Flat	0.768	0.991	0.519
EF-1926	-0.979	0.809	Flat	0.755	0.992	0.491

Legend:

EC   Emcompress/CTM mixed nonscored/scored
EN   Emcompress/CTM nonscored
ES   Emcompress/CTM scored
EF   Emcompress/CTM flat

NS/S   mixed nonscored/scored

(bias/SEB) was included in the summary tables. It is desirable that this ratio be less than 3.0 for best model fit.

It is complicated to compare equations on an individual basis, since each was generated independently. Each was developed from a unique combination of wavelengths and calibration samples. For instance, while developing one equation, an outlier may be detected which was not an outlier for another calibration. This calibration set may work well at a particular wavelength as a second derivative, but the raw data from the same calibration set may regress at a different wavelength. This resulted in a unique set of calibration samples for that equation. Also, changing the individual samples in a calibration set may cause the computer software to select a different wavelength for regression. As previously explained, the basis of selection of the regression wavelength (by the NSAS software) is the degree of variation at that point. One set of samples may have a greater standard deviation at one wavelength; if samples are added or deleted from this set, the highest variability may occur at a different wavelength.

There were no outstanding features to note concerning calibration of Emcompress® based tablets in comparison to Avicel® based tablets. The process was the same, and similar patterns of behavior were noted for both matrices.

1.4.5.1   *Hardness Calibration of SRC Avicel®/CTM Tablets*

General calibration equations were developed for SRC tablets using several different calibration, or training, sets. All four replicates of NIR tablet scans were averaged (AC data set) and subject to random sample selection for the calibration set. MLR and PLS regression were used to develop equations using raw and second derivative spectral data. Improvement of the MLR models was obtained by regressing on more than one wavelength. In some cases, the first regression wavelength was preselected based on spectral information, or to provide a basis of comparison to the other groups of calibrations (e.g., scored, nonscored, mixed).

Table 17 summarizes the calibration and validation process for the AC data set. Seven MLR equations were developed using second derivative spectra. Several of these predictions resulted in good agreement ($r = 0.991$ or better) and two predictions resulted in agreement of $r = 0.981$ or better. When the same AC calibrations were applied to data sets consisting solely of nonscored or scored data, a large bias resulted. Linearity was still 0.989 or better, but large values for bias and bias/SEB ratio were observed. Two AC calibrations were able to satisfactorily predict values from an AN (nonscored) data set and an AS (scored) data set.

Four MLR equations were developed using the raw AC data. A series of three of these equations was applied to one validation set. The first model was based on one wavelength (2422 nm), the second on two wavelengths (2422 nm + 2378 nm), and the third equation was based on three wavelengths (1460 nm + 1740 nm + 2040 nm). The best prediction came from the two-term equation. The prediction values for r were as follows: one-term, $r = 0.997$, two-term, $r = 0.992$ and three-term, $r = 0.994$.

Four PLS calibrations were developed using the second derivative AC data. All four of these fit the two validation sets well. As expected, increasing the number of factors improved the calibration. When AC calibrations were applied to AN or AS validation sets, only one calibration gave acceptable results, with values for bias and bias/SEB within specified tolerances. Results were slightly better for the nonscored validation set (bias/SEB = 0.63) versus the scored data set (bias/SEB = 1.53).

Two calibrations were developed using raw AC data in a PLS regression. Both equations accurately predicted the validation set. The two equations were unable to predict values from the AN or the AS validation sets. The first calibration employed the full spectral range of 1100 nm to 2500 nm. The second was restricted to the range of 1500 nm to 2150 nm. The SEE's were very close (0.315 versus 0.312), and the validation of the first equation (SEP = 0.349) was slightly better than the second (SEP = 0.369).

To summarize the calibration process for AC data sets, all of the AC calibrations were able to predict AC validation sets with a good degree of accuracy. None of the calibrations based on raw data were able to sufficiently predict AN or AS data. One second derivative PLS calibration was able to predict an AN ($r^2 = 0.994$) as well as an AS ($r^2 = 0.995$) validation set. Two second derivative MLR equations adequately fit both AN and AS data from one validation set. In general, a higher bias/SEB value resulted when an model was used to predict an AN or AS model. There did not appear to be a difference in performance between PLS models developed from raw data versus second derivative data. MLR models were slightly better when second derivative data was used.

Table 18 summarizes the validation of nonscored Avicel®/CTM tablets (AN) using MLR. Using second derivative spectral data, six out of seven equations successfully (SEP<0.5) predicted the AN validation set. The r^2 value was consistently 0.994 to 0.995. The equation that did not fit the validation set was a calibration based on 1930 nm, the water band. The SEE at this wavelength was 0.81. However, when using 1930 nm with a second wavelength (1456 nm), the equation was able to fit the validation data (SEE = 0.375 and SEP = 0.500).

AN calibrations using second derivative data were only marginally successful at fitting AS or AC validation sets. One equation fit the AC data, and two others were marginally acceptable. When applying AN calibrations to scored data sets (AS), two out of seven equations produced a fair prediction. Performance of the models appeared to be the same between raw and second derivative data for both PLS and MLR models.

Calibrations based on spectral data from scored (AS) tablets followed the same pattern as the nonscored (AN) tablets: equations developed specifically for AS data were able to fit AS validation sets but not AN or AC validation sets. Calibration and validation results are summarized in Table 19. Performance of raw data PLS models was slightly better than second derivative. Raw and second derivative MLR models were about equal in performance.

Table 17.   Summary of hardness calibration/validation summary for AC (combined scored and nonscored) tablets. Reference SE for all Avicel/CTM SRC tablets is 0.68 kg.

MLR- 2d hardness data

Cal.file	mult r	SEE	Val.File	bias/SEB	mult r	SEP
acm-cal1	-0.994	0.468	NS/S	1.14	0.982	0.780
acm-cal2	0.997	0.326	NS/S	1.45	0.997	0.341
			Nonscored	0.67	0.997	0.382
			Scored	0.01	0.996	0.414
acm-cal3	0.996	0.402	NS/S	0.92	0.997	0.310
			Nonscored	11.00	0.998	0.300
			Scored	10.81	0.997	0.317
ac-cal1	-0.983	0.790	NS/S	0.00	0.995	0.439
			Nonscored		0.995	0.451
			Scored		0.994	0.495
ac-cal2	0.996	0.408	NS/S		0.997	0.350
			Nonscored		0.997	0.369
			Scored		0.995	0.456
ac-cal3	0.997	0.327	NS/S		0.991	0.571
			Nonscored		0.994	0.512
			Scored	0.07	0.993	0.513
acm-cal4	0.992	0.529	NS/S	0.62	0.983	0.810
			Nonscored	8.19	0.989	0.632
			Scored	8.28	0.986	0.687

MLR-Raw hardness data

Cal.file	mult r	SEE	Val.File	bias/SEB	mult r	SEP
ac-cal4	0.971	0.976	NS/S	0.04	0.969	1.060
acm-cal5	0.993	0.490	NS/S	0.84	0.992	0.555
acm-cal6	0.998	0.268	NS/S	2.72	0.997	0.342
			Nonscored	6.42	0.996	0.405
acm-cal7	0.995	0.423	NS/S	0.14	0.994	0.468
			Nonscored	7.98	0.997	0.355
			Scored	4.26	0.991	0.568

Table 17. Calibration and validation summary of AC hardness (continued).

PLS- 2d hardness data

Cal.file	mult r	SEE	Val.File	bias/SEB	mult r	SEP
acm-pls1	0.996	0.363	NS/S	0.99	0.996	0.399
			Nonscored	3.51	0.993	0.646
			Scored	2.24	0.996	0.470
acm-pls2	0.997	0.348	NS/S	0.60	0.995	0.443
			Nonscored	8.24	0.995	0.907
			Scored	6.67	0.995	0.753
ac-pls1	0.997	0.317	NS/S	0.47	0.994	0.516
			Nonscored	0.63	0.994	0.588
			Scored	1.53	0.995	0.449
ac-pls2	0.998	0.296	NS/S	0.21	0.995	0.417

PLS-Raw hardness data

Cal.file	mult r	SEE	Val.File	bias/SEB	mult r	SEP
acm-pls3	0.998	0.315	NS/S	0.21	0.997	0.349
			Nonscored	4.09	0.997	0.313
			Scored	3.10	0.995	0.405
acm-pls4	0.998	0.312	NS/S	0.65	0.996	0.369
			Nonscored	5.42	0.997	0.315
			Scored	4.35	0.995	0.423

Table 18.　Summary of hardness calibration and validation results for AC (nonscored) tablets. Reference SE for Avicel/CTM SRC tablets is 0.68.

MLR- 2d hardness data

Cal.file	mult r	SEE	Val.File	bias/SEB	mult r	SEP
acn-cal1	-0.992	0.512	NS/S	7.50	0.995	0.435
			Nonscored	0.40	0.995	0.456
			Scored	11.80	0.993	0.488
acn-cal2	0.997	0.345	NS/S	0.90	0.995	0.419
			Nonscored	0.97	0.995	0.456
			Scored	0.10	0.993	0.522
acn-cal3	-0.996	0.370	NS/S	0.14	0.994	0.455
			Nonscored	1.40	0.994	0.502
			Scored	0.14	0.993	0.515
acn-cal4	-0.980	0.811	NS/S	8.70	0.987	0.707
			Nonscored	1.80	0.989	0.705
			Scored	13.70	0.984	0.937
acn-cal5	-0.996	0.375	NS/S	0.70	0.995	0.439
			Nonscored	0.84	0.994	0.500
			Scored	0.91	0.993	0.518
acn-cal7	0.989	0.597	NS/S	7.90	0.992	0.567
			Nonscored	0.85	0.995	0.445
			Scored	12.70	0.988	0.678

MLR-Raw hardness data

Cal.file	mult r	SEE	Val.File	bias/SEB	mult r	SEP
acn-cal8	0.997	0.303	NS/S	3.7	0.997	0.377
			Nonscored	1.9	0.995	0.448
			Scored	6.5	0.993	0.609

PLS- 2d hardness data

Cal.file	mult r	SEE	Val.File	bias/SEB	mult r	SEP
acn-pls1	0.997	0.313	NS/S	3.60	0.997	0.352
			Nonscored	0.23	0.995	0.470
			Scored	6.10	0.995	0.438
acn-pls2	0.998	0.310	Nonscored	0.90	0.997	0.317
			Scored	4.50	0.996	0.412

Table 19.   Summary of hardness calibration and validation results for ACS (scored) tablets. Reference SE for Avicel/CTM SRC tablets is 0.68.

MLR- 2d hardness data

Cal.file	mult r	SEE	Val.File	bias/SEB	mult r	SEP
acs-cal1	-0.994	0.455	NS/S	5.90	0.995	0.463
			Nonscored	12.76	0.994	0.458
			Scored	1.23	0.993	0.541
acs-cal2	0.997	0.310	Nonscored		0.994	0.468
			Scored	1.72	0.996	0.385
acs-cal3	-0.994	0.472	NS/S	6.36	0.995	0.456
			Nonscored		0.995	0.436
			Scored	1.04	0.993	0.527
acs-cal4	0.996	0.399	Scored	1.09	0.994	0.458

MLR-Raw hardness data

Cal.file	mult r	SEE	Val.File	bias/SEB	mult r	SEP
acs-cal5	0.993	0.513	NS/S	6.11	0.991	0.603
			Scored	0.13	0.985	0.728
acs-cal6	0.995	0.416	Scored	0.84	0.992	0.531
acs-cal7	0.997	0.360	Scored	1.05	0.992	0.519

PLS- 2d hardness data

Cal.file	mult r	SEE	Val.File	bias/SEB	mult r	SEP
acs-pls1	0.998	0.281	Scored	2.28	0.996	0.430

PLS- Raw hardness data

Cal.file	mult r	SEE	Val.File	bias/SEB	mult r	SEP
acs-pls2	0.999	0.250	Scored	0.81	0.994	0.498

These findings conclude that separate calibrations are needed for an accurate prediction of scored tablets. This further indicates that there is a difference in the NIR signal due to scoring of Avicel®/CTM tablets.

1.4.5.2   *Hardness Calibration of FF Avicel®/CTM Tablets*

Table 20 summarizes the calibration and validation process for FF Avicel®/CTM tablets using MLR and PLS regression. The equations developed for the flat tablets were able to adequately predict AF validation sets. The SEE values for three out of four MLR models were far below the reference SEE (AF SEE = 0.66 kg), which raises the suspicion of overfitting the model. These models also produced SEP's that were less than the SEE, an unexpected result since SEP's are normally greater than SEE's.

None of the AF equations were able to predict AC data sets. There did not appear to be a significant difference in calibration performance using raw data versus second derivative data for either MLR or PLS models.

1.4.5.3   *Hardness Calibration of Mixed FF & SRC Avicel®/CTM Tablets*

Table 21 summarizes the results of calibrations developed for spectral data consisting of mixed AC and AF samples (ACAF). In general, it was possible to model the combined sets of Avicel® tablet data. PLS calibrations were better than MLR for these samples, and raw data produced slightly better results than second derivative data. The calibrations performed best when applied to validation sets of mixed samples. When applied to sets of flat, scored or nonscored tablet data, a large bias value resulted.

Better calibrations resulted from data sets that excluded AF hardness levels 2 and 4. These two sample sets were very close to the "adjacent" sample sets in spectral appearance. These findings provide valuable information about the suitability of the calibration sample set.

The effect of increasing the number of regression wavelengths can be observed in the first three MLR second derivative calibrations of Table 21. Regression at 2054 nm

213

Table 20.   Summary of hardness calibration/validation results for AF (flat-faced) tablets. Reference SE for Avicel/CTM FF tablets is 0.39. (# denotes a deleted sample).

MLR-2d hardness data

Cal.file	mult r	SEE	Val.File	bias/SEB	mult r	SEP
afc1-c1	0.9955	0.405	NS/S	4.6	0.939	2.160
			Flat	0.48	0.997	0.359
afc1-c2	0.9975	0.309	NS/S	7.09	0.966	2.130
			Flat	0.7	0.998	0.275
afc1-c3			NS/S	8.05	0.969	2.250
			NS/S #	0.49	0.973	0.962
			Flat	0.11	0.999	0.250
afc1-c4	-0.993	0.509	NS/S	25.17	0.928	9.550
			Flat	0.51	0.993	0.519
afc1-c5	0.9978	0.288	NS/S	21.58	0.966	5.710
			Flat	0.95	0.998	0.296

MLR-Raw hardness data

Cal.file	mult r	SEE	Val.File	bias/SEB	mult r	SEP
afc1r-c1	0.9986	0.229	NS/S	14.11	0.983	2.740
			Flat	0.56	0.999	0.231
afc1r-c2	0.9957	0.396	NS/S	44.38	0.990	6.410
			Flat	0.38	0.998	0.304

214

Table 20. Summary of AF calibration and validation results (continued).

PLS- 2d hardness data

Cal.file	mult r	SEE	Val.File	bias/SEB	mult r	SEP
afc1-p1	0.9979	0.2945	NS/S	10.89	0.971	2.820
afc1-p2	0.9982	0.2727	Flat	0.67	0.998	0.277
			NS/S	24.2	0.940	8.390
			Flat	0.7	0.998	0.258

PLS- Raw hardness data

Cal.file	mult r	SEE	Val.File	bias/SEB	mult r	SEP
afc1r-p1	0.9978	0.2874	Flat	0.25	0.9980	0.277
afc1r-p2	0.9987	0.2359	NS/S	9.60	0.995	1.070
			Flat	0.65	0.999	0.235

215

Table 21.   Summary of hardness calibration/validation results for ACAF
              (combined FF and SRC) tablets. Reference SE for all (flat and SRC)
              Avicel/CTM tablets is 0.54.

MLR-2d hardness data

Cal.file	mult r	SEE	Val.File	bias/SEB	mult r	SEP
acf2d-c1	-0.990	0.644	ACAF	0.62	0.991	0.619
			NS/S	0.99	0.969	1.050
			Flat	1.69	0.994	0.541
acf2d-c2	0.992	0.566	ACAF	0.17	0.993	0.539
acf2d-c3	0.994	0.505	ACAF	0.05	0.993	0.521
acf2d-c4	0.995	0.467	ACAF	0.09	0.996	0.426
acf2d-c5	0.997	0.347	ACAF	0.67	0.996	0.393

MLR- Raw hardness data

Cal.file	mult r	SEE	Val.File	bias/SEB	mult r	SEP
acf2-c1 (h135)	0.992	0.586	NS/S	0.11	0.991	0.659
			Flat	0.80	0.994	0.513
			ACAF	1.24	0.991	0.624
acf2-c2 (h135)	0.995	0.461	Flat	0.03	0.735	0.224
			Scored	0.57	0.992	0.841
			ACAF	0.60	0.992	0.579
			NS/S	0.70	0.991	0.696
			Flat H2	9.22	0.899	0.342
			Nonscored	10.62	0.996	1.080
amix-cal1	0.998	0.264	ACAF	4.23	0.981	1.020
			Flat	16.20	0.996	1.410
amix-cal2	0.993	0.482	ACAF	8.05	0.837	4.380

216

Table 21. Summary of calibration/validation results of ACAF hardness (continued).

PLS- 2d hardness data

Cal.file	mult r	SEE	Val.File	bias/SEB	mult r	SEP
acf2d-p1	0.997	0.386	ACAF	1.21	0.997	0.396
acf2d-p2	0.998	0.334	ACAF	0.13	0.997	0.388
			Scored	1.19	0.995	0.455
			NS/S	1.92	0.993	0.598
			Nonscored	5.29	0.995	0.705

PLS- Raw hardness data

Cal.file	mult r	SEE	Val.File	bias/SEB	mult r	SEP
acf2-p1 (h135)	0.998	0.331	ACAF	0.51	0.997	0.340
acf2-p2 (h135)	0.998	0.265	ACAF	0.04	0.998	0.279
amixpls1	0.999	0.213	ACAF	6.04	0.929	2.300
amixpls2	0.998	0.271	ACAF	7.08	0.976	1.560
amixpls3	0.997	0.313	ACAF	8.04	0.884	3.670

(calibration filename acf2d-c1) produced a satisfactory calibration, with an SEE of 0.644 kg. The addition of a second regression term at 2136 nm (calibration filename acf2d-c2) improved the SEE to 0.566. The SEP improved from 0.619 to 0.539, and the bias was significantly reduced. The addition of a third wavelength (2460 nm, calibration filename acf2d-c3) further improved the model. Linearity improved only slightly with the addition of the second and third wavelengths.

Figures 42 to 46 display the residual versus NIR calculated hardness plots for several unsuccessful Avicel®/CTM calibration models. Each of the models produced a high degree of bias in the validation process. The bias is obvious in each of the plots, as there appeared to be two distinct populations. Further analysis showed that this was indeed the case, leading to the conclusion that the residual data are segregated by geometry.

1.4.5.4   Hardness Calibration of SRC Emcompress®/CTM Tablets

Hardness calibration and validation results for EC (combined scored and nonscored data) tablets are summarized in Table 22. The reference SE for hardness of EC tablets was 0.55 kg. Second derivative models came closest to this value in the SEE's. Linearity was also slightly better in second derivative calibrations. Second derivative models were used to predict three types of validation sets: nonscored, scored and mixed (nonscored plus scored) data. The best performance (SEP values) resulted unexpectedly from validation sets containing only scored data. Since scoring is probably responsible for much of the variability factor in the calibrations, we might conclude that some of the calibration samples contain too much variability, and the calibration set should be reevaluated. Remembering that both calibration and validation sets are representative of the entire sample population, we would ideally want outliers excluded, and our validation sets to be similar to the calibration samples. If they are not, then a new calibration set should be selected, which more closely resembles the entire population to be modeled. The present calibration set is not realistic, from a manufacturing perspective, since we would probably not use mixed data of this type.

218
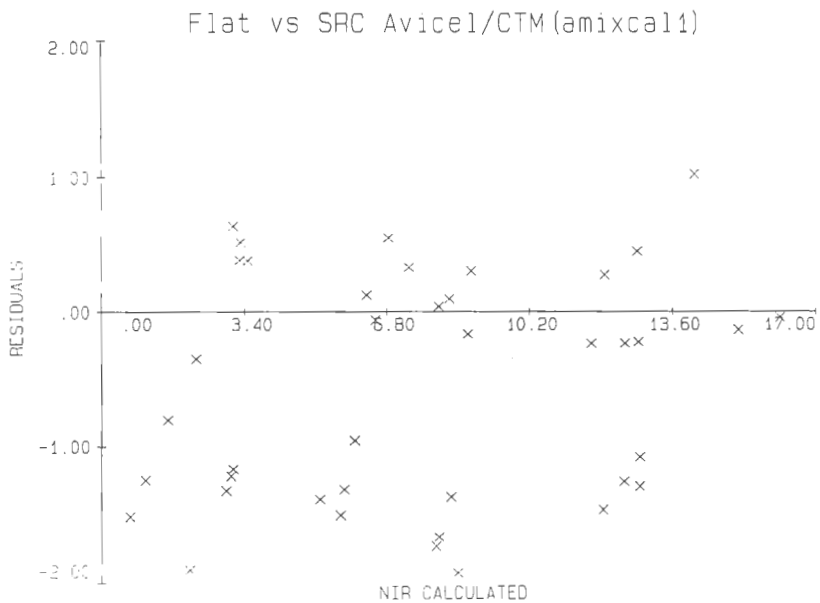
Figure 42. Residual versus NIR calculated hardness ACAF (Flat and SRC) Avicel®/CTM tablets (MLR calibration filename amixcal1).
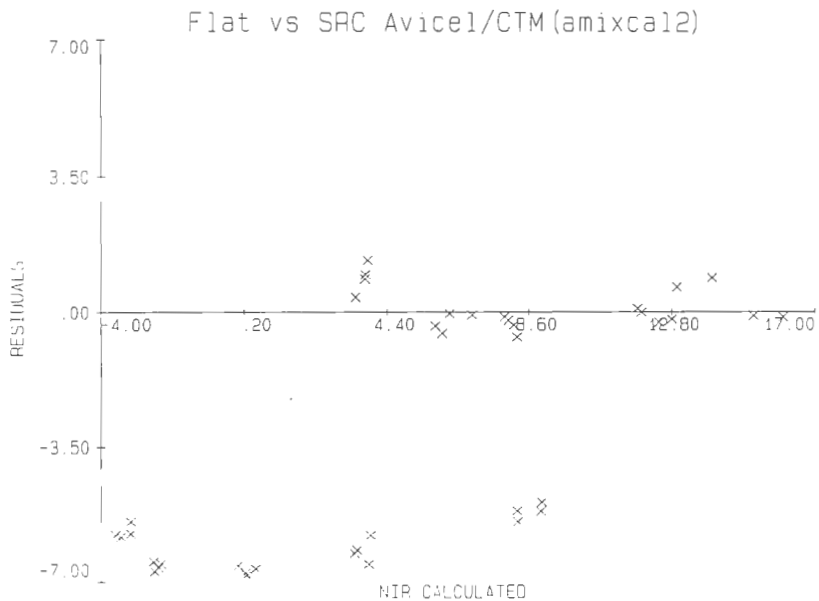
Figure 43. Residual versus NIR calculated hardness: ACAF (Flat and SRC) Avicel®/CTM tablets (MLR calibration filename amixcal2).
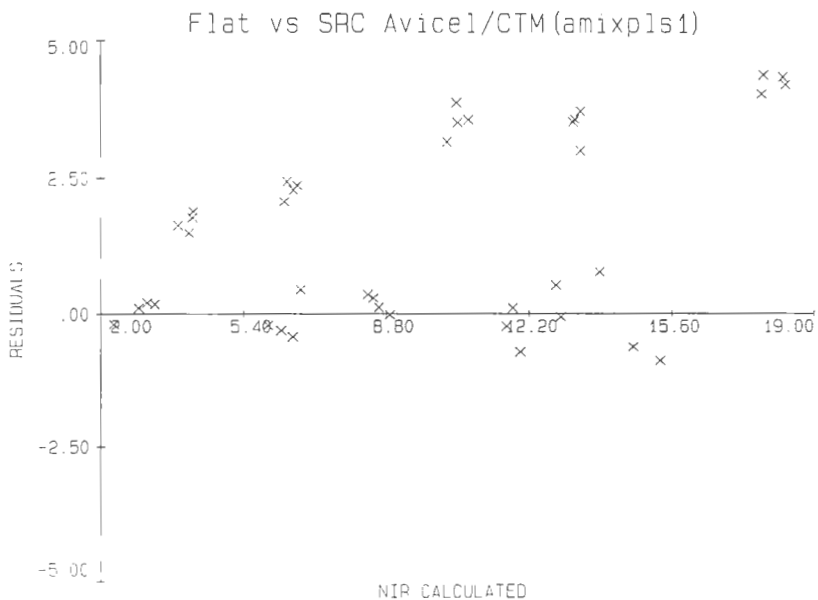
Figure 44. Residual versus NIR calculated hardness: ACAF (Flat and SRC) Avicel®/CTM tablets (PLS calibration filename amixpls1).
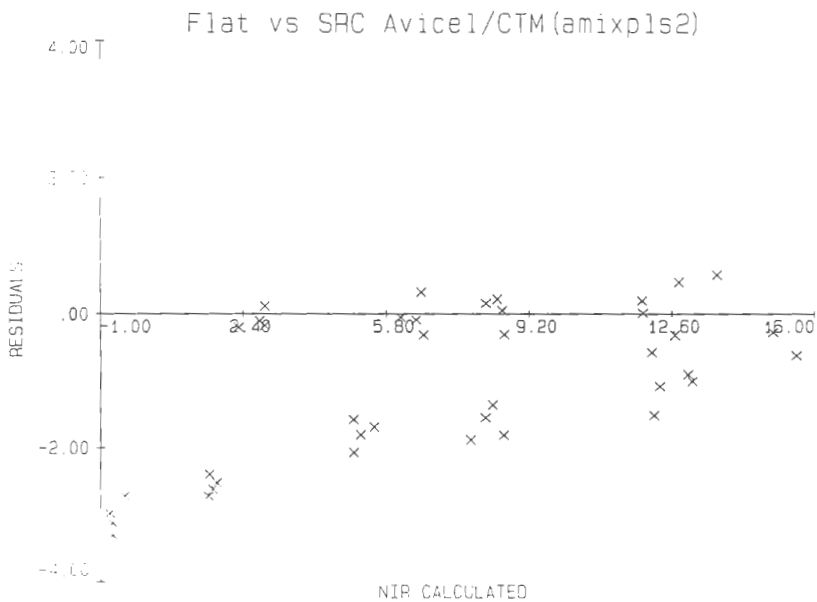
Figure 45. Residual versus NIR calculated hardness: ACAF (Flat and SRC) Avicel®/CTM tablets (PLS calibration filename amixpls2).
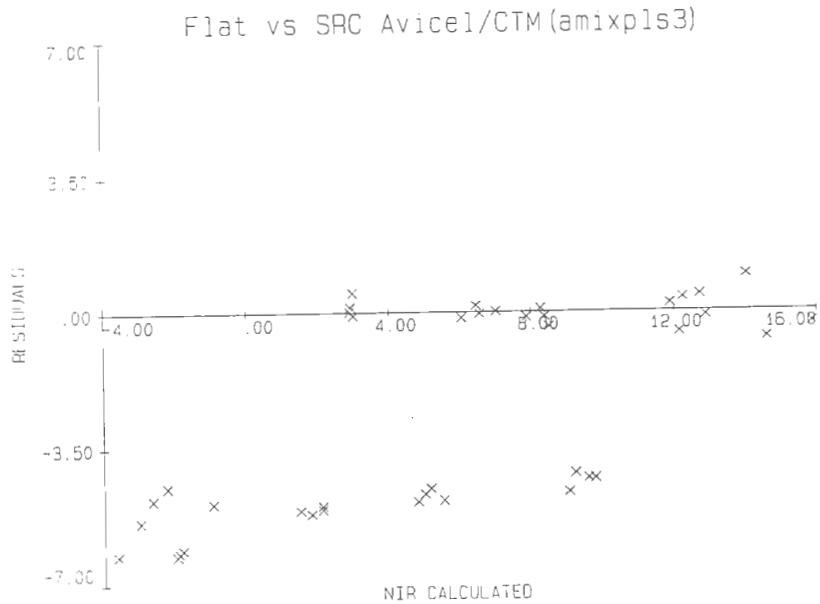
Figure 46. Residual versus NIR calculated hardness: ACAF (Flat and SRC) Avicel®/CTM tablets (PLS calibration filename amixpls3).

Table 22.   Summary of calibration/validation results of EC (combined) hardness data.
Reference SE is 0.55 for Emcompress/CTM SRC tablets.

MLR- 2d hardness data

Cal.file	mult r	SEE	Val.File	bias/SEB	mult r	SEP
ecacal2	0.984	0.465	Nonscored	0.61	0.969	0.677
			Scored	0.79	0.967	0.666
			NS/S	0.02	0.933	0.933
ecacal3	0.963	0.674	Nonscored	2.31	0.971	0.758
			Scored	0.91	0.978	0.548
			NS/S	0.70	0.968	0.655

MLR- Raw hardness data

Cal.file	mult r	SEE	Val.File	bias/SEB	mult r	SEP
ecacal1	0.952	0.745	NS/S	0.39	0.972	0.624

PLS- 2d hardness data

Cal.file	mult r	SEE	Val.File	bias/SEB	mult r	SEP
ecapls4	0.9869	0.442	Nonscored	2.19	0.977	0.676
			Scored	0.85	0.977	0.566
			NS/S	0.22	0.936	0.911

PLS- Raw hardness data

Cal.file	mult r	SEE	Val.File	bias/SEB	mult r	SEP
ecapls2	0.960	0.695	NS/S	0.74	0.968	0.680
ecapls3	0.973	0.568	NS/S	0.15	0.974	0.589

Results of hardness calibration and validation for ECN (nonscored) tablets are summarized in Table 23. Raw MLR calibrations were much better than second derivative MLR. The first set of MLR models (second derivative) differs in the number of wavelengths regressed. The first was developed at 1752 nm and the second at 1752 and 1348 nm. Linearity was fair for both, and SEE values were close to the reference SE of 0.55 kg. Prediction results were not as good, with relatively high bias/SEB and SEP values. In fact, these two models were better at predicting scored and mixed (scored with nonscored) data. This might be explained by the high regression coefficients obtained for each of the models. The regression coefficient for the first equation was 5950, and for the second the coefficients were 10,508 and 5,836; over 5,000 is undesirable and indicate overfitting.

In contrast, one of the raw data MLR models had regression coefficient values in the low hundreds, and a SEE of 0.552 kg. Prediction based on this model resulted in a SEP of 0.353. This was a two-term equation, based on regression at 2492 and 1922 nm. The other equation in the raw data MLR section of Table 23 was a one-term model at 2492 nm. Although prediction with this equation was good (SEP = 0.700 kg), this model was deemed unacceptable because the calibration multiple r value was only 0.919 and the SEE was 0.923.

PLS models for EC nonscored tablets also appear in Table 23. The best calibration was a second derivative model with a SEE of 0.587 kg and a SEP of 0.579 kg. It can be noted from the table that these PLS models seemed to fit scored, nonscored and mixed (scored with nonscored) data nearly equally. However, the linearity of each of the models is marginal, with calibration multiple r value of 0.970 or less. If the calibration sample set was changed, linearity might improve. Of the two PLS models developed from raw EC nonscored data, one had a SEP of 0.623 kg, although the calibration multiple r value was only 0.954. Overall, calibration of nonscored Emcompress®/CTM tablets was only moderately successful.

Table 23.   Summary of hardness calibration/validation of EC nonscored tablets.
Reference SE is 0.55 for Emcompress/CTM SRC tablets.

MLR-2d hardness data

Cal.file	mult r	SEE	Val.File	bias/SEB	mult r	SEP
ecncal1	-0.961	0.643	Nonscored	2.57	0.972	0.844
			Scored	2.36	0.972	0.726
			NS/S	0.12	0.969	0.682
ecncal2	0.969	0.594	Nonscored	2.35	0.961	0.980
			Scored	3.93	0.961	1.030
			NS/S	1.12	0.949	0.877

MLR- Raw hardness data

Cal.file	mult r	SEE	Val.File	bias/SEB	mult r	SEP
ecnrcal1	0.919	0.923	Nonscored	0.35	0.967	0.700
ecnrcal2	0.973	0.552	Nonscored	1.91	0.989	0.353

Table 23. Summary of hardness calibration/validation of EC nonscored tablets (continued).

PLS- 2d hardness data

Cal.file	mult r	SEE	Val.File	bias/SEB	mult r	SEP
ecnpls1	0.942	0.787	Scored	0.20	0.975	0.659
			NS/S	1.09	0.976	0.652
ecnpls2	0.969	0.625	Nonscored	2.52	0.973	0.820
			Scored	0.93	0.955	0.852
			NS/S	1.07	0.967	0.733
ecnpls3	0.970	0.587	Nonscored	0.75	0.975	0.579
			Scored	0.92	0.975	0.587
			NS/S	0.11	0.976	0.567

PLS- Raw hardness data

Cal.file	mult r	SEE	Val.File	bias/SEB	mult r	SEP
ecnrpls1	0.969	0.607	Nonscored	2.81	0.955	1.010
ecnrpls2	0.954	0.784	Nonscored	0.07	0.970	0.623

Hardness calibration and validation results for ES (scored) tablets are summarized in Table 24. A series of second derivative MLR equations was developed by successively adding a wavelength term to the model. The first two models were created using one wavelength (2172 nm and 2170 nm, respectively). The second model had a better SEE, but the prediction results were better with the first equation (SEP = 0.766 kg versus 0.872). SEE's were further reduced by the addition of another regression term, but overall performance was not as good as expected. Although SEE values were very low, the performance of the models was not acceptable (i.e., SEP values were much higher than the reference SE). None of the scored MLR models could predict nonscored or mixed data sets; all predictions resulted in high bias/SEB and SEP values.

Two MLR calibrations were created for scored tablets using raw data. The wavelengths used were the same as those in the nonscored data, with the same results. The two-term equation was better than the one term equation and SEP values were in the same range as the reference SE.

One PLS calibration was developed for scored tablets using second derivative data. The SEE was 0 .854 and the SEP was 0.567 for scored tablets. This model predicted nonscored and mixed (scored with nonscored) nearly as well as it predicted scored data. This result indicates that the PLS model is not precise enough to discriminate the different data sets.

1.4.5.5   Hardness Calibration of FF Emcompress®/CTM Tablets

Table 25 summarizes hardness calibration and validation results for EF (flat-faced) tablets. Overall, prediction results (SEP) for EF validation sets were at least as good as the reference SE of 0.46 kg. The first section contains two MLR models developed from raw data. The difference between them is that the first was constructed with a single wavelength (2288 nm, SEE = 0.692 kg) and the second from two wavelengths (2288 + 1910 nm, SEE = 0.697 kg). In this case, the addition of a second term did not

Table 24.   Summary of hardness calibration/validation results for EC scored tablets .
Reference SE is 0.55 for Emcompress/CTM SRC tablets. (*denotes an
adjustment to bias/slope).

MLR- 2d hardness data

Cal.file	mult r	SEE	Val.File	bias/SEB	mult r	SEP
ecscal1	0.962	0.700	Nonscored	5.00	0.951	1.370
			Scored	0.59	0.955	0.766
			NS/S	3.05	0.959	0.938
ecscal2	0.983	0.476	Nonscored	6.71	0.940	1.880
			Scored	1.13	0.948	0.872
			NS/S	2.49	0.952	0.961
ecscal3	0.988	0.416	Nonscored	7.01	0.929	2.100
			Scored	1.17	0.932	1.000
			NS/S	4.07	0.940	1.330
ecscal4	0.989	0.397	Nonscored	6.47	0.931	1.960
			Scored	1.03	0.935	0.979
			NS/S	3.67	0.942	1.250

MLR- Raw hardness data

Cal.file	mult r	SEE	Val.File	bias/SEB	mult r	SEP
ecsrcal1	0.932	0.933	Scored	1.80	0.967	0.733
ecsrcal2	0.948	0.830	Scored	0.12	0.975	0.579

Table 24. Summary of hardness calibration/validation results for EC scored tablets (continued).

PLS- 2d hardness data

Cal.file	mult r	SEE	Val.File	bias/SEB	mult r	SEP
ecspls1	0.943	0.854	Nonscored	1.52	0.967	0.744
			Scored	0.03	0.975	0.567
			NS/S	0.84	0.976	0.581

Table 25.   Summary of hardness calibration/validation results for EF (flat-faced)
tablets. Reference SE for Emcompress/CTM flat-faced tablets is 0.46.

MLR-Raw hardness data

Cal.file	mult r	SEE	Val.File	bias/SEB	mult r	SEP
efr-cal1	0.985	0.692	NS/S	8.09	0.951	1.870
efr-cal2	0.985	0.697	Flat	1.22	0.996	0.377

MLR-2d hardness data

Cal.file	mult r	SEE	Val.File	bias/SEB	mult r	SEP
ef-cal1	-0.985	0.688	Flat	0.71	0.994	0.471
ef-cal2	0.990	0.583	Flat	0.26	0.994	0.440
ef-cal3	0.988	0.620	Flat	0.98	0.993	0.516

PLS- Raw hardness data

Cal.file	mult r	SEE	Val.File	bias/SEB	mult r	SEP
efr-pls1	0.984	0.700	NS/S*	9.12	0.949	2.120
			Flat	1.30	0.996	0.366

PLS- 2d hardness data

Cal.file	mult r	SEE	Val.File	bias/SEB	mult r	SEP
ef-pls1	0.980	0.800	Flat	0.73	0.993	0.473
ef-pls2	0.987	0.680	Flat	0.81	0.995	0.415

significantly improve the model. The SEP obtained upon prediction of an EF validation set using the two-term model was 0.377 kg.

The second section of Table 25 contains MLR models developed from second derivative (2d) data. These were based on one, three, and two terms, respectively. The three-term model produced the best SEE (0.583 kg) and SEP (0.440 kg).

PLS models follow the MLR results in Table 25. The raw data PLS model utilized one factor and produced acceptable results (SEE = 0.700 kg, SEP = 0.366 kg). The second derivative models varied in the number of factors, which were one and three, respectively. The three-factor model had a better SEE (0.680 kg) than the one-factor model (SEE = 0.800) and a better SEP (from 0.473 to 0.415 kg). It appeared that PLS and MLR models performed equally well, and second derivative models were slightly better than raw data models (bias/SEB ratios were lower for second derivative models).

1.4.5.6   Hardness Calibration of Mixed FF & SRC Emcompress®/CTM Tablets

Numerous calibration equations were generated for Emcompress®/CTM tablets of mixed geometry (ECEF). Results of hardness calibration and validation for ECEF data are summarized in Table 26. Raw data and second derivative data performed equally well for ECEF data sets. All of the MLR and PLS models adequately fit validation sets of mixed EC and EF spectra. The addition of a second or more regression wavelengths improved the models. This point is illustrated by calibration files ecef-p3, ecef-p4, ecef-c5 and ecef-c7 in Table 26. File ecef-p3 is based on one wavelength (1824 nm). The next three calibration files include the successive addition of regression wavelengths 2436 nm, 1620 nm and 2236 nm, respectively. Each additional wavelength resulted in an improvement in both correlation coefficient (from 0.9877 to 0.9957) and SEE (from 0.500 to 0.306). However, the SEP's did not improve as expected in the validation process. In this case, the SEP increased with each additional wavelength, and leveled out after three terms.

Table 26.   Summary of hardness calibration/validation of ECEF tablets.
             Reference SE is 0.50 for all Emcompress/CTM tablets.

MLR- 2d hardness data

Cal.file	mult r	SEE	Val.File	bias/SEB	mult r	SEP
ecef-c1	0.969	0.823	ECEF	0.34	0.981	0.618
			NS/S	0.47	0.946	0.818
			Nonscored	2.18	0.956	0.913
			Scored	1.1	0.969	0.659
ecef-c2	0.982	0.602	NS/S	0.27	0.939	0.894
			ECEF	1.21	0.981	0.653
ecef-p3	0.988	0.500	ECEF	1.57	0.981	0.681
ecef-p4	0.993	0.390	ECEF	1.91	0.982	0.702
ecef-c5	0.995	0.319	NS/S	1.86	0.939	1.050
			ECEF	1.83	0.980	0.732
ecef-c7	0.996	0.306	NS/S	1.68	0.940	1.040
			ECEF	1.62	0.979	0.754
ecef-c6	0.990	0.471	ECEF	1.83	0.979	0.763

MLR- Raw hardness data

Cal.file	mult r	SEE	Val.File	bias/SEB	mult r	SEP
emixcal1	0.964	0.893	ECEF	0.2	0.980	0.634
			NS/S	0.59	0.967	0.780
			Flat	1.6	0.995	0.458
emixcal2	0.971	0.810	ECEF	0.27	0.985	0.550
emixcal4	0.980	0.690	ECEF	0.52	0.986	0.550

Table 26. (continued) Summary of hardness calibration/validation of ECEF tablets.

PLS- 2d hardness data

Cal.file	mult r	SEE	Val.File	bias/SEB	mult r	SEP
ecef-p1	0.974	0.779	ECEF	0.03	0.986	0.542
			Nonscored	1.25	0.961	0.792
			Scored	0.25	0.974	0.606
ecef-p2	0.983	0.647	ECEF	0.54	0.974	0.749
ecef-pl3	0.982	0.654	ECEF	0.65	0.986	0.548
ecef-pl4	0.993	0.420	ECEF	1.32	0.975	0.814
ecef-pl5	0.981	0.674	ECEF	1.09	0.983	0.626
			Nonscored	2.28	0.961	1.050
			Scored	2.88	0.971	0.905
ecef-pl6	0.985	0.595	ECEF	1.63	0.981	0.706
			Nonscored	1.59	0.960	1.140
ecef-pl7	0.992	0.460	ECEF	2.07	0.980	0.759

PLS- Raw hardness data

Cal.file	mult r	SEE	Val.File	bias/SEB	mult r	SEP
emixpls1	0.980	0.689	ECEF	0.51	0.985	0.552

1.4.6　　　　*Calibration of Compression Force*

　　　　Upper and lower punch compression forces were calibrated against NIR data for flat faced tablets using both raw and second derivative data. As with hardness calibrations, the addition of a second regression term tended to improve a MLR model. Tablet matrix appeared to be a factor in the success of the calibrations, as it was possible in this study to calibrate Avicel® /CTM but not Emcompress® /CTM tablets.

1.4.6.1　　　　*Compression Calibration of FF Avicel®/CTM Tablets*

　　　　The upper compression force (UC) calibration and validation results for Avicel® /CTM tablets are summarized in Table 27. The reference SEE for flat Avicel® /CTM tablets was 0.099 kN (the overall SEE for Avicel® /CTM flat and convex tablets was 0.118 kN) for upper compression force. Regression coefficient values were under 2000 for second derivative data, and in the hundreds for raw data models. Two PLS models were developed for each type of data, using the full spectral range for one (1100 to 2500 nm) and a restricted range for the other model (1500-1990). Reducing the wavelength range improved the calibration statistics but did not improve prediction performance. Both of the raw data calibrations made adequate predictions of the validation set. Comparisons of raw data versus second derivative models were inconclusive, since there were only two models for each data type.

　　　　Table 28 summarizes the calibration and validation efforts for lower compression (LC) force data. The reference SE for Avicel®/CTM LC flat tablets was 0.075 kN, and the overall SE for Avicel®/CTM flat and convex tablets was 0.086 kN. The same wavelengths as the UC calibrations were used for LC MLR models. Calibration statistics for LC data were slightly better than for UC data, with linearity being equal.

　　　　Overall, calibration of Avicel®/CTM upper and lower compression force with NIR absorbance was successful despite the small number of samples in the calibration set.

Table 27.   Near-infrared calibration/validation of upper compression force for Avicel®
/CTM tablets.

MLR- 2d UC data

Cal.file	mult r	SEE	Val.File	bias/SEB	mult r	SEP
afc2-c1	-0.991	0.121	afcval2d	0.963	0.993	0.121
afc2-c2	0.995	0.097	afcval2d	1.797	0.988	0.179

MLR-Raw data

Cal.file	mult r	SEE	Val.File	bias/SEB	mult r	SEP
afc2r-c1	0.978	0.195	afc-val	0.304	0.979	0.196
afc2r-c3	0.993	0.116	afc-val	0.654	0.993	0.128

PLS-2d data

Cal.file	mult r	SEE	Val.File	bias/SEB	mult r	SEP
afc2-p1	0.999	0.052	afcval2d	0.214	0.989	0.144
afc2-p2	0.993	0.112	afcval2d	1.606	0.995	0.114

PLS- Raw data

Cal.file	mult r	SEE	Val.File	bias/SEB	mult r	SEP
afc2r-p1	0.991	0.129	afc-val	0.35	0.993	0.118
afc2r-p2	0.993	0.116	afc-val	1.818	0.989	0.167

Table 28.   Near-infrared calibration and validation of lower compression force for Avicel®/ CTM tablets.

MLR-2d data

Cal.file	mult r	SEE	Val.File	bias/SEB	mult r	SEP
afc3-c1	-0.991	0.103	afcval2d	0.312	0.992	0.099
afc3-c2	0.995	0.080	afcval2d	1.461	0.988	0.136
afc3-c3	0.997	0.059	afcval2d	2.024	0.992	0.123

MLR-Raw data

Cal.file	mult r	SEE	Val.File	bias/SEB	mult r	SEP
afc3r-c1	0.977	0.163	afc-val	0.066	0.978	0.165
afc3r-c2	0.992	0.097	afc-val	0.032	0.992	0.106

PLS-2d data

Cal.file	mult r	SEE	Val.File	bias/SEB	mult r	SEP
afc3-p1	0.990	0.111	afcval2d	0.448	0.988	0.122
afc3-p2	0.993	0.090	afcval2d	0.862	0.995	0.084

PLS- Raw data

Cal.file	mult r	SEE	Val.File	bias/SEB	mult r	SEP
afc3r-p1	0.991	0.107	afc-val	0.253	0.991	0.107
afc3r-p2	0.997	0.066	afc-val	1.795	0.989	0.135

1.4.6.1   Compression Calibration of FF Emcompress® /CTM Tablets

Results of the upper punch calibration and validation for Emcompress® /CTM tablets are summarized in Table 29. The reference SE was an inflated 1.277 kN. This value dropped to 0.226 kN with the exclusion of level EF1 data. Since the models were created using all five compression force levels, 1.277 kN is the relevant value.

MLR models constructed from second derivative data had very high regression constants, despite conformance to acceptable SEE and SEP levels. These findings indicate the presence of high variability or an outlier in the calibration set. Emcompress® /CTM spectral and reference data contained more variability than the Avicel® /CTM tablets.

Lower punch calibration and validation results appear in Table 30. Again, the reference SE for this data inflated to 0.925 kN with all data included, and 0.141 kN without EF1 data. SEE and SEP values fell below the reference SE, but there was a high amount of bias in the validations. Raw data models were slightly better than second derivative models.

Due to the small sample size (n=20) and high amount of variability, the calibration of Emcompress® /CTM flat tablets was deemed unsatisfactory. The process might be improved by using a larger calibration set and excluding the EF1 tablet data. It has been shown in other studies[7] that a greater matrix variability requires that many more samples be included in order to have a valid calibration. It is evident from the Avicel® /CTM results that compression force can be modeled using NIRS, however improper selection of the calibration set can produce inadequate results.

1.7   Conclusions

These results describe the utility of the hardness/NIR relationships for different formulations. The NIR/hardness relationship established in Manuscript II still holds true for other matrices: an increase in tablet compression force resulted in an increased NIR

Table 29.   Near-infrared calibration and validation of upper compression force for
Emcompress® /CTM flat tablets.

MLR-Raw data

Cal.file	mult r	SEE	Val.File	bias/SEB	SEP	mult r
efr2-c1	0.985	0.938	efc-val	0.129	0.439	0.993
efr2-c2	-0.990	0.793	efc-val*	0.856	0.572	0.997
efc2r-c1	0.998	0.296	efc-val	1.09	1.280	0.936
efc2r-c2	-0.996	0.372	efc-val	1.336	0.702	0.997
efc2r-c3	0.999	0.227	efc-val	0.035	1.570	0.976

*restored deleted samples

MLR-2d data

Cal.file	mult r	SEE	Val.File	bias/SEB	SEP	mult r
efc-cal1	-0.994	0.583	efcval2d	1.536	0.708	0.997
efc-cal2	0.997	0.436	efcval2d	4.835	0.950	0.999
efc2-c1	-0.999	0.225	efcval2d	1.167	0.357	0.995
efc2-c2	0.999	0.183	efcval2d	2.026	0.425	0.995

PLS- Raw data

Cal.file	mult r	SEE	Val.File	bias/SEB	SEP	mult r
efc2r-p1	1.000	0.150	efc-val	4.338	0.278	0.999

PLS-2d data

Cal.file	mult r	SEE	Val.File	bias/SEB	SEP	mult r
efc-pls1	0.985	1.030	efcval2d	3.063	1.230	0.992
efc2-p1	0.999	0.226	efcval2d	2.207	0.321	0.998

Table 30.   Near-infrared calibration/validation of lower compression force for
             Emcompress® /CTM tablets.

MLR-Raw data

Cal.file	mult r	SEE	Val.File	bias/SEB	SEP	mult r
efc3-c1	0.985	0.693	efc-val	1.35	0.513	0.997
efc3-c2	-0.989	0.597	efc-val	0.142	1.160	0.976

MLR-2d data

Cal.file	mult r	SEE	Val.File	bias/SEB	SEP	mult r
efc-cal3	-0.973	0.915	efcval2d	2.222	0.933	0.995
efc-cal4	-0.995	0.403	efcval2d	1.439	0.531	0.997
efc-cal5	0.997	0.319	efcval2d	3.993	0.679	0.998
efc-cal6	0.998	0.269	efcval2d	4.44	0.773	0.998

PLS- Raw data

Cal.file	mult r	SEE	Val.File	bias/SEB	SEP	mult r
efc3-p1	0.984	0.718	efc-val	1.105	0.512	0.997

PLS-2d data

Cal.file	mult r	SEE	Val.File	bias/SEB	SEP	mult r
efc-pls2	0.985	0.751	efcval2d	3.199	0.893	0.993

absorbance. There is a matrix effect involved in the NIR calibration of hardness and compression force. Calibration models must be formulation (matrix) specific.

Tablet geometry also has an effect on the NIR calibration of hardness. Calibration models designed specifically for one geometry type did not fit another shape of tablet surface. Raw data models had smaller regression coefficients than second derivative models, suggesting an increase in the amount of noise in the second derivative models. Mixed geometry models gave variable results, supporting the assertion that calibration models should contain samples of homogeneous composition.

The NIR spectra of scored sides of tablets contained more variability between replicates (higher standard deviation) than the nonscored sides of tablets. This study did not find a statistical difference in NIR response to hardness due to scoring of Emcompress®/CTM tablets, possibly due to the higher variability in reference and spectral data versus the Avicel®/CTM data. There was a significant difference in NIR response due to scoring of the Avicel®/CTM tablets. This portion of the study suggests that separate calibrations should be developed for scored and nonscored tablets.

This document described the determination of several tablet properties and subsequent calibration using NIRS. Further work may lead to an explanation of the mechanism behind changing NIR absorbance in response to increased tablet hardness. Specific studies may be undertaken to determine which features of the tablet surface are most responsible for the change in NIR response to increased compression force.

References

1)   Leuenberger, H. and Rohera, B. D., *Pharm. Res.* 3(1), 12-22 (1986).

2)   Nyström,C. and P. G. Karehill, "The Importance of Intermolecular Binding Forces and the Concept of bonding Surface Area", in Pharmaceutical Powder Compaction Technology, G. Alderborn and C. Nystrom, ed., Marcel Dekker, Inc., New York, NY, 1996, pp. 17-53.

3)   King, R. E., "Tablets, Capsules and Pills", in Remington's Pharmaceutical Sciences, Osol, A., et al, editors, Mack Publishing Co., Easton, Pennsylvania, pp. 1553-1584 (1980).

4)   Corti, P., et al, *Pharm. Acta Helv.*, 64(5-6), 140-143 (1989).

5)   Wade, A. and P. J. Weller, "Handbook of Pharmaceutical Excipients", second edition, American Pharmaceutical Association, Washington, D.C., pp. 56-60, 1994.

6)   ibid, pp 84-87.

7)   Corti, P., et al, *Pharm. Acta Helv.*, 64(5-6), 140-143 (1989).

Addendum to Manuscript IV

The following observations were made with regard to the results of Manuscripts III and IV.

Data from two tablet presses

There was a difference in the NIR spectra between two batches of CTM 6% tablets manufactured with two different tablet presses. One batch was produced at the University of Rhode Island (URI), using one station of a sixteen-station Stokes Rotary Tablet Press. The second batch was made at Pfizer Central Research, using a Korsch six-station tablet press. The same raw materials were used in both blends. The same NIR spectrophotometer was used to obtain the reflectance spectra of all of the samples. When the spectra were plotted together, there was one region (Figure 1a) where the spectra were different; the plot was essentially the same for the remainder of the spectra.

This finding has implications in the validation process of a NIR hardness testing method. The spectral variation may be due to inhomogeneity of the blend or differences in the concentration of one or more of the components. As the URI press was not instrumented, upper and lower punch data were not available for comparison to the Pfizer press data. In any case, a good NIR calibration set for this product would include this type of variation if a company produced these tablets at several manufacturing sites.
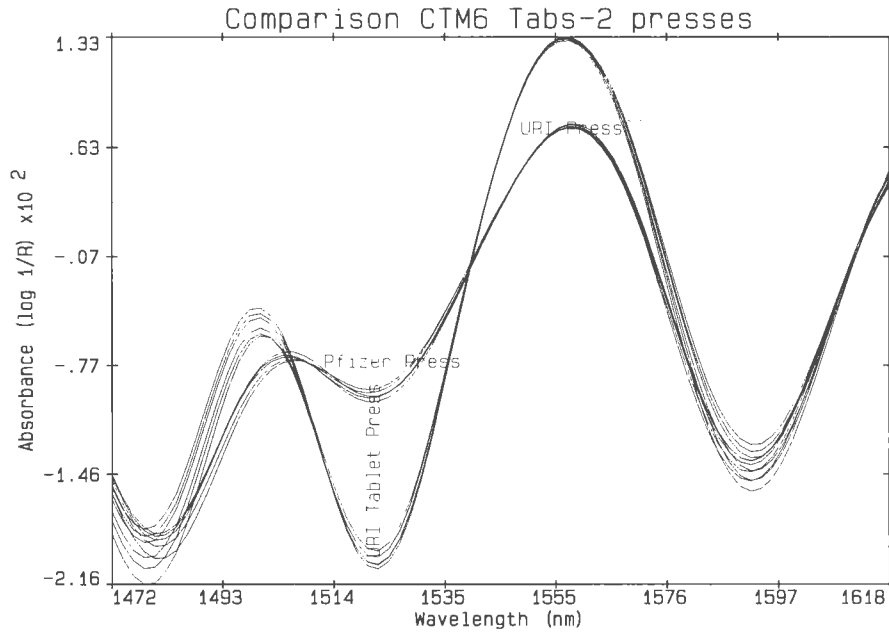
Figure 1a. Comparison of NIR spectra of chlorpheniramine maleate 6%/ Avicel ᴿ/magnesium stearate tablets manufactured on two different tablet presses.

<u>Data from two hardness testers</u>

The overall standard error of the Pfizer hardness tester was 0.50 kg, as compared to 0.32 kg for the Erweka hardness tester at URI. This difference may be attributed to the number and type of samples available for calculation. The error calculation for the Erweka Hardness Tester was based on sampling 20 flat faced, nonscored tablets from 20 batches of 300. All of these samples were of the same excipient matrix, so the calculation was based on the testing of 400 similar samples.

The calculation of the overall standard error of the hardness tester at Pfizer was based on a combination of flat faced and standard round convex tablets (with one scored side) and two different excipient matrices. Ten tablets from each batch of 200 tablets were included in the calculation, for a total of 200 samples tested. Hardness testing of the flat tablets resulted in a much lower (0.41 kg) standard error than convex tablets (0.60 kg). This difference should be considered when calibrating hardness with NIRS. The standard error for all batches containing Avicel® was 0.52 kg, while that for Emcompress® was 0.49 kg. This finding was unexpected, since NIR spectral data for the Avicel® -containing tablets appeared to be less variable than the Emcompress® tablet data.

SUMMARY OF CONCLUSIONS

1)   Near-infrared (NIR) spectrophotometric methods are becoming increasingly utilized by the pharmaceutical industry. However, the appearance of NIR methods in the pharmaceutical literature has been sparse, and indicates the reluctance of the industry to accept the technology.

2)   Although the potential of NIR to predict tablet parameters has been suggested, the published literature appears to have little data in this area. The present work appears to be the first study to evaluate the practical utility of the NIR/compression force relationship.

3)   Feasibility studies using chlorpheniramine/Avicel and hydrochlorothiazide/Avicel tablets indicated that a relatively simple relationship may exist between NIR absorbance and tablet hardness. An increase in tablet compression force resulted in a consistent increase in NIR absorbance.

4)   Chlorpheniramine/Avicel and hydrochlorothiazide/Avicel tablets of increasing hardness levels were successfully differentiated by principal component analysis. This result indicates the potential use of NIR as a useful and non-destructive, quality control mechanism. The NIR signal responded in the same way to a change in hardness, regardless of the drug.

5)   A series of formulation specific equations was developed by calibrating tablet hardness data against NIR reflectance response (absorbance) for each formulation. The results of NIRS hardness prediction were at least as precise as the reference hardness test (SE = 0.32).

6)   Calibration models developed using the calculated tablet density were better than those from hardness data. This was probably due to the accuracy of weight and thickness measurements and the high quality tablet press tooling. However, the predictive ability (SEP) of the hardness models was better than the density models. These results indicate that the hardness models contained built in variability and were thus more rugged. Conversely, the density models may have been overfitted.

7)   Separate calibration models are required for scored versus nonscored tablets, regardless of the tablet matrix. Mixed models consisting of scored and nonscored tablets adequately predicted mixed validation sets, but better predictions resulted when the calibration and validation sets contained only scored or nonscored tablets.

8)   NIR spectra are different for tablets of different excipient matrices, thus separate calibration models are required.

9)   Tablets composed of the same excipient matrix required slightly different calibration equations when the geometry was changed. Mixed models, composed of both flat and convex tablets, satisfactorily predicted mixed validation sets, but better predictions resulted when the calibration and validation sets contained tablets of only one type of geometry.

10)   It may be possible to predict tablet hardness using a NIR model based on only one wavelength. Good linearity and SEP values were obtained from simple linear regression equations from one or two wavelengths.

11)   NIR calibrations for tablet hardness performed best when formulation specific
models were constructed. Ruggedness was improved when all expected types of
variability were included in the model. Linearity and SEE were improved when the
calibration and validation sets contained a single type of product.

12)   The key factor in calibration development is the selection of the calibration set. It
was illustrated in this work that careful selection of representative samples is imperative to
the successful performance of the calibration model.

13)   This project demonstrated that it is possible to calibrate various tablet parameters
with NIR absorbance data and achieve successful predictions of those parameters. NIR
models for tablet hardness, density, upper and lower compression force data were
developed using several different tablet matrices.

SECTION III

Appendix A.   List of terms used in Statistical Summary Report[1]

(*reprinted with permission of Paul Entrop, Marketing Manager, Perstorp Analytical Co.,
Silver Spring, MD)

Bias	The average difference between the calculated and reported results.
Standard Error of Bias (SEB)	The standard error expressing the confidence interval of the reported bias.
Standard Error of Difference(SDD)	The bias corrected estimate of random errors.
Root Mean Square (RMS)	A non-bias corrected estimate of random errors. RMS will be equal to the SDD when the bias is zero.
Slope Adjustment	Factor by which the slope and bias terms are multiplied to adjust the existing equation to fit the current data. 1.00 = no adjustment.
Standard Error of Slope	Estimate of the error on the computed slope.
Intercept Adjustment	Adjustment to be made to the intercept term of the calibration when a slope adjustment is made. 0 is equivalent to no adjustment.
Standard Error of Performance	Estimate of the error in the computed values using a slope and bias corrected equation.
Simple Correlation	Correlation between the calculated and reported values using the slope and bias corrected equation.
Achievable Standard Error of Prediction (achievable SEP)	The best estimate of the achievable standard error of performance using the available data from each group.
Prediction Stability Coefficient	Ratio of the achievable SEP to the actual root mean square deviation (SEP). Thus, the achievable is more often less than the actual SEP.

1 Reference Manual for Near Infrared Spectral Analysis Software (NSAS) Version 3.30a,
NIRSystems, Inc./Perstorp Analytical Co., Silver Spring, MD, pp.3-1 to 3-62, 1995.

APPENDIX B.

Hardness calibration results for chlorpheniramine maleate (CTM), hydrochlorothiazide (HCTZ) and placebo tablets in Manuscript III.

Legend:

MLR	Multiple linear regression	
PLS	Partial least squares regression	
SEE	Standard error of estimation (or calibration)	
*	deleted outlier	
#	nonrandom sample selection in calibration set	

Table 1a.   CTM 2% MLR Calibration

Cal.file	k(0)	k(1)	k(2)	k(3)	λ nm	mult r	SEE
ctm2cal	-24.582	-4985.83	0	0	1458	-0.986	0.51
ct2cal4*	-24.244	-4934.89	0	0	1458	-0.9878	0.482
ct2cal2	-2.81	-4284.59	1075.8	0	1458+1528	0.9905	0.423
ct2cal3	1.266	4039.43	1231.8	-117.2	1458+1528+1728	0.9912	0.411
ct2cal5	-2.461	-4300.2	1102.4	0	1458+1528	0.9929	0.372

Hardness calibration results for CTM, HCTZ and Placebo tablets in Manuscript III.

Table 1b.   CTM 2% PLS calibration

Cal. file	# factors	MSECV	(min)	λ range nm	mult r	SEE
pls2ctm2	2	0.071	1.25	1100-2500	0.9871	0.4902
pls3ctm2	2	0.069	1.24	1300-2350	0.9873	0.4857
plsctm2	3	0.077	1.23	1100-2500	0.9884	0.4738
pls4ctm2	1	0.055	1.04	1300-2500	0.9903	0.4258
pls5ctm2	3	0.055	1.23	1174-1414	0.9906	0.4306
pls6ctm2	4	0.062	1.17	1950-2360	0.9911	0.4171

Hardness calibration results for CTM, HCTZ and Placebo tablets in Manuscript III.

Table 2a.   CTM 6% MLR Calibration

Cal.file	K(0)	K(1)	k(2)	k(3)	k(4)	λ nm	mult r	SEE
c6sscal10	-18.86	-396.54	-536.91	-422.92	0	2236+1932+1436	0.976	0.554
c6sscal6	35.81	14.04	0	0	0	1558/1784	0.987	0.394
c6sscal1	-28.37	-5523.27	0	0	0	1784	-0.989	0.365
c6sscal8	-29.83	-441.25	-7523.23	0	0	2236+1780	0.992	0.325
c6sscal2	-23.53	-3084.61	0	0	0	1590+1760	-0.992	0.318
ctm6cal	-28.37	-5520.97	0	0	0	1784	0.992	0.313
c6sscal3	-28.58	-5579.67	-229.45	0	0	1784+2254	0.993	0.298
c6sscal9	-29.77	-947.64	-6894.04	-992.57	0	2236+1780+2078	0.993	0.291
c6sscal7	22.47	12.77	4527.15	0	0	1558/1784+1698	0.994	0.285
c6sscal5	-35.59	-5934.56	-314.08	2686.51	-1113.249	1784+2254+1180 +1720	0.994	0.271

Hardness calibration results for CTM, HCTZ and Placebo tablets in Manuscript III.

Table 2b.   CTM 6% PLS Calibration

Cal. file	# factors	MSECV	(min)	λ range nm	mult r	SEE
pls4ctm6	5	0.023	1.21	1300-2350	0.9942	0.2771
pls3ctm6	5	0.022	1.06	1100-2500	0.9944	0.2721
pls2ctm6	7	0.022	1.10	1100-2500	0.9961	0.2237
pls1ctm6	8	0.024	1.06	1100-2500	0.9969	0.2038

Hardness calibration results for CTM, HCTZ and Placebo tablets in Manuscript III.

Table 3a.   CTM 2 & 6% MLR Calibration

Cal.file	K(0)	K(1)	k(2)	λ range nm	λ nm	mult r	SEE
ct26cal5	-24.826	-1325.83	-1930.18	1100-2500	2018+1436+2236+2268	0.9439	0.982
ct26cal1	-33.124	-5821.95	0	1100-2500	1824	-0.951	0.912
ct26cal3	-32.4	152.738	-7151.95	1930	1930+1824	0.9538	0.887
ctm26cal2	-20.653	-9243.32	1510.452	1100-2500	1824+2324	0.9676	0.746

Table 3b.   CTM 2 & 6% PLS Calibration

Cal. file	# factors	MSECV	(min)	λ range nm	mult r	SEE
c26pls1	11	0.064	1.18	1100-2500	0.9908	0.4121

Hardness calibration results for CTM, HCTZ and Placebo tablets in Manuscript III.

Table 4a.   HCTZ 15% MLR Calibration

Cal.file	K(0)	K(1)	K(2)	K(3)	λ nm	mult r	SEE
hct15c2#	-21.81	511.34	0.00	0	1998	0.944	1.010
6hc15cal	21.54	-139.21	0.00	0	1572/1998	-0.985	0.513
4hc15cal	-9.21	235.44	-2027.65	0	1998+1578	-0.959	0.441
hct15cal#	-31.17	-1399.01	0.00	0	2076	-0.984	0.547
2hc15cal	-29.89	-1345.28	0.00	0	2076	-0.983	0.541
5hc15cal	-27.78	-992.81	771.80	0	2076+1316	0.989	0.445
3h15c1*	-29.37	-1323.68	0.00	0	2076	-0.991	0.412
3h15c2*	-26.25	-896.24	-1232.31	0	2076+1822	0.994	0.330
3h15c3	-22.25	-479.63	-2172.43	292.36	2076+1822+1902	0.996	0.295
7hc15cal	-2.11	-955.78	0.00	0	1360+2262	0.990	0.502
9hc15cal	71.97	-51.69	0.00	0	1580/1676	-0.989	0.430
8hc15cal	-25.11	-1372.35	908.01	0	2320+1328	0.990	0.417
10hc15ca	-12.16	-631.55	-3582.01	0	1520+1576	0.991	0.393

Hardness calibration results for CTM, HCTZ and Placebo tablets in Manuscript III.

Table 4b.   HCTZ 15% PLS Calibration

Cal. file	# factors	MSECV	λ range nm	(min)	mult r	SEE
pls2hc15*	4.00	0.03	1100-2500	1.13	0.995	0.301
pls4hc15	4.00	0.03	1300-2350	1.18	0.995	0.294
7hc15pls	6.00	0.04	1100-2500	1.21	0.994	0.341
plshct15	6.00	0.04	1100-2500	1.01	0.995	0.310
3h15pl	4.00	0.06	1100-2500	1.12	0.996	0.289

Hardness calibration results for CTM, HCTZ and Placebo tablets in Manuscript III.

Table 5a. HCTZ 20% MLR Calibration

Cal.file	K(0)	K(1)	K(2)	λ nm	mult r	SEE
5hc20cal	-13.7	499.789	0	1394	0.9799	0.446
6hc20cal	-14.002	73.401	760.654	1930+1390	0.9808	0.442
hc20cal2	-14.801	1205.011	0	1334	0.9871	0.426
hc20cal3	-14.613	1203.062	0	1332	0.989	0.385
hct20cal#	-14.395	1184.126	0	1332	0.99	0.356
hc20cal4#	-14.636	1204.486	0	1332	0.991	0.354

Table 5b. HCTZ 20% PLS Calibration

Cal. file	# factors	MSECV	λ range nm	mult r	SEE
pls2hc20	3	0.054	1100-2500	0.9882	0.4142
pls4hc20	3	0.054	1300-2350	0.9893	0.393
pls3h20	3	0.046	1100-2500	0.99	0.3743
plshct20#	3	0.038	1100-2500	0.9905	0.3588

Hardness calibration results for CTM, HCTZ and Placebo tablets in Manuscript III.

Table 6a. HCTZ 15% & 20% MLR Calibration

Cal.file	K(0)	K(1)	k(2)	λ nm	mult r	SEE
hcAcal1	-26.655	-1101.81	0	2262	-0.971	0.665
hcAcal2	-26	-1077.04	0	2262	-0.977	0.575
hcAcal4	-26.585	-1098.62	0	2262	-0.979	0.556
hcAcal3	-25.747	-1067.43	0	2262	-0.979	0.551
hcAcal5	-18.999	-129.26	-2503.114	1930+1820	-98.41	0.464

Table 6b. HCTZ 15% & 20% PLS Calibration

Cal. file	# factors	MSECV	λ range nm	mult r	SEE
pls1hcA	7	0.065	1100-2500	0.9877	0.4478
pls2hcA	4	0.052	1100-2500	0.988	0.4075
pls3hcA	5	0.043	1100-2500	0.9905	0.3615
pls4hcA	5	0.042	1100-2500	0.991	0.3502

Hardness calibration results for CTM, HCTZ and Placebo tablets in Manuscript III.

Table 7a. MLR Calibration of Placebo (1200-2450nm)

Cal.file	K(0)	K(1)	k(2)	k(3)	k(4)	λ nm	mult r	SEE
pl3c1	-15.47	8077.78	-3246.33	621.31	0	1320+2220+2400	0.99	0.400
pl3c2*	-15.24	8246.67	-3307.55	601.46	0	1320+2220+2400	0.993	0.338
pl4c1	-19.24	7123.99	2160.32	-2683.24	666.02	1320+1700+2220+2400	0.991	0.383

Table 7b. PLS Calibration of Placebo (1200-2450nm)

Cal. file	# factors	MSECV	(min)	mult r	SEE
pl2p2	7	0.034	1	0.9936	0.3144
pl2p3	6	0.043	1.25	0.9921	0.3452
pl2p4	6	0.046	1.2	0.9914	0.3593
pl2p5	7	0.031	1	0.9942	0.3006
pl2p6	6	0.043	1.38	0.9928	0.3294
pl2p7	6	0.03	1.24	0.9939	0.2949
pl2p8	5	0.043	1.77	0.9894	0.382

APPENDIX C.

The following tables contain density calibration coefficients and other data from Manuscript III.

Table 1a. MLR density calibration results for CTM 2% in Manuscript III.

Cal.file	K(0)	K(1)	k(2)	λ nm	mult r	SEE
dct2c1	-0.671	444.071	0.000	1292	0.9778	0.0204
dct2lsc2	-0.891	272.346	21.136	1292+2228	0.9867	0.0159
dct2c3	2.071	0.213	0.000	1524/1292	0.9821	0.0182
dct2c4	-0.235	-6.208	0.000	1292/1524	-0.9815	0.0187

Table 1b. PLS density calibration results for CTM 2% in Manuscript III.

Cal. file	# factors	MSECV	(min)	λ range nm	mult r	SEE
dct2pl1	5	0	1.20	1100-2500	0.9938	0.0112
dct2pl2	4	0	1.18	1100-2500	0.9927	0.0118

Table 2a. MLR density calibration results for CTM 6% in Manuscript III.

Cal.file	K(0)	K(1)	k(2)	λ nm	mult r	SEE
dct6c1	-1.156	-96.739	0.000	2352	-0.9779	0.0224
dct6c2	-0.922	-74.151	93.802	2352+2172	0.9826	0.0200
dct6c3	2.228	3.409	0.000	1568/2352	0.9832	0.0195
dct6c4	2.036	-0.338	0.000	2352/1454	0.9860	0.0179

Table 2b. PLS density calibration results for CTM 6% in Manuscript III.

Cal. file	# factors	MSECV	(min)	λ range nm	mult r	SEE
dct6pl1	6	0	1.00	1100-2500	0.9956	0.0104
dct6pl2	6	0	1.00	1100-2500	0.9958	0.0100

Table 3a. MLR Density calibration results for HCTZ 15% in Manuscript III.

Cal.file	K(0)	K(1)	k(2)	λ nm	mult r	SEE
dh15c1	-0.161	-201.146	0.000	1820	-0.9850	0.0217
dh15c3	-0.093	-2.339	0.000	1820/1556	-0.9943	0.0135
dh15lsc2	0.760	-187.750	-70.132	1820+1558	0.9951	0.0127

Table 3b. PLS Density calibration results for HCTZ 15% in
Manuscript III.

Cal. file	# factors	MSECV	(min)	λ range nm	mult r	SEE
dhc15pl1	5	0	1.24	1100-2500	0.9966	0.0109
dh15pl2	5	0	1.16	1100-2500	0.9972	0.0098

Table 4a. MLR Density calibration results for HCTZ 20% in Manuscript III.

Cal.file	K(0)	K(1)	k(2)	λ nm	mult r	SEE
dh20c1	0.300	-82.442	0.000	2318	-0.9740	0.0178
dh20c2	0.155	-73.691	-82.157	2318+1814	0.9887	0.0119
dh20c3	0.602	-0.469	0.000	2318/1568	0.9680	0.0197
dh20c4	1.709	0.641	0.000	1568/2318	0.9832	0.0144

Table 4b. PLS Density calibration results for HCTZ 20% in Manuscript III.

Cal. file	# factors	MSECV	(min)	λ range nm	mult r	SEE
dh20pl1	6	0	1.00	1100-2500	0.9972	0.0062
dh20pl2	6	0	1.00	1100-2500	0.9984	0.0048

BIBLIOGRAPHY

Abrams, S. M., Shenk, J. S., Westerhaus, M. O. and Barton, F. E., **Journal of Dairy Science** 70, 806-813 (1987).

Aldridge, P. K., Mushinsky, R. F., Andino, M. M. and Evans, C. L. "Identification of tablet formulations inside blister packages by near-infrared spectroscopy", **Applied Spectroscopy** 48(10), 1272-1276 (1994).

Aldridge, P. K., Pfizer, Inc. Apparatus for mixing and detecting on-line homogeneity. European Patent Publication 0 631 810 A1, 1993.

American Society for Testing and Materials, "Standard Practices for Infrared, Multivariate, Quantitative Analysis", Official ASTM Publication No. E1655, pp. 1-25 (1995).

Association of Analytical Chemists, Conference Publication, November (1993).

Baer, R. J., Frank, J. F. and Morrison, L., "Compositional analysis of nonfat dry milk by using near infrared diffuse reflectance spectroscopy", **Journal of the Association of Official Analytical Chemists** 66(4), 858-863 (1983).

Bohme, W. and Liekmeier, W., "Water determination by near infrared spectroscopy", **International Labmate** 14(1), 1-4 (1986).

Bouveresse, E. and Massart, D. L., "Modified algorithm for standardization of near-infrared spectrophotometric instruments", **Analytical Chemistry** 67(8), 1381-1389, 1995.

Brereton, R. G., "Chemometrics in analytical chemistry", **Analyst**, 112, 1635-1657 (1987).

Brook, D. B. and Marshall, K., "Crushing-strength of compressed tablets I. Comparison of testers", **Journal of Pharmaceutical Sciences** 57, 481-484 (1968).

Buchanan, B. R., Baxter, M. A., Chen, T., Qin, X. and Robinson, P. A., "Use of near-infrared spectroscopy to evaluate an active in a film coated tablet", **Pharmaceutical Research** 13(4), 616-621 (1996).

Carroll, J. E., "Real-time-saving spectroscopy", **Dateline PerPharma** 1(1), 124-126 (February 1994).

Church, G. J., **Time** 120, 16 (October 18, 1982).

Ciurczak, E. W and Torlini, R. P., "Analysis of solid and liquid dosage forms using near-infrared reflectance spectroscopy", **Spectroscopy** 2(3), 41-43 (1987)

Ciurczak, E. W, Torlini, R. P. and Demkowicz, M. P., "Determination of particle size of pharmaceutical raw materials using near-infrared reflectance spectroscopy", **Spectroscopy** 1(7), 36-39 (1986).

Ciurczak, E. W. and Maldacker, T. A., "Identification of actives in multicomponent pharmaceutical dosage forms using near-infrared reflectance analysis", **Spectroscopy** 1(1), 36-39 (1986).

Ciurczak, E. W. and Pope, J. M. presented at PittCon, March (1993).

Ciurczak, E. W., "Analytical applications of near-infrared spectroscopy", **Chemtech** 6, 374-380 (1992).

Ciurczak, E. W., "Pharmaceutical mixing studies using near-infrared spectroscopy", **Pharmaceutical Technology** 15(9), 140 (1991).

Ciurczak, E. W., "Questions and answers on process analysis: Tips for selecting and calibrating IR instruments", **Spectroscopy** 10(9), 19-20, 1995.

Corti, P. and Dreassi, E., "Near infrared reflectance analysis: Features and applications in pharmaceutical and biomedical analysis", **Farmaco** 48(1), 3-20 (1993).

Corti, P., and Dreassi, E., "Application of NIRS to the quality control of pharmaceuticals: Ketoprofen assay in different pharmaceutical formulae", **Pharmaceutica Acta Helvetaie** 64(5-6), 140-143 (1989).

Corti, P., Dreassi, E., Corbini, G., Lonardi, S., Viviani, R. Mosconi, L. and Bernuzzi, M., "Application of near infrared reflectance to the analytical control of pharmaceuticals: Assay of ranitidine chlorhydrate and water content in tablets", **Pharmaceutica Acta Helvetaie** 65(1), 28 (1990).

Dempster, M. A., Jones, J. A., Last, I. R., MacDonald, B. F. and Prebble, K. A., "Near-infrared methods for the identification of tablets in clinical trial supplies", **Journal of Pharmaceutical and Biomedical Analysis** 11(11/12), 1087-1092 (1993).

Drennen, J. K. and Lodder, R. A., "Nondestructive near-infrared analysis of intact tablets for determination of degradation products", **Journal of Pharmaceutical Sciences** 79(7), 622-627 (1990).

Dubois, P., Martinez, J. R. and Levillain, P., "Determination of five components in a pharmaceutical formulation using near infrared reflectance spectrophotometry", **Analyst** 112(12), 1675-1679 (1987).

Duff, G. A., and Ciurczak, E. W., presented at PittCon, March (1993).

Entrop, P., **Dateline: Pharma,** a Perstorp Analytical publication, October 1995.

Gemperline, P. J. and Boyer, N. R., "Classification of near-infrared spectra using wavelength distances: Comparison to the Mahalanobis distance and residual variance methods", **Analytical Chemistry** 67(1) 160-166 (1995).

Gemperline, P. J. and Webber, L. D., "Raw materials testing using soft independent modeling of class analogy analysis of near-infrared reflectance spectra", **Analytical Chemistry** 61, 138-144 (1989).

Grant, A., Davies, A. M. C. and Bilverstone, T., "Simultaneous determination of sodium hydroxide, sodium carbonate and sodium chloride concentrations in aqueous solutions by near-infrared spectrometry", **Analyst** 114(7), 819-822 (1989).

Gunsel, W. C., et al, "Tablets", in The Theory and Practice of Industrial Pharmacy, L. Lachman, H. A. Lieberman, and Kanig, J. L., editors, Lea & Febiger, Philadelphia, 305-345 (1970).

Hansen, W. G., "Shifting of -OH absorption bands on NIR spectra of esters", **Applied Spectroscopy** 47(10), 1623-1625 (1993).

Higuchi, T., et al, **Journal of the American Pharmaceutical Association**, Scientific Edition 42, 194 (1953).

Jones, J. A., et al, "Development and transferability of near infrared methods for determination of moisture in a freeze-dried injection product", presented at the "Fourth International Symposium on Pharmaceutical and Biomedical Analysis", Baltimore, MD, pp. 1-9 (April 1993).

Kamat, M. S., Lodder, R. A., and DeLuca, P. P., "Near-infrared spectroscopic determination of residual moisture in lyophilized sucrose through intact glass vials", **Pharmaceutical Research** 6(11), 961-965 (1989).

King, R. E., "Tablets, Capsules and Pills", in Remington's Pharmaceutical Sciences, Osol, A., et al, editors, Mack Publishing Co., Easton, Pennsylvania, pp. 1553-1584 (1980).

Kortum, G., in Reflectance Spectroscopy: Principles, Methods & Applications, Springer-Verlag, New York (1969).

Kubelka, P., "New contributions to the optics of intensely light-scattering materials Part I.", **Journal of the Optical Society of America** 38, 448 (1948).

Kumar, V. V. and Raghunathan, P., "Spectroscopic investigations of the water pool in lecithin reverse micelles", **Lipids** 21(12), 764-768 (1986).

Lafford, T. A., Cornelis, Y. and Forster, P., "Near-infrared spectroscopy for quantitative and qualitative quality control", **Analyst** 117(10), 1543-1545 (1992).

Leuenberger, H. and Rohera, B. D., "Fundamentals of powder compression. I. The compactibility and compressibility of pharmaceutical powders", **Pharmaceutical Research** 3(1), 12-22 (1986).

Libnau, F. O., Kvalheim, O. M., Christy, A. A. and Toft, J., "Spectra of water in the near- and mid-infrared region", **Vibrational Spectroscopy** 7, 243-254 (1994).

Lin, J. and Brown, C. W., "Universal approach for determination of physical and chemical properties of water by near-IR spectroscopy", **Applied Spectroscopy** 47(10), 1720-1727 (1993).

Lodder, R. A. and Hieftje, G. M., "Analysis of intact tablets by near-infrared reflectance spectrometry", **Applied Spectroscopy** 42(4), 556-558 (1988).

Lodder, R. A., Selby, M. and Hieftje, G. M., "Detection of capsule tampering by near-infrared reflectance analysis", **Analytical Chemistry** 59(15), 1921-1930 (1987).

Lonardi, S., Viviani, R., Mosconi, L., Bernuzzi, M., Corti, P., Dreassi, E., Murratzu, C. and Corbini, G., "Drug analysis by near-infrared reflectance spectroscopy. Determination of the active ingredient and water content in antibiotic powders.", **Journal of Pharmaceutical and Biomedical Analysis** 7, 303-308 (1989).

MacDonald, B. F. and Prebble, K. A., "Some applications of near-infrared reflectance analysis in the pharmaceutical industry", **Journal of Pharmaceutical and Biomedical Analysis** 11(11), 1077-1085 (1993).

Mark, H. L. and Tunnell, D., "Qualitative near-infrared reflectance analysis using Mahalanobis distances", **Analytical Chemistry** 57(7), 1449-1456 (1985).

Mark, H. L., "Data Analysis: Multilinear Regression and Principal Component Analysis", in Handbook of Near-Infrared Analysis, ed. D. A. Burns and E. W. Ciurczak, Marcel Dekker, Inc., New York, NY, pp. 107-158 (1992).

Marshall, K. and Rudnic, E. M., "Tablet Dosage Forms", in Modern Pharmaceutics, second edition, G. S. Banker and C. T. Rhodes, editors, Marcel Decker, Inc., New York, NY, pp. 355-425 (1990).

Massart, D. L., et al, Data Handling in Science & Technology, (New York: Elsevier Publishing, 1988), vol. 2, Chemometrics: a textbook, pp. 5.

McClure, W. F. "Near-infrared spectroscopy,: the giant is running strong", **Analytical Chemistry** 66(1), 42A-53A (1994).

Noble, D., "Illuminating Near-IR", **Analytical Chemistry** 67(23), 735A-740A (1995).

Norris, K. H. and Hart, J. R., Proceedings of the 1963 International Symposium on Humidity and Moisture: Principles and Methods of Measuring Moisture in Liquids and Solids, Vol. 4., Reinhold, New York, p. 19 (1965).

Norris, K. H. and Williams, P. C., "Optimization of mathematical treatments of raw near-infrared signal in the measurement of protein in hard red spring wheat", **Cereal Chemistry**, 61(2), 158-165 (1984).

Nyström,C. and P. G. Karehill, "The Importance of Intermolecular Binding Forces and the Concept of bonding Surface Area", in Pharmaceutical Powder Compaction Technology, G. Alderborn and C. Nystrom, ed., Marcel Dekker, Inc., New York, NY, 1996, pp. 17-53.

Olinger, J. M. and Griffiths, P. R. **Applied Spectroscopy** 47(6):687-694 (1993).

Osborne, B. G. and Fearn, T., "Collaborative evaluation of near infrared reflectance analysis for the determination of protein, moisture and hardness in wheat", **Journal of the Science Food and Agriculture** 34:1011-1017 (1983).

Osborne, B. G. and Fearn, T., Near Infrared Spectroscopy in Food Analysis, Wiley & Sons, Inc., New York, pp. 117-161 (1986).

Plugge, W. and Van Der Vlies, C., "Near-infrared spectroscopy as an alternative to assess compliance of ampicillin trihydrate with compendial specifications", **Journal of Pharmaceutical and Biomedical Analysis** 11(6), 435 (1993).

Plugge, W. and Van Der Vlies, C., "The use of near infrared spectroscopy in the quality control laboratory of the pharmaceutical industry", **Journal of Pharmaceutical and Biomedical Analysis** 10(10-12), 797-803 (1992).

Reference Manual for Near Infrared Spectral Analysis Software (NSAS) Version 3.30 a, NIRSystems, Inc./Perstorp Analytical Co., Silver Spring, MD, pp. 3-1 to 3-62, 1995.

Ryan, J. A., Compton, S. V., Brooks, M. A., and Compton, D. A., "Rapid verification of identity and content of drug formulations using mid-infrared spectroscopy", **Journal of Pharmaceutical and Biomedical Analysis** 9(4), 303 (1991).

Sekulic, S. S., Ward, H. W., Brannegan, D. R., Stanley, E. D., Evans, C. L., Sciavolino, S. T., Hailey, P. A. and Aldridge, P. K., "On-line monitoring of powder blend homogeneity by near-infrared spectroscopy", **Analytical Chemistry** , 68(3), 509-513, 1996.

Shenk, J. S., J. J. Workman, Jr., and M. O. Westerhaus, "Applications of NIR Spectroscopy to Agricultural Products", in <u>Handbook of Near-Infrared Analysis</u>, D. A. Burns and E. W. Ciurczak, editors, Marcel Dekker, Inc., New York, pp. 383-431 (1992).

Sinsheimer, J. E. and Poswalk, N. M., "Pharmaceutical applications of the near-infrared determination of water", **Journal of Pharmaceutical Sciences** 57(11), 2007-2010 (1968).

Thomas, .E. V., "A primer on multivariate calibration", **Analytical Chemistry** 66(15), 795A-804A, 1994.

Tudor, A. M., Melia, C. D., Binns, J. S., Hendra, P. J., Church, S. and Davies, M. C., "The application of Fourier-transform Raman spectroscopy to the analysis of pharmaceuticals and biomaterials", **Journal of Pharmaceutical and Biomedical Analysis** 8(8-12), 717-720 (1990).

United States Pharmacopoeia XXIII/National Formulary XVIII, USP Convention, Inc., Rockville, MD, printed by Rand McNally, Taunton, Massachusetts, pp. 1680 (1995).

United States Pharmacopoeia XXIII/National Formulary XVIII, USP Convention, Inc., Rockville, MD, Rand McNally, Taunton, Massachusetts, pp. 1838-1982 (1995).

Vornheder, P. F. and Brabbs, W. J., "Moisture determination by near-infrared spectrometry", **Analytical Chemistry** 42(12), 1454-1456 (1970).

Wade, A. and P. J. Weller, "Handbook of Pharmaceutical Excipients", second edition, American Pharmaceutical Association, Washington, D. C., pp. 56-60, 1994.

Wetzel, D. L., "Near-infrared reflectance analysis: sleeper among spectroscopic techniques", **Analytical Chemistry** 55(12), 1165A-1175A (1983).

Weyer, L. G., "Near-infrared spectroscopy of organic substances", **Applied Spectroscopy Reviews** 21(1&2), 1-43 (1985).

Whitfield, R. G. and Fox, L. E., "Near infrared spectrophotometry (NIRS) for pharmacopoeial identity testing", **Pharmeuropa** 4(1), 60 (1992).

Whitfield, R. G., "Near-infrared reflectance analysis of pharmaceutical products", **Pharmaceutical Manufacturing** 4(1), 31 (1986).

Willard , H. H. et al, "Infrared Spectroscopy", Chapter 11, in, Instrumental Methods of Analysis, 7th edition, Wadsworth Publishing Company, Belmont, California, p. 287 (1988).

Windham, W. R., Gaines, C. S. and Leffler, R. G., "Effect of wheat moisture content on hardness scores determined by near-infrared reflectance and on hardness score standardization", **Cereal Chemistry** 70, 662-666 (1993).

Workman, J. and Brown, J., "A new standard practice for multivariate, quantitative infrared analysis- Part I", **Spectroscopy** 11(2), 48-51, 1996.

Workman, J. J., "NIR Spectroscopy Calibration Basics", in Handbook of Near-Infrared Analysis, ed. D. A. Burns and E. W. Ciurczak, Marcel Dekker, Inc., New York, NY, pp. 247-280 (1992).

Workman, J., "A review of process near infrared spectroscopy: 1980-1994", **Journal of Near Infrared Spectroscopy** 1, 221-245 (1993).